

UNCLASSIFIED

---

AD 274 282

*Reproduced  
by the*

ARMED SERVICES TECHNICAL INFORMATION AGENCY  
ARLINGTON HALL STATION  
ARLINGTON 12, VIRGINIA



---

UNCLASSIFIED

NOTICE: When government or other drawings, specifications or other data are used for any purpose other than in connection with a definitely related government procurement operation, the U. S. Government thereby incurs no responsibility, nor any obligation whatsoever; and the fact that the Government may have formulated, furnished, or in any way supplied the said drawings, specifications, or other data is not to be regarded by implication or otherwise as in any manner licensing the holder or any other person or corporation, or conveying any rights or permission to manufacture, use or sell any patented invention that may in any way be related thereto.

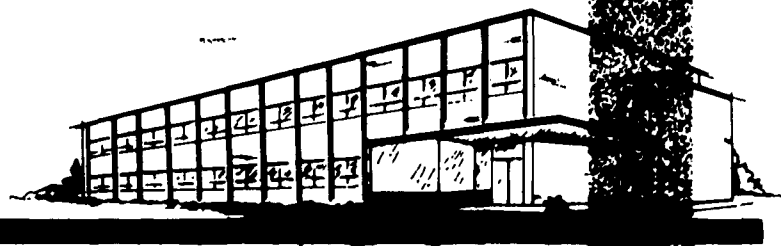
CATALOGED BY ASTIA 274282  
AS AD NO.

274 282

Copy No. \_\_\_\_\_

NOX

ASTIA  
RECEIVED  
APR 20 1962  
62-3-1  
TISIA A



THE *Bendix* CORPORATION

BENDIX SYSTEMS DIVISION • ANN ARBOR, MICHIGAN


SCADAR FINAL REPORT

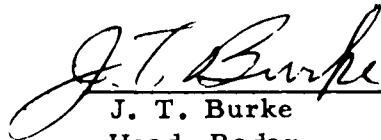
BSR-628

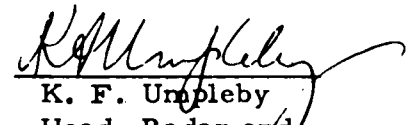
December 1961

Prepared by:

Approved by:

  
R. G. Peltzer  
Radar Systems Group

  
J. T. Burke  
Head, Radar  
Systems Section

  
K. F. Umpleby  
Head, Radar and  
Acoustics Department

BENDIX SYSTEMS DIVISION  
of  
THE BENDIX CORPORATION  
Ann Arbor, Michigan

AF 30(602) - 1861

Prepared  
for  
Rome Air Development Center  
Air Research and Development Command  
United States Air Force

Griffiss Air Force Base  
New York

## TABLE OF CONTENTS

	<u>Page</u>
1. INTRODUCTION AND SUMMARY	1-1
2. SYSTEM DESIGN	2-1
2.1 DESIGN CONSIDERATIONS	2-3
2.2 SYSTEM DESCRIPTION	2-6
3. COMPONENT DESIGN	3-1
3.1 MODIFICATIONS TO EXISTING EQUIPMENT	3-1
3.1.1 FRC-45 Radio Frequency Oscillator	3-1
3.1.2 Design and Development of Special Equipment	3-1
3.2 DESIGN AND DEVELOPMENT OF SPECIAL EQUIPMENT	3-1
3.2.1 Mixer, 5-Mc Amplifiers and Notch Filters	3-4
3.2.2 Limiter Discriminator	3-4
3.2.3 Integrator	3-4
3.2.4 5X Multiplier	3-4
3.2.5 6X Multiplier	3-11
3.2.6 Target Oscillator	3-11
4. LABORATORY TESTS	4-1
4.1 Mixer, 5-Mc Amplifier and Notch Filter Chassis	4-1
4.2 Limiter-Discriminator Chassis	4-2
4.3 Overall System Test	4-6
5. FIELD TESTS	5-1
5.1 FIELD TEST LOCATION	5-1
5.2 EQUIPMENT PERFORMANCE	5-1
5.3 FIELD TEST RESULTS	5-3
6. CONCLUSIONS AND RECOMMENDATIONS FOR FUTURE STUDY	6-1
6.1 CONCLUSIONS	6-1
6.2 RECOMMENDATIONS FOR FUTURE STUDY	6-1
APPENDIX A THEORETICAL ANALYSIS	A-1

## LIST OF ILLUSTRATIONS

<u>Figure</u>	<u>Title</u>	<u>Page</u>
2-1	SCADAR System Block Diagram	2-4
3-1	0-469/FRC-45(318F1) Radio Frequency Oscillator Modification	3-2
3-2	REL Receiver Modification	3-3
3-3	Mixer, 1 <sup>st</sup> IF, Filter Driver, and AOC	3-5
3-4	IF Amplifier, Filter Driver, and AOC	3-6
3-5	Filter Schematic	3-7
3-6	Band Reject Filter Response	3-8
3-7	Limiter-Discriminator Schematic	3-9
3-8	Crystal Discriminator	3-10
3-9	Integrator	3-11
3-10	25 Mc Multiplier	3-12
3-11	30 Mc Multiplier	3-13
3-12	Target Oscillator	3-14
3-13	Receive Test Switch Schematic	3-16
4-1	Mixer, Amplifier, and Notch Filter Block Diagram	4-1
4-2	Amplifier-Notch Filter Chassis Test Configuration	4-2
4-3	Frequency Response Curve — Filter No. 1	4-3
4-4	Frequency Response Curve — Filter No. 2	4-4
4-5	Limiter-Discriminator Swept Frequency Response	4-5
4-6	Discriminator Response	4-7
4-7	Discriminator Curve	4-8
5-1	AM Envelope Detector	5-2
5-2	Crossings 1, 2, and 3	5-5
5-3	Crossings 4 and 5	5-7
5-4	Crossings 6 and 7	5-8
5-5	Crossing 8	5-9
5-6	Crossing 9	5-10
5-7	Crossing 10	5-11
5-8	Crossings 11 and 12 (a and b)	5-12
5-9	Simulated Target Crossings	5-13
5-10	Simulated Target Crossings With Noise	5-14

# LIST OF ILLUSTRATIONS (CONT.)

<u>Figure</u>	<u>Title</u>	<u>Page</u>
A-1	Baghdady's Variable Trap Method	A-4
A-2	Vector Diagram of Two Unmodulated Radio Waves	A-5
A-3	Instantaneous Frequency Distribution (after Granlund')	A-7
A-4	Instantaneous Frequency Distribution for $W_d = kt$	A-8
A-5	Discriminator Block Diagram	A-15
A-6	Transfer Function	A-16

## SECTION 1

### INTRODUCTION AND SUMMARY

For some years Bendix has been working under contract to the Rome Air Development Center on a project known as SCADAR, a method for detecting moving targets by bistatic radar techniques. Most people have observed the flickering produced in a television set when an airplane flies by. This is caused by the fact that the signal reflected (or refracted) from the airplane beats with the signal being received directly from the transmitting station, producing alternately an increase or decrease in signal level as the difference in path lengths is an even or odd number of half-wavelengths. SCADAR is an attempt to apply this phenomenon to a military system of airplane detection, using existing communications links. In addition, the SCADAR technique makes use of the principle of "forward scatter enhancement". By extrapolation from optical theory, it can be shown that the effective cross section of an object can be much greater in the forward scatter mode than in the back scatter mode. The combination of this enhancement, and the sophisticated data processing which is possible, should lead to a superior ability to detect small or low-flying airplane targets.

During the course of this project a variety of experimental implementations (in addition to analytical work) have fully substantiated the claims made for the system. Field tests have been performed in several geographical locations both within and outside the United States, at frequencies ranging from 50 to 4000 Mc under all meteorological (and ionospheric) conditions, using a variety of targets, different spacings between transmitter and receiver (including line of sight and over the horizon), and using a variety of data processing systems. A system using a dual transmitter-receiver link was tested, and shown to be capable of yielding additional information about the motion of the target. All of this work has been fully described in previous interim reports.

The SCADAR principle has been fully demonstrated to be capable of detecting airplanes crossing a base line established by an existing communications link. This technique is sensitive, reliable, and low in cost. The next most logical step would be to install such a system as an extension of the nation's early warning capabilities, or for local application as a gap filler.

The final six months of the SCADAR work (described in detail in this report) were concerned with the implementation of a new technique for data processing, which it was anticipated would yield even greater detection sensitivity. This technique, which is described in detail later in following sections, was shown to have considerable promise when implemented by simulation in the laboratory. For example, it was shown to be quite capable of recognizing a signal 40 db below the noise level. As a further check, a system using sound as the propagating signal was installed in the Bendix parking lot to detect the motion of automobiles. At this point it became apparent that the presence of the direct signal, which had been previously considered innocuous, was a serious factor in limiting the sensitivity of the system since it tended to "capture" the receiver. Accordingly, it was necessary to incorporate rejection filters to reduce this signal to an acceptable level. Since the final implementation visualized operation at 806 Mc, with receiver (discriminator) bandwidths of a few hundred cycles, very high stabilities and very high ratios of center frequency to bandwidth were involved. This led to filters and discriminators using crystals of very high accuracy and stability, and accounted for most of the technical difficulties encountered.

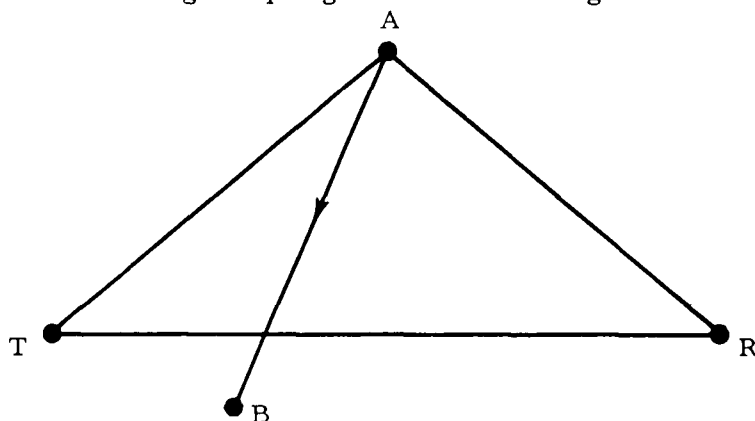
These difficulties were eventually overcome, and a working system was installed on the tropo-scatter DEW line training link in Illinois. For reasons incident to the problem described above, it was necessary to modify the already quite stable transmitter at Streator to provide a stability that was several orders of magnitude greater.

Field tests were conducted during November 1961, using commercial airplane traffic as targets. Many difficulties arose, which at first cast doubt on the validity of the technique. The principle difficulties stemmed from sheer volume of traffic, which tended to confuse the results, and very slow aircraft, which provided low doppler frequencies. Later in the tests a random spurious modulation of the transmitter was observed to occur from causes beyond control. By operating at night when the traffic density was lower, and by choosing times when the transmitter was operating properly, satisfactory results were obtained which clearly demonstrated that, under better field-test conditions and in the presence of a typical enemy threat, the technique under evaluation would provide a detection capability superior to the methods previously employed. To this extent the project is considered to have been satisfactorily concluded.

## SECTION 2

### SYSTEM DESIGN

The technique investigated in the final portion of the SCADAR is illustrated by the following simple geometrical configuration.



Energy from a transmitter at point T is received by a receiver at R. An aircraft at point A, proceeding towards B, re-radiates energy which enters the receiver via the path TAR. Since  $TAR > TR$ , there will be a phase difference in the two paths. As the aircraft approaches the line TR, the path TAR will shorten until  $TAR = TR$ , and then increase again. The signals arriving by the two paths therefore alternately add and subtract when  $TAR - TR = N \lambda / 2$ , resulting in a modulation of the direct signal by the aircraft signal. Demodulation produces frequencies in the low audio range, varying from a maximum when the target enters the common antenna pattern, falling to zero as the aircraft crosses TR, and rising again to a maximum as the aircraft leaves the common antenna pattern.

This system is simple, and makes no stringent demands on transmitter and receiver stability, or on the type of modulation (if any) superimposed on the carrier. However, signal processing is usually by some form of spectrum analysis, which requires human interpretation for maximum detectability. Previous SCADAR work has used a variety of spectrum analyzers, but all had the common feature that analysis was performed after the two signals had beat in an amplitude detector.

Two other limitations exist:

1. For practical reasons, analyzer bandwidths have been limited to a minimum of 5 cps, whereas narrower bandwidths (or conversely longer integration times) would improve the detectability of weak signals.
2. The direct signal is frequently quite weak, in fact comparable to the aircraft signal, and both are noisy. Recovery of modulation products by square law detection results in a further degradation of signal/noise ratio.

The following technique was investigated in an effort to improve the detectability of weak signals.

Suppose the direct signal (via path TR) is not present. This may be because the spacing of the stations exceeds line of sight. Because the airplane is at some altitude, however, let us suppose that energy is arriving via path TAR. For the reasons explained previously, this will manifest itself in the receiver as a signal which is initially higher than the carrier frequency, and falls (through the carrier frequency), to a value below the carrier frequency. After conversion, the same signal will be observed as one sliding through the IF pass band.

Suppose some of the IF signal from the receiver is abstracted and passed through a discriminator, with a bandwidth equal to the audio bandwidth required in the original system. The output of the discriminator will then consist of a slowly varying DC voltage, starting with some polarity (say positive) falling to zero, and increasing in the negative direction. In fact, the familiar S-curve associated with a discriminator will be traced out. This waveform bears a close resemblance to a single cycle of a sine wave, having a period equal to the time the airplane takes to traverse the common antenna pattern. In a typical case this may be 30 seconds. The discriminator can therefore be followed with a low pass filter having a time constant of this order, and the same waveform may be observed with little loss of amplitude. (There will, of course, be a phase delay).

Having done this, the signal is now being observed with an integration time of 30 seconds, or a bandwidth of  $1/30$  cps. This represents a considerable reduction in bandwidth, and a consequent increase in detectability

over the original system. Furthermore, the discriminator itself has an inherent noise rejection capability, since noise contributions from above and below the center frequency will produce voltages of opposite polarity, which tend to cancel. In fact, the only noise appearing in the output of the discriminator will result from those components of unbalance which lie below  $1/30$  cps.

It is apparent that there is considerable potential here for an improvement in the detection of weak signals. The practical advantage lies in the freedom to use stations spaced beyond line of sight, and/or to detect lower altitude targets. In addition, it should be relatively easy to implement an alarm system which would recognize the positive-going-through-zero-to-negative signal characteristics of a target.

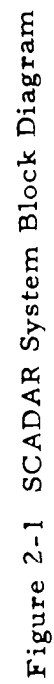
Some additional restrictions are imposed by the use of this technique. A fairly high degree of stability is required of both transmitter and receiver, since differential shifts of the order of 100 cps will produce target-like signals. At 1000 Mc this would correspond to a stability better than 1 part in  $10^7$ . The situation is somewhat alleviated, because we are really concerned only with frequency shifts which take place in periods of the order of 30 seconds. Much slower shifts can be recognized as not representative of typical target speeds. To accommodate these slow shifts, however, it might be necessary to servo the discriminator to the carrier frequency (after conversion). This would be possible if the direct signal is available; if not, multiple discriminators could be provided to bracket the expected drift or  $10^{-8}$  stable oscillators provided to reduce the drift.

Later sections of this report will describe the implementation and field test of a detection system of this kind.

The block diagram of the system that was used to detect the target signal by the FM techniques described above and compared with the detection by AM techniques as shown in Figure 2-1. In addition to the equipment that is necessary to receive and detect the desired signal, there is equipment to test the system in the absence of a signal and also to align the system.

## 2.1 DESIGN CONSIDERATIONS

At this point it is appropriate to record all that is known about the character of the carrier and target signals. The carrier signal  $S_c$  is



derived from a source that has a stability of  $1 \times 10^{-8}$  cps/day, but it is not this stable in short periods of time because it arrives at the receiver via the tropospheric scatter mode. This tropospheric scatter signal has, by nature, random amplitude<sup>1</sup> and phase<sup>2</sup> fluctuations.

The target signal  $S_t$  is derived from the same stable source as  $S_c$  but its frequency differs from  $S_c$  because of the doppler effect. When the target is in the common volume,  $S_t$  is not subject to the rapid fluctuations in amplitude and phase that are associated with  $S_c$  but has smooth changes in amplitude and phase as a function of time. When the target is not in the common volume,  $S_t$  will be similar in character to  $S_c$ . The amplitude of  $S_t$  is inversely related to the frequency difference  $W_d$ . The limits of the amplitude changes and frequency difference are known, but their behavior within these limits is not predictable even when it is smooth.

In general, the doppler frequency will be less than 150 cps and for the application of this problem will be less than 60 cps. It is, therefore, advisable to limit the bandwidth of the discriminator to  $\pm 150$  cps.

Since  $E_c > E_t$ , it will be necessary to reduce  $E_c$  to a value that is at least 40 db below  $E_t$  to prevent  $E_c$  from capturing  $E_t$ . Very narrow-band rejection filters were used to achieve strong rejection of  $E_c$  without appreciably affecting  $E_t$ , since none of the weak signal enhancement methods of Appendix A could achieve this amount of rejection.

The frequency stability of the receiver must be equal to or better than that of the received signal. This requirement arises from the fact that  $E_c$  must be rejected in the filters while rejecting a minimum amount of  $E_t$ .

Since the doppler frequency  $\frac{W_t - W_c}{2\pi}$  can be expected to go from +60 cps through 0 to -60 cps, some of  $E_t$  will be rejected by the filters.

---

<sup>1</sup> Finney, R. G., "Short-Time Statistics of Tropospheric Radio Wave Propagation," General Electric Research Lab. Report No. 58-RL02030

<sup>2</sup> von Baeyer, H. J., "Selective Fading Effects on UHF Tropospheric Scatter Paths," Proc. IRE, Nov. 1959, pp. 2021.

<sup>3</sup> The common volume is the volume that is common to both antenna beams.

The basic bandwidth requirements of the discriminator and filter prescribed the use of crystal elements. After a thorough search of the state of the art of crystal filters and discriminators it was found that these units would have to be designed and built to the specifications that were desired. A center frequency of 1 to 5 Mc was necessary to achieve the bandwidths that were required while remaining within the limits of the state of the art.

The 5-Mc second IF center frequency was chosen for the following reasons. The first intermediate frequency of 30 Mc had already been determined by the receiver. A 5-Mc frequency standard with a stability of  $1 \times 10^{-9}$  cps/day was available for aligning the discriminator. The output of the 5-Mc frequency standard could be multiplied by 5 to obtain the 25-Mc local oscillator signal to convert the first IF of 30 Mc to the second IF of 5 Mc. The 5-Mc standard could also be multiplied by 6 to obtain a 30-Mc signal to align the 30-Mc IF strip or to supply a synthetic signal for system test in the absence of  $S_c$ . In addition to a synthetic  $S_c$  the test equipment supplies broad band noise centered at 30 Mc and a variable oscillator that produces a simulated  $S_t$  as it would appear at the output of the 30-Mc IF amplifier. The inherent difficulty with this choice of second IF frequency is that the 5 X multiplier will have a 5-Mc component. This is reduced considerably by cascaded, tuned amplifiers so that the amplitude of this component is much lower than the smallest expected amplitude of  $S_c$  at the second mixer.

The high cost and long lead time in the procurement of the crystal notch filters prescribed that an overload protection device and an AGC be inserted ahead of the filters to reduce the possibility of their being damaged as a result of abnormally high signal strengths or operator ineptitude.

The output of the discriminator is integrated in a low pass filter and presented on a Sanborn recorder. A selection of from 0.1 to 30 seconds of integration time is available to the operator; the optimum integration time to be determined during the field test of the equipment.

## 2.2 SYSTEM DESCRIPTION

The system block diagram shown in Figure 2-1 can be conveniently broken into three basic parts. These are the FM detection system, the AM detection comparison system, and the target simulator.

The basic FM detection system consists of a transmitter, receiver, signal processing circuits, and a recorder. The transmitter is a standard 1-kw klystron type which has been modified by replacing the two exciter crystal oscillators with a  $10^{-8}$  stable oscillator which will provide an 806-Mc carrier signal. The carrier signal is transmitted and arrives at the receiver via the tropo-scatter mode, where it is mixed with an 836-Mc signal that has been obtained from a  $10^{-8}$  stable oscillator. The difference frequency of 30 Mc is amplified and fed into the second mixer where it beats with the 25-Mc signal that was obtained from the  $10^{-9}$  stable 5-Mc oscillator. The 5-Mc output of the second mixer is amplified and fed to a notch filter which reduces the carrier signal by 40 db but does not appreciably reduce targets with high doppler frequencies. The output of the filter is amplified and filtered a second time. (Overload protective circuits monitor the signal inputs to the notch filters to guard against their damage by excessively high signal levels.) The signal is amplified and limited before being fed into a discriminator whose bandwidth is 300 cps. The output of the discriminator is integrated over an operator selected time constant of from 0.1 to 30 seconds before being displayed on the Sanborn recorder.

The signal that is used to obtain comparison AM detection is obtained from the 30-Mc output of the receiver and then amplified and AM detected by standard techniques. The audio doppler frequency is then multiplied by 50 in the frequency multiplier which consists of a tape recorder that records the signal at a tape speed of 1-7/8 ips and plays back at 50 times 1-7/8 ips by using a high speed spinning head. The multiplied doppler frequency is then analyzed and presented on a Helix recorder. For a more detailed description of the AM detection system see the "SCADAR Final Report", BSR 256, June 1960.

The main purpose of the target simulator is to provide the system with a self check capability. The three signals that are generated within the target simulator are a  $10^{-9}$  stable 30-Mc signal, a noise source that is centered about 30 Mc, and a signal which is swept in frequency from 30 Mc + 150 cps to 30 Mc - 150 cps. The signal selector switch allows the operator to select any combination of the three signals or the received signal. The 30-Mc signal is used to align the system and to provide a stable carrier signal for system tests. The noise generator provides a noise source when conducting system tests. The slowly swept oscillator provides a simulated target signal of known amplitude and frequency which is used in system tests and as a quick self test. This oscillator can also be manually set to provide a stable signal for determining the frequency response of the notch filters and the discriminator.

## SECTION 3

### COMPONENT DESIGN

The design of the components contained in the system can be divided into two categories. The first category is the modification of the existing equipment that was used during past SCADAR contracts. The second category to be presented is the design and development of the special equipment that is needed in this system.

#### 3.1 MODIFICATIONS TO EXISTING EQUIPMENT

##### 3.1.1 FRC-45 Radio Frequency Oscillator

It was necessary to modify the FRC-45 RF Oscillator, as shown in Figure 3-1 below, before it would accept the signal from the 67.166666 Mc stable oscillator. In the normal operating mode for this equipment, the RF oscillator output is fed to the exciter unit where it is mixed with the 16.5 Mc FM modulated signal to obtain the 806 Mc FM modulated carrier. In order to achieve the frequency stability that was required for the field tests, the 16.5-Mc input to the exciter was disconnected and the 67-Mc stable oscillator signal was inserted into the RF Oscillator unit in place of the  $10^{-5}$  stable crystal oscillator. Essentially, the modification consisted of replacing the 40-Mc oscillator doubler (V1301) with an amplifier and converting V1302 to an amplifier doubler by removing the oscillator and ungrounding the grid.

##### 3.1.2 REL Receiver

The modification of the REL receiver consisted of replacing the  $10^{-5}$  stable/crystal oscillator with the 46.444444-Mc stable oscillator and amplifier. The modification, as shown in Figure 3-2 below, was necessary to achieve the required frequency stability.

#### 3.2 DESIGN AND DEVELOPMENT OF SPECIAL EQUIPMENT

A majority of the design and development of the equipment that is presented below was completed in the laboratory of Bendix Systems Division. The notch filters, discriminator and stable oscillators were purchased from a company that specializes in the design and development of these items.

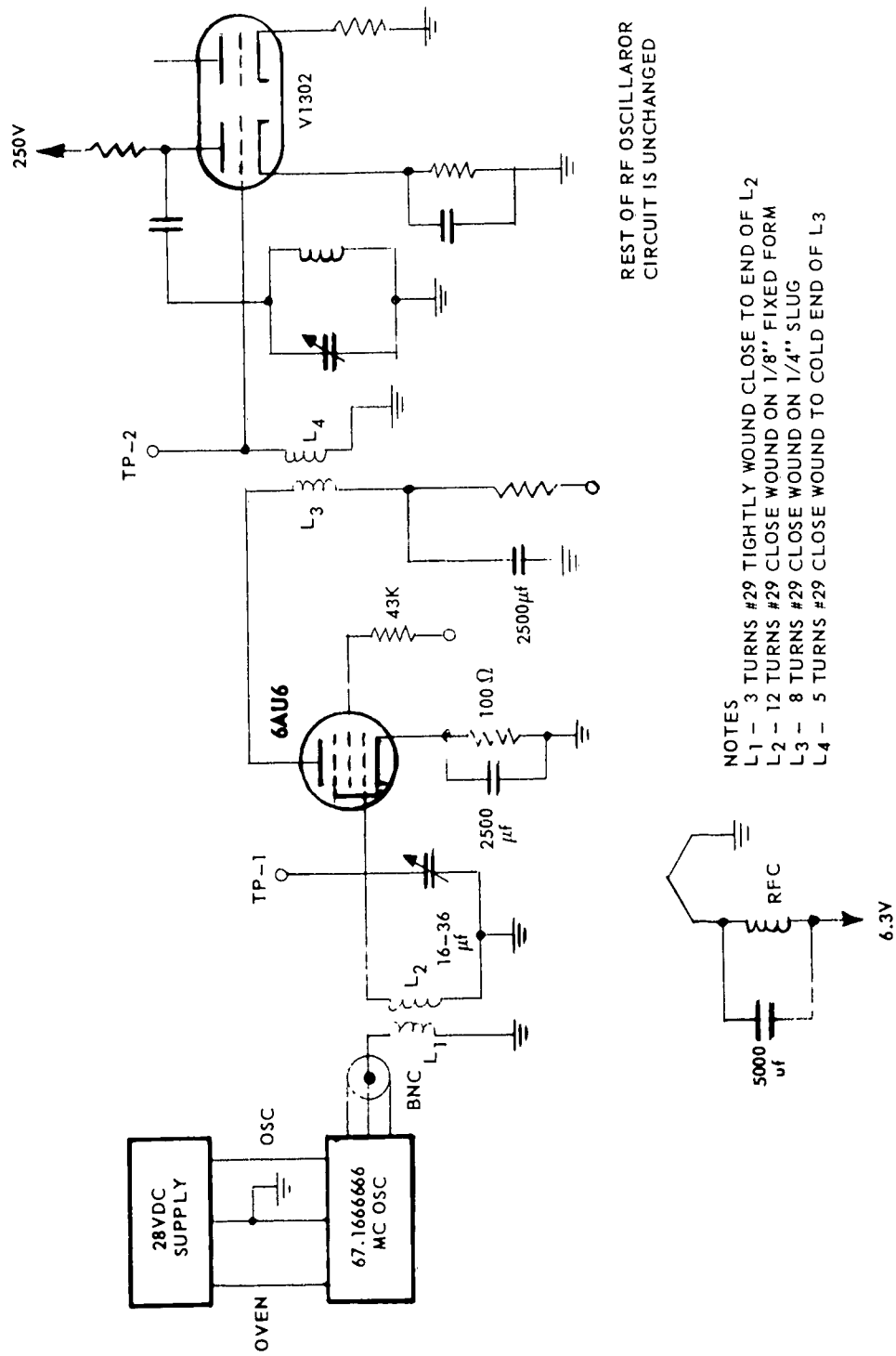


Figure 3-1 0-469/FRC-45(318F1) Radio Frequency Oscillator Modification



### 3. 2. 1 Mixer, 5-Mc Amplifiers and Notch Filters

The schematic diagram for this unit is shown in Figures 3-3 and 3-4 below. The notch or band reject filter schematic diagram and ideal band reject characteristics are shown below in Figure 3-5 and Figure 3-6.

L matching networks are used to match the 25-Mc and 30-Mc inputs to the mixer. The 5-Mc output of the mixer is amplified and impedance matched to the filter by means of a cathode follower and a resonant tank. The notch filter requires resistive and reactive impedance matching at both the input and the output in order to perform to specifications. A resistive mismatch will cause the notch to shift in frequency and a reactive mismatch will cause asymmetry. The 5-Mc signal with 40 db of the carrier frequency removed by the first notch filter is amplified and filtered again to remove another 40 db of carrier before being sent to the limiter-discriminator chassis.

### 3. 2. 2 Limiter-Discriminator

The limiter-discriminator chassis contains five stages of amplification, a limiter pair, another amplifier stage, an impedance matching stage and the discriminator. The schematic diagram is shown in Figure 3-7. Figure 3-8 is a schematic diagram of the discriminator.

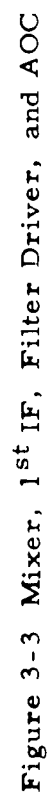
The limiter pair has been designed for a wide bandwidth to improve the transient response to noise bursts. The discriminator must be impedance matched on its input and is tuned for symmetry by a trimmer capacitor. The signal output of the discriminator is fed into the integrator.

### 3. 2. 3 Integrator

The integrator is a simple RC network as shown in Figure 3-9. The operator selects the appropriate integration time for the targets that are to be detected.

### 3. 2. 4 5X Multiplier

The 5-Mc input to the 5X multiplier, that is shown in Figure 3-10, is obtained from the  $10^{-9}$  stable oscillator. The 5-Mc signal is amplified and then clipped to obtain odd harmonics. The clipped signal is amplified





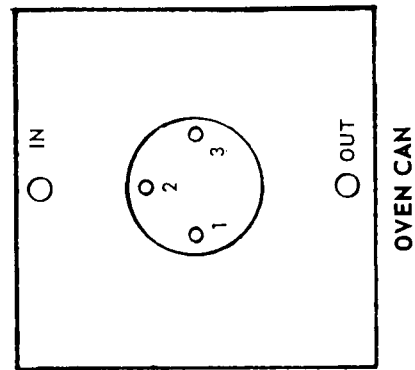
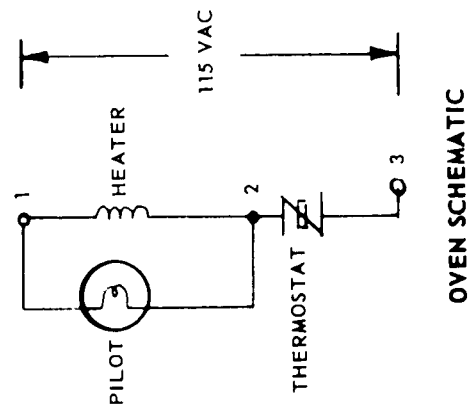
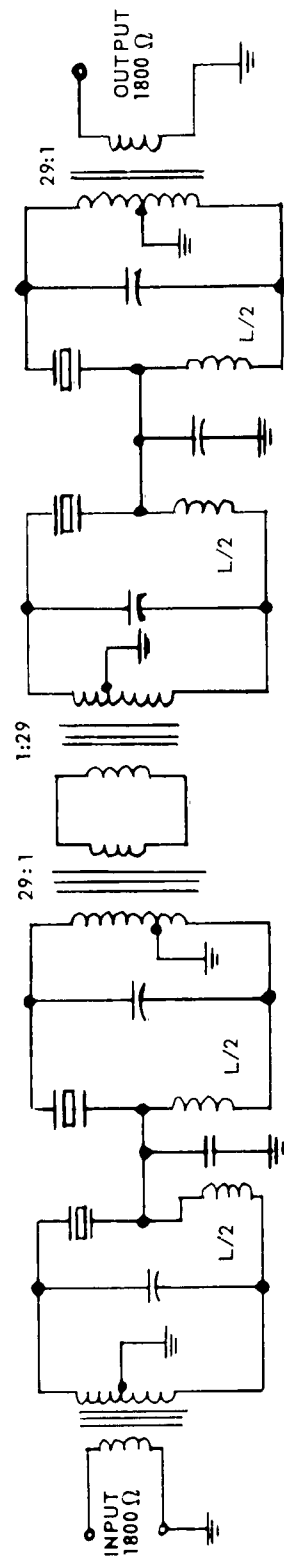


Figure 3-5 Filter Schematic

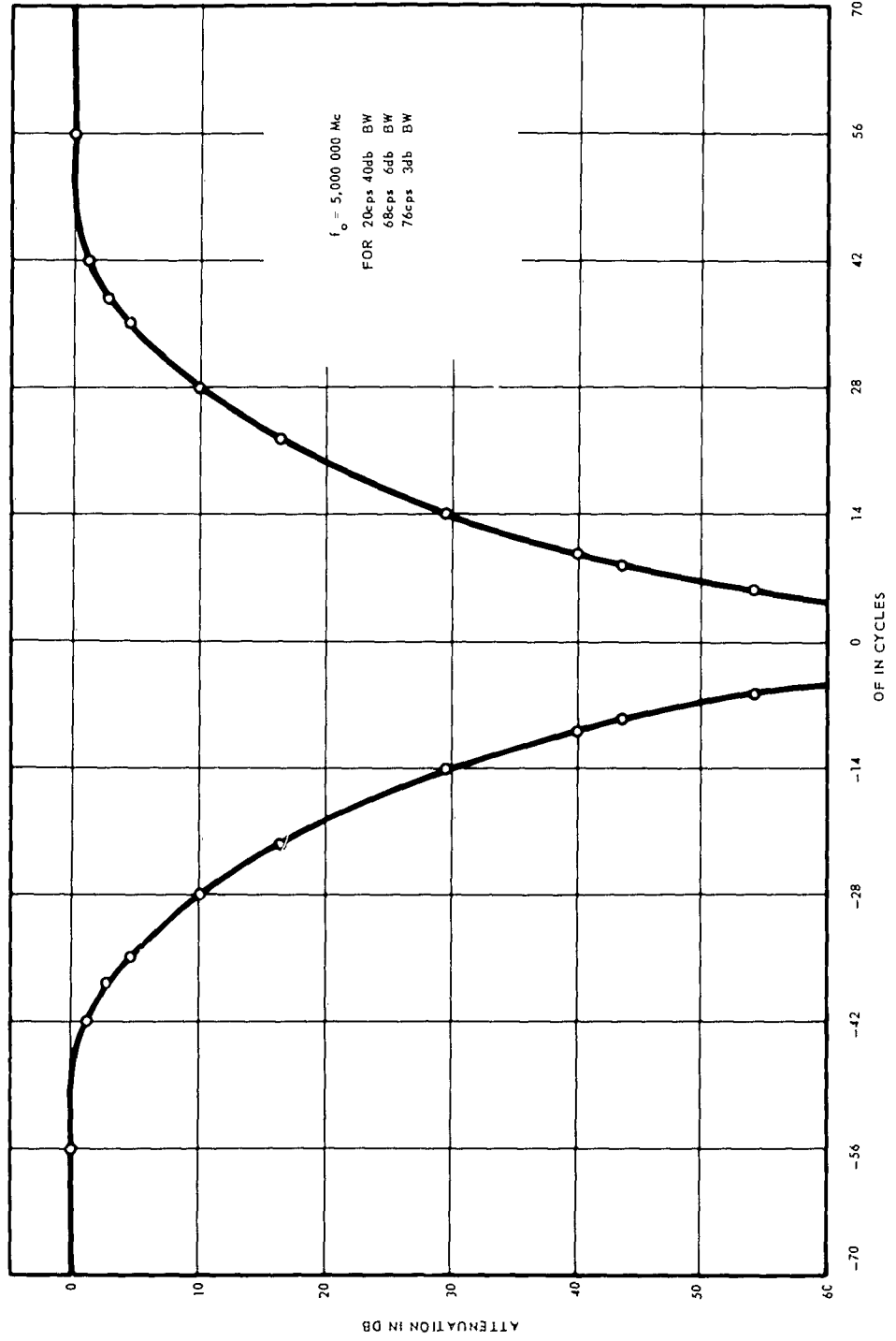


Figure 3-6 Band Reject Filter Response



**Figure 3-7 Limiter-Discriminator Schematic**

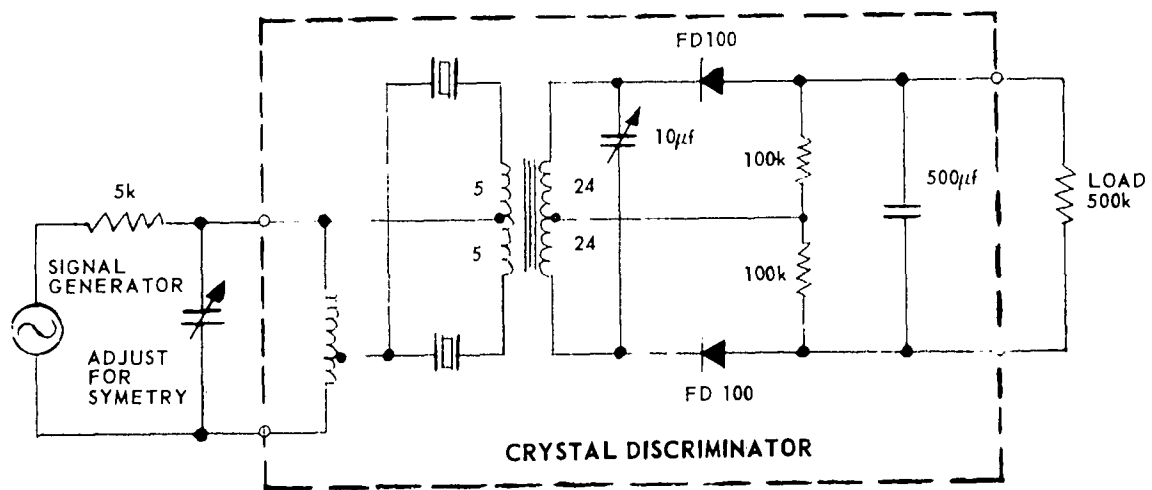


Figure 3-8 Crystal Discriminator

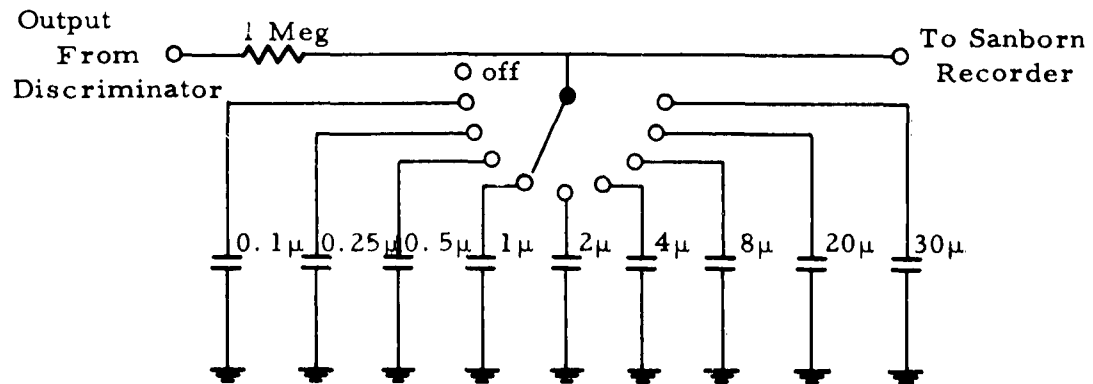


Figure 3-9 Integrator

in 25-Mc tuned circuits, passed through a 5-Mc twin-T rejection filter, amplified in another 25-Mc tuned circuit and impedance matched to the output with a cathode follower.

### 3.2.5 6X Multiplier

The schematic diagram for the 6X multiplier is shown in Figure 3-11 below. The 5-Mc input signal is obtained from the  $10^{-9}$  stable oscillator, amplified, distorted to produce a sixth harmonic, filtered and amplified in 30-Mc tuned circuits, passed through a 5-Mc twin-T rejection filter, amplified in another 30 Mc tuned circuit, and impedanced matched to the output with a cathode follower.

### 3.2.6 Target Oscillator

The target oscillator is a crystal oscillator that is swept in frequency by a motor driven trimmer capacitor as shown in Figure 3-12 below. The speed of the 2 rpm drive motor is controlled by the variac. Manual frequency control of the oscillator is obtained by adjusting a second trimming capacitor. The manual control is also used to select the center of the swept frequency range.

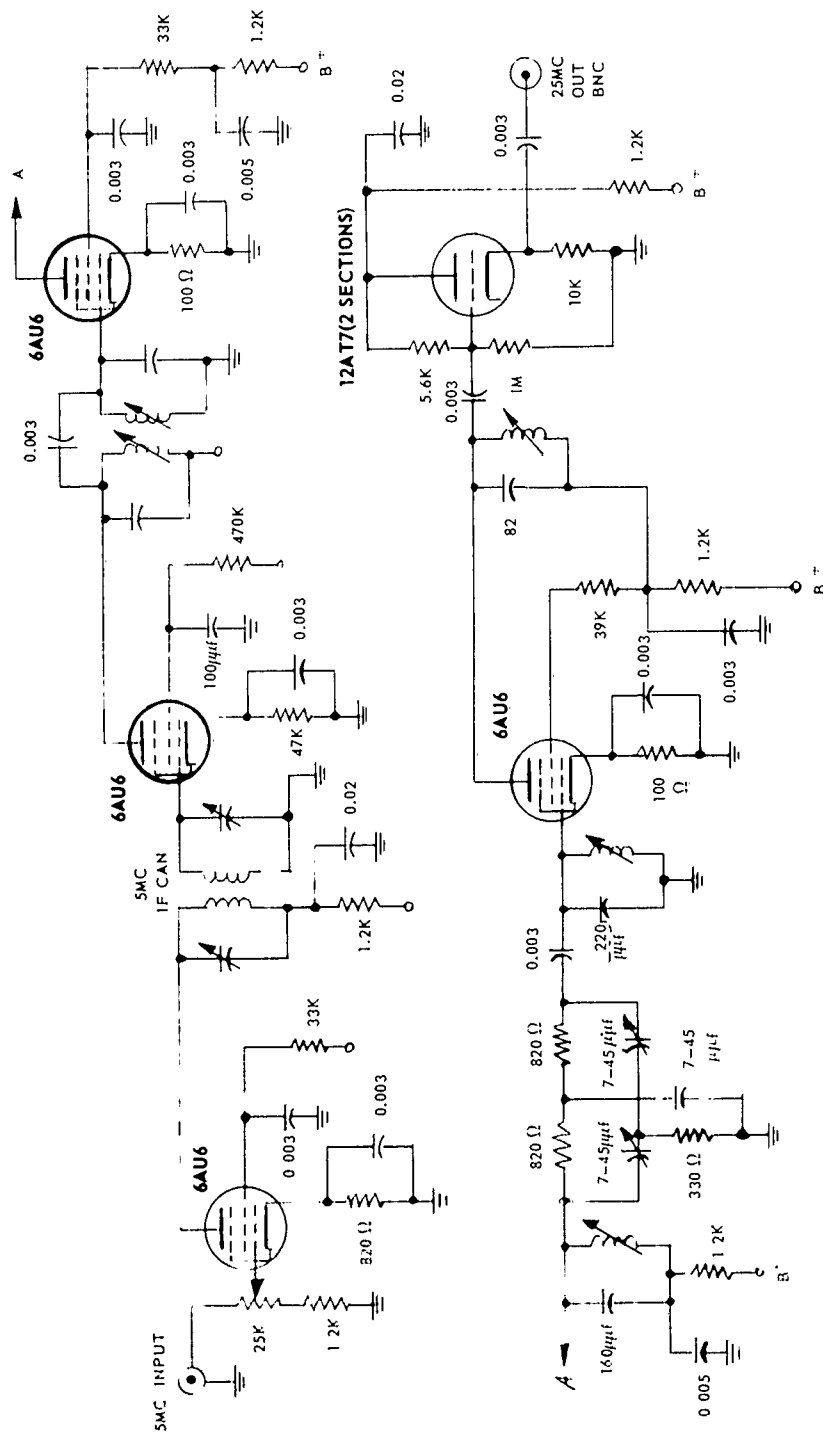


Figure 3-10 25 McMultiplier

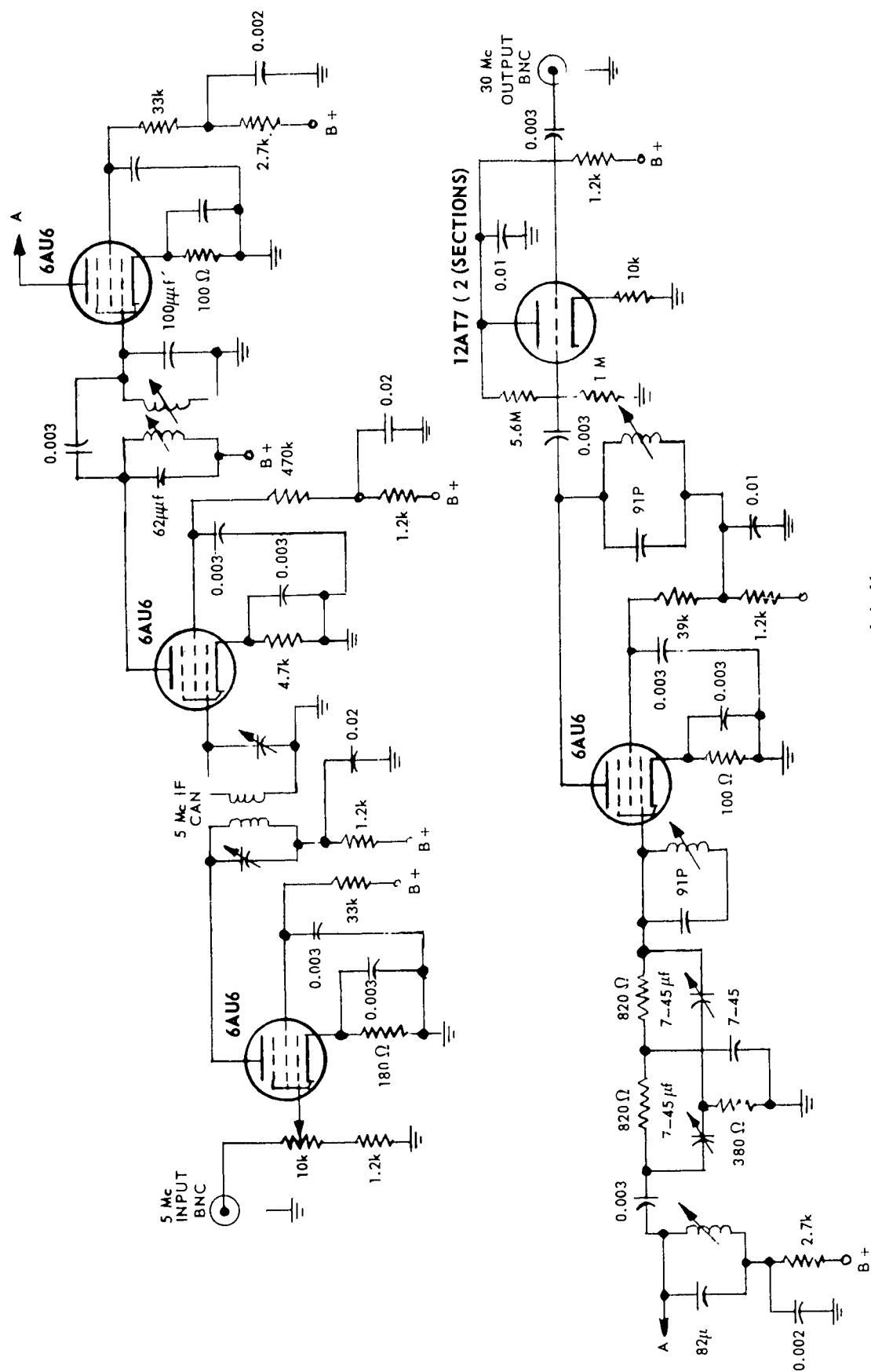


Figure 3-11 30 McMultiplier

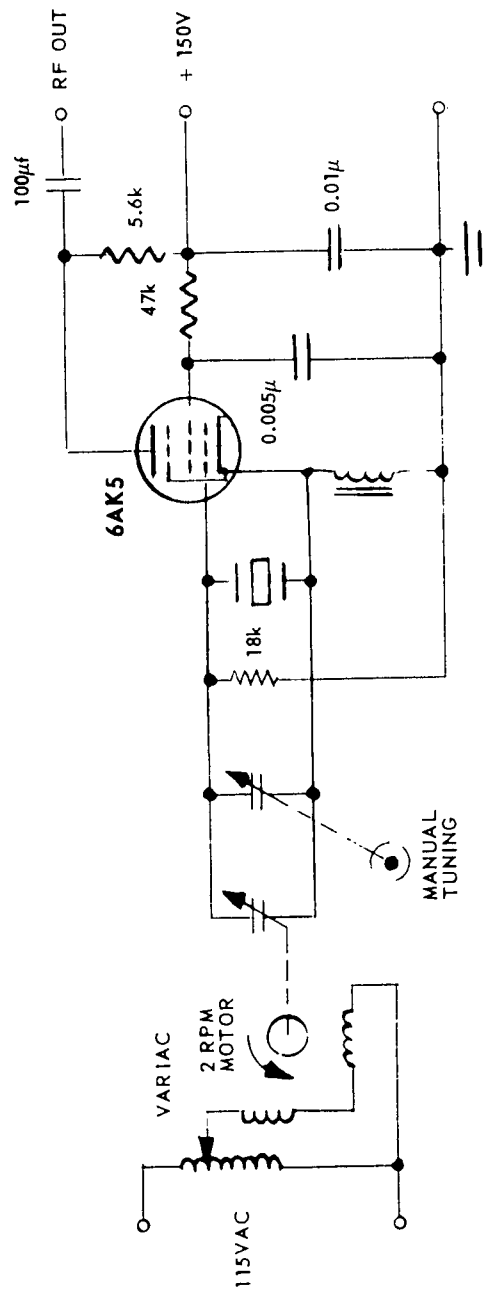


Figure 3-12 Target Oscillator

### 3.2.7 Receive-Test Selector Switch

The receive-test selector switch is used to conveniently select the desired signal input to the system. Figure 3-13 shows the diagram and the connections for the four wafers.

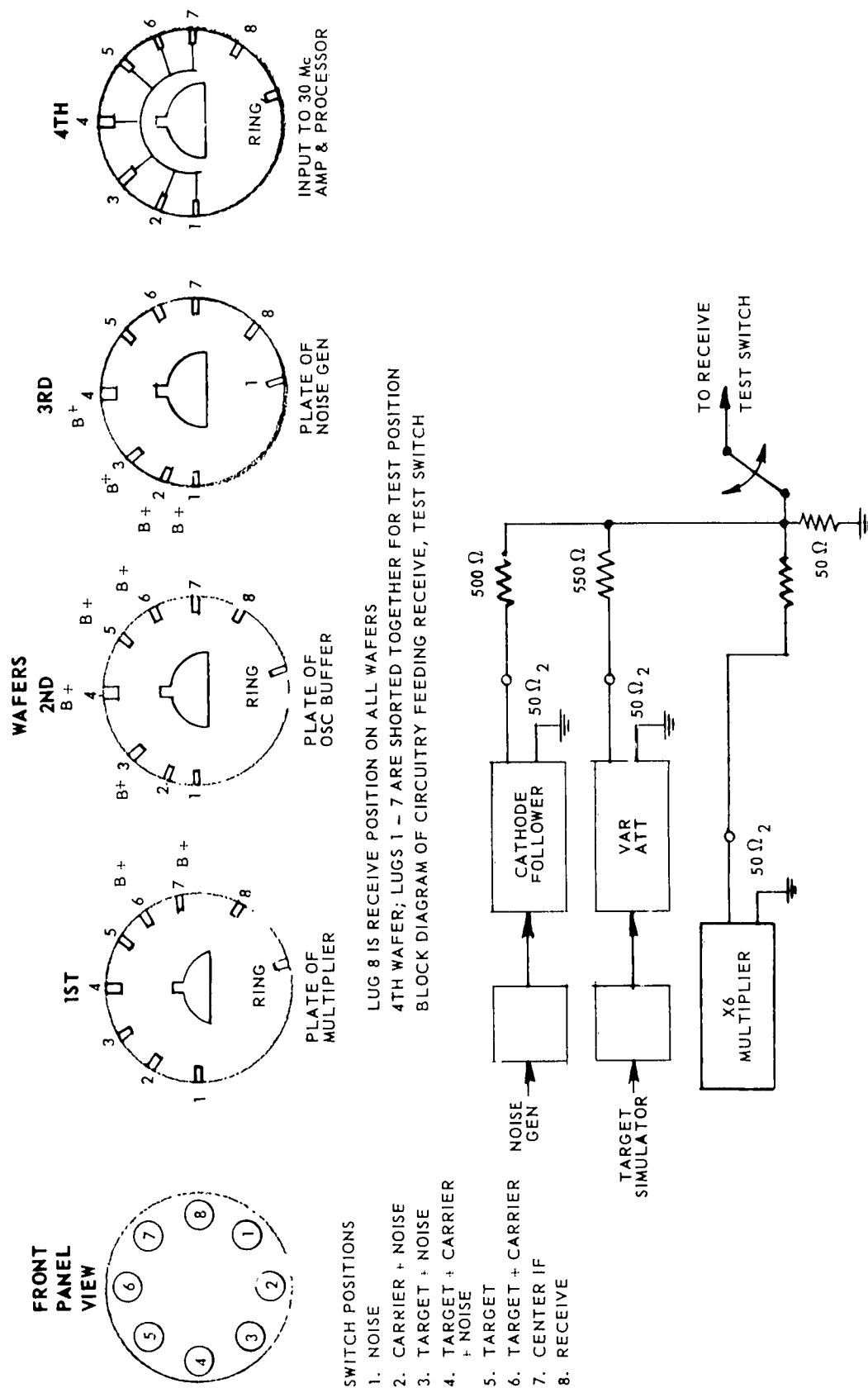


Figure 3-13 Receive Test Switch Schematic

## SECTION 4

### LABORATORY TESTS

The laboratory tests presented here were performed for the complete detection system and for those units that are unique to this system. The procedures for testing the stock units of equipment are presented in the equipment manuals and will not be covered here.

#### 4.1 MIXER, 5-Mc AMPLIFIER, AND NOTCH FILTER CHASSIS

This chassis contains a mixer to convert the 30-Mc input signal to 5 Mc, a 5-Mc buffer amplifier to isolate the first notch filter from the mixer, AGC and overload protection for each filter, a 40-db amplifier between the two filters, and a cathode follower output as shown in the block diagram of Figure 4-1 below. The schematic diagram is shown in Figures 3-3 and 3-4 above.

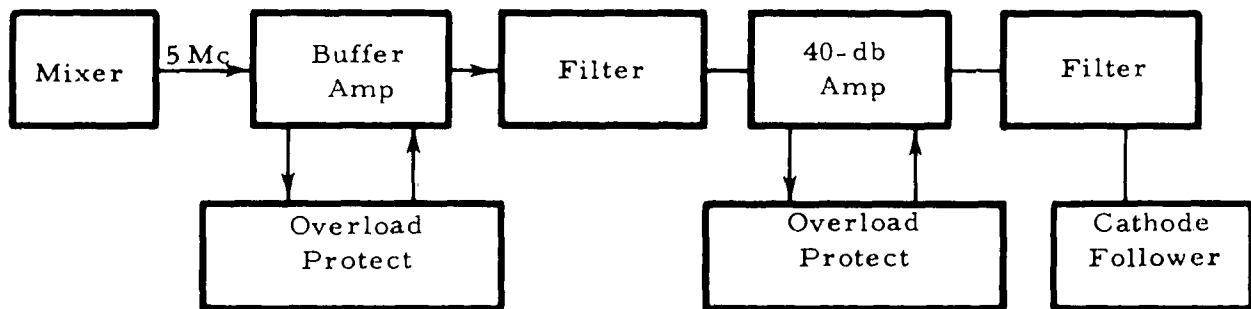


Figure 4-1 Block Diagram of Mixer, Amplifier, and Notch Filter

The unit was partially tested without the filters to determine the gain and bandwidth for both the buffer amplifier and the 40-db amplifier. The available gain was sufficient to obtain limiting on receiver input noise and the bandwidth was very wide compared to the bandwidth of the limiter-discriminator.

The unit was then tested with one filter to determine the band reject characteristics of the filter in its circuitry. The test configuration is shown in Figure 4-2 and the filter characteristics that were obtained from the manufacturer are shown in Figures 4-3 and 4-4. The response curve for the first filter was verified in the lab before the field test. The second filter was rejected before the field test and was not returned by the manufacturer until after the conclusion of the field test.

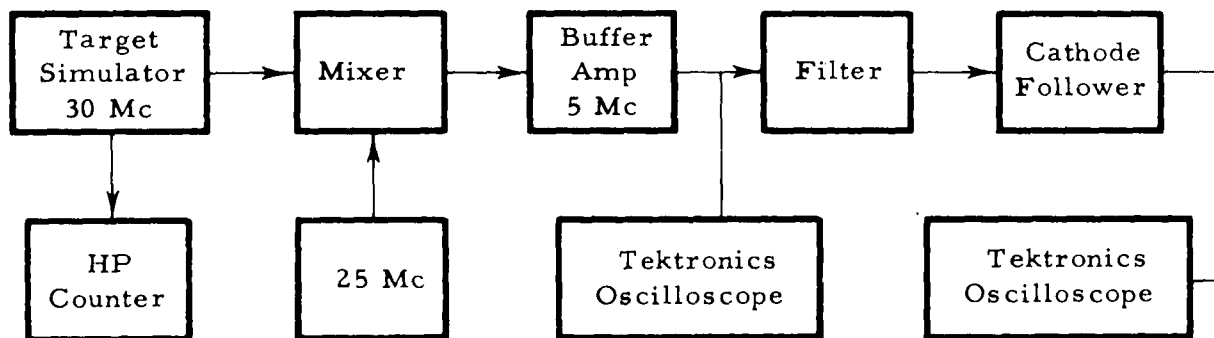


Figure 4-2 Amplifier-Notch Filter Chassis Test Configuration

#### 4.2 LIMITER-DISCRIMINATOR CHASSIS

The chassis contains an amplifier with approximately 60 db of gain, a two stage wide-band limiter and a narrow-band discriminator. The schematic diagram was shown in Figure 3-7. Measurement tests performed on this chassis determined that the amplifier-limiter bandwidth for signals below the limiter threshold is between 25 and 28 kc. The inaccuracy of the bandwidth measurement is caused by the lack of a highly-stable signal generator that can be varied over this frequency range. Oscilloscope photographs of the swept bandwidth for a limited and an unlimited signal are shown in Figure 4-5 below.

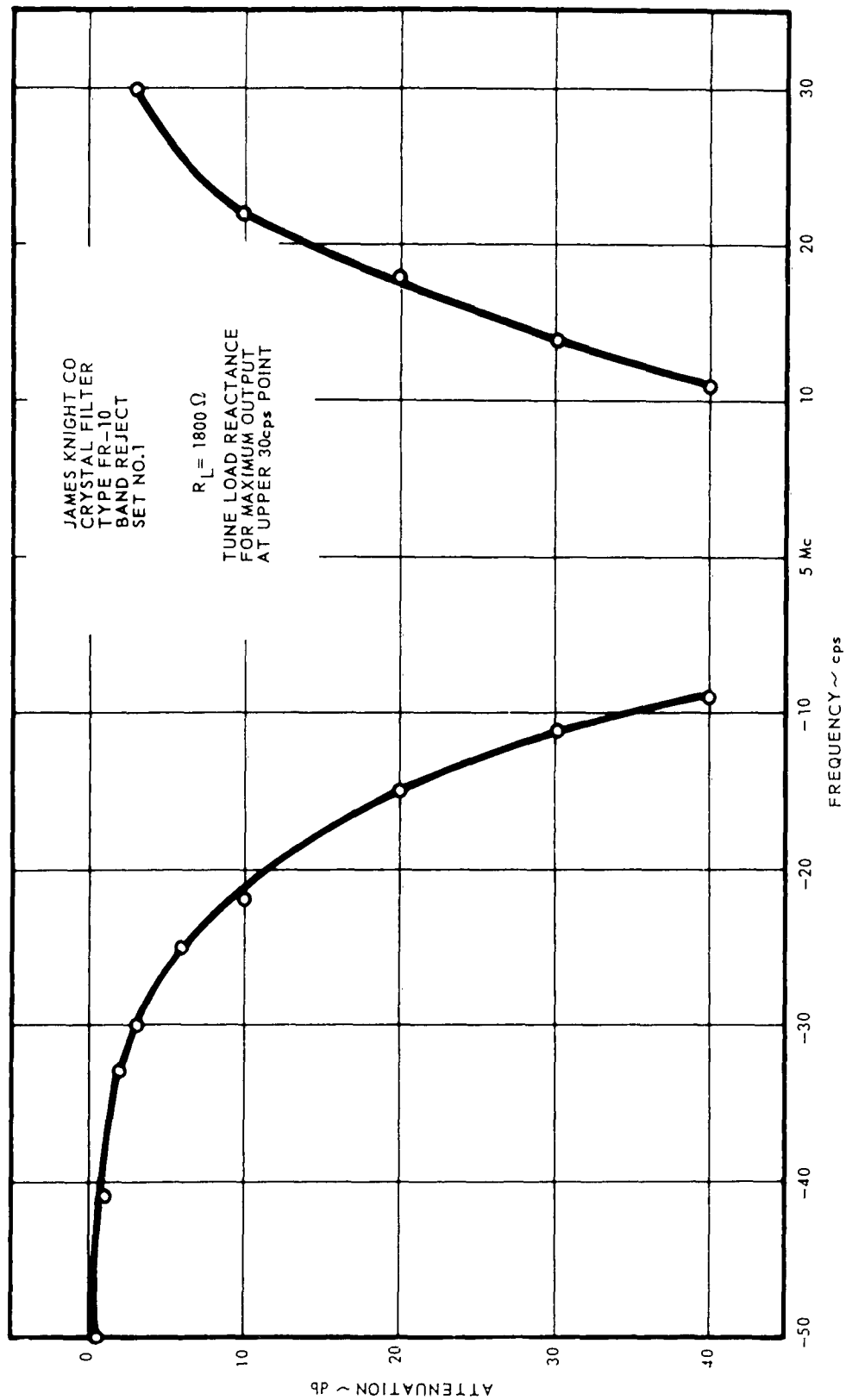


Figure 4-3 Frequency Response Curve-Filter No. 1

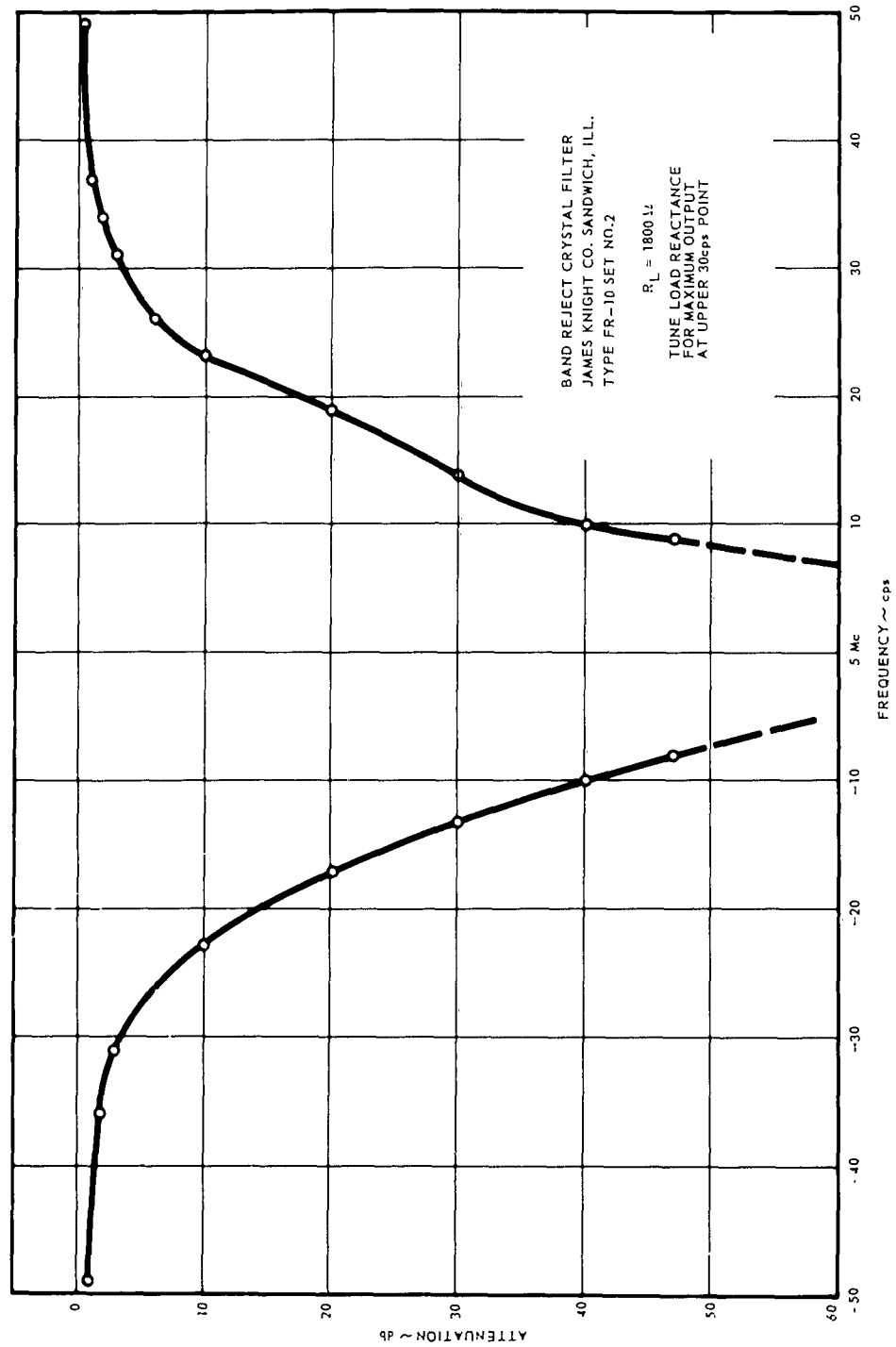
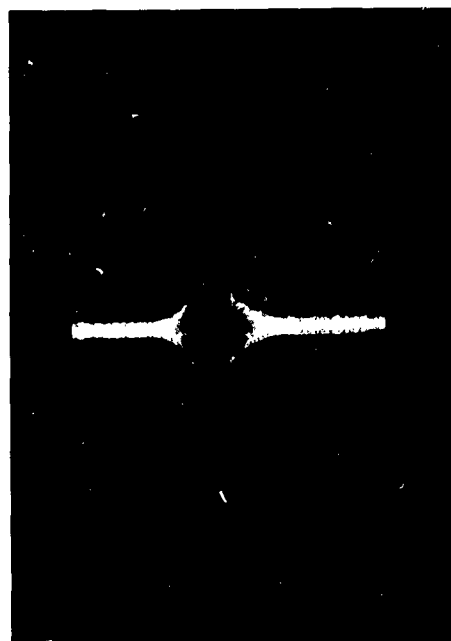
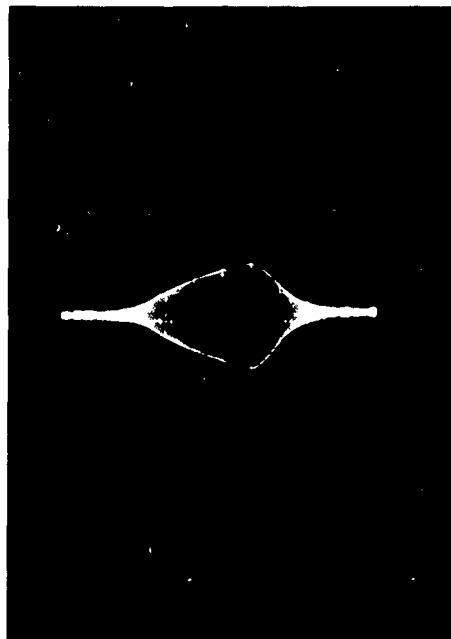


Figure 4-4 Frequency Response Curve—Filter No. 2



UNLIMITED NOISE  
 25 Kc/div SWEEP RATE  
 0.05 V/div VERTICAL  
 0.5msec/div SWEEP  
 3 $\mu$  V INPUT



LIMITED NOISE  
 25 Kc/div SWEEP RATE  
 0.1 V/div VERTICAL  
 0.5msec/div SWEEP  
 100 $\mu$  V INPUT

Figure 4-5 Limiter-Discriminator Swept Frequency Response

The strong signal discriminator characteristic curve was also obtained in a conventional manner except that an extremely stable signal generator was required and had to be monitored continuously during the measurements. The data points near the center of the discriminator (zero volts out) were the most difficult to obtain accurately. The response curve as obtained immediately after receipt of the discriminator is shown in Figure 4-6.

The capture ratio was obtained by simultaneously injecting a strong 5-Mc constant amplitude signal and a controlled amplitude signal at a variable frequency of  $5 \text{ Mc} \pm \Delta f$  (where  $\Delta f < 150 \text{ cps}$ ). The capture ratio was 65 db when the 5-Mc signal was at the center of the discriminator and no noise was present.

#### 4.3 OVERALL SYSTEM TEST

The overall system test was conducted in a conventional manner with the very stable 806-Mc signal generator that was obtained by modifying the FRC-45 Ratio Frequency Oscillator.

The overall system response curve, shown in Figure 4-7, was obtained by varying the input frequency over the range of  $806 \text{ Mc} \pm 280 \text{ cps}$ . The discriminator output voltage was obtained by a G. R. Electrometer due to the nonlinearity of the Sanborn DC Recorder.

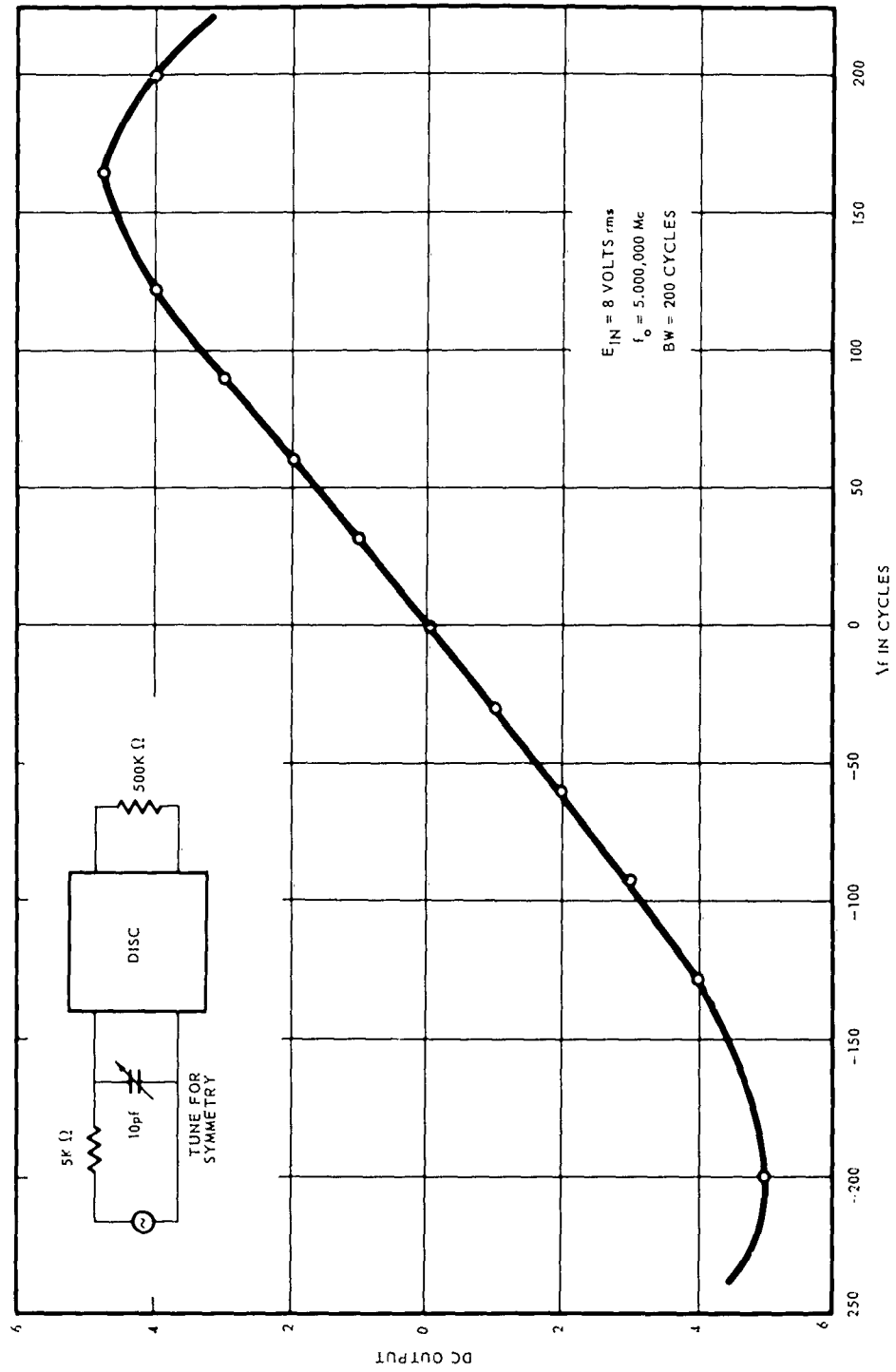


Figure 4-6 Discriminator Response

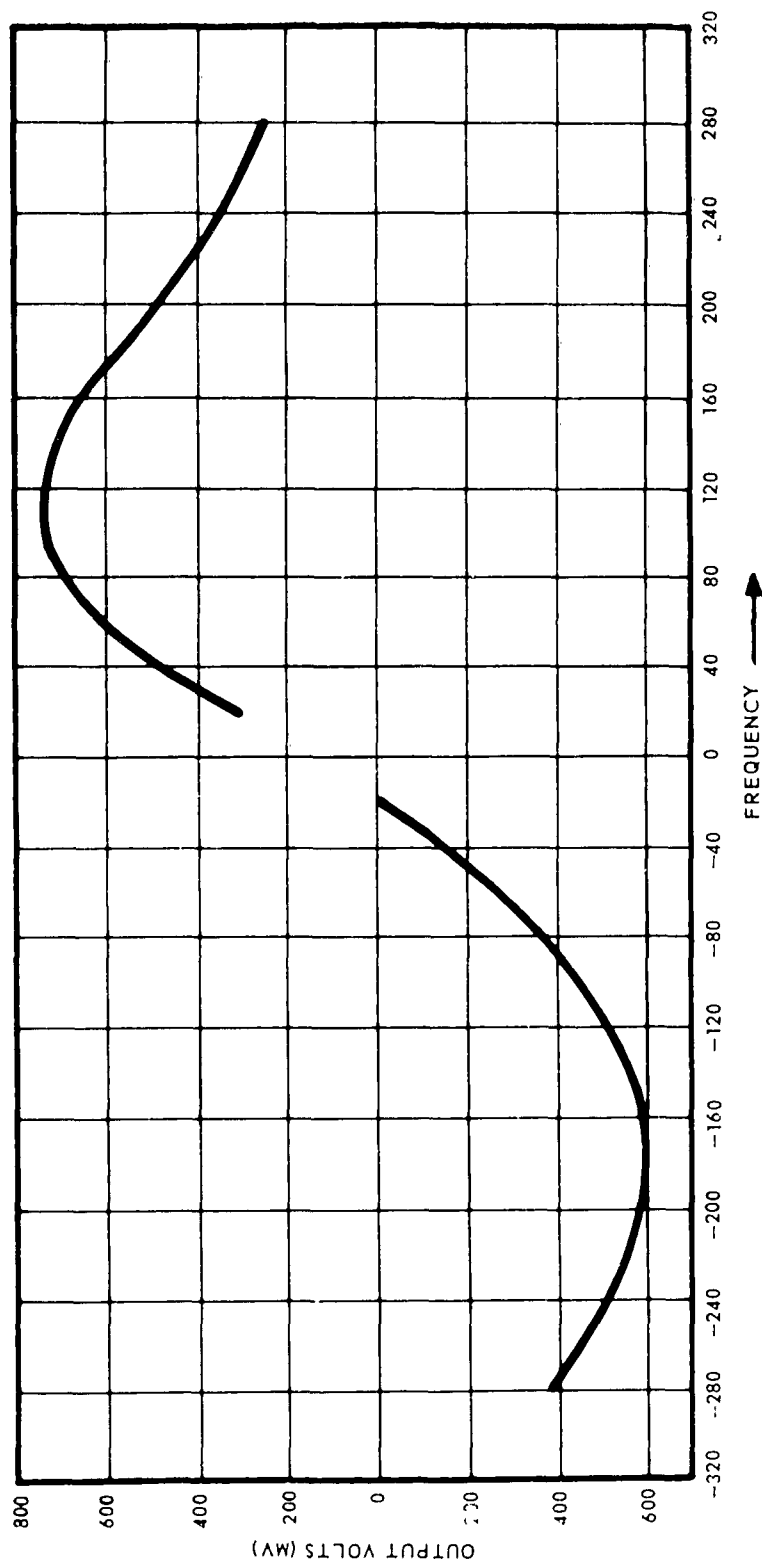


Figure 4-7 Discriminator Curve

## SECTION 5

### FIELD TESTS

#### 5.1 FIELD TEST LOCATION

The site chosen for the field test was the DEW line training link (operated by Federal Electric Corporation) in north-central Illinois with terminals west of Rockford and southwest of Streator. This site was chosen because of the availability of casual air traffic and the knowledge of link parameters that had been gained during previous tests.

Federal Electric Corporation personnel indicated their interest and their willingness to aid in expediting the field test, with the understanding that the tests be conducted and the facilities be used on a non-interference basis with their training program. This stipulation produced no hardships since the Domestic Auxiliary Station (DAS) west of Rockford was not being used in the training program and the installation of the modified FRC-45 Radio Frequency Oscillator at the Domestic Main Site (DMS) southwest of Streator did not interfere with the normal training operations there. The 1-kw transmitter at Streator was used to supply the tropo-scatter signal which was received at the DAS.

Upon completion of final laboratory tests, the equipment was dismantled on 1 November and placed aboard a truck; it was driven to the DAS at Seward on 2 November and was reassembled on 3 November. The FRC-45 Radio Frequency Oscillator was taken to the Streator site and installed in place of the regular unit there. Initial system checkout was completed by 4 November and the equipment was operated continually until 30 November with the exception of the Thanksgiving weekend. On 30 November the equipment was dismantled and prepared for shipment back to Ann Arbor on 1 December. The FRC-45 Radio Frequency Oscillator was removed from the Streator site on 1 December, thereby completing the field test operation.

#### 5.2 EQUIPMENT PERFORMANCE

The receiver equipment performed satisfactorily with the exception of the discriminator. The center frequency was  $5 \text{ Mc} \pm 0 \text{ cps}$  when the discriminator was first received from the manufacturer and one month later

it had become 5 Mc - 13 cps. After the first week of the field tests the center frequency had changed to 5 Mc - 29 cps where it remained for the duration of the test. The offset discriminator caused an increase in the noise output due to the resulting noise unbalance and an increase in output voltage due to the carrier. The noise output was further increased by the presence of the notch filter which is centered about 5 Mc and therefore offset with respect to the center of the discriminator.

The system block diagrams show the AM detection system which consist of an IF amplifier, a spectrum analyzer, and a display. The AM detection system was changed after a few days of operation because the Alfax display unit was causing interference on the FM and the AM system. This interference was caused by the normal arcing in the Alfax recorder. The AM detection system that was adopted is as sensitive for detection purposes but yields little information about the spectrum of the target signal above 10 cps. This AM envelope detection is shown in Figure 5-1.

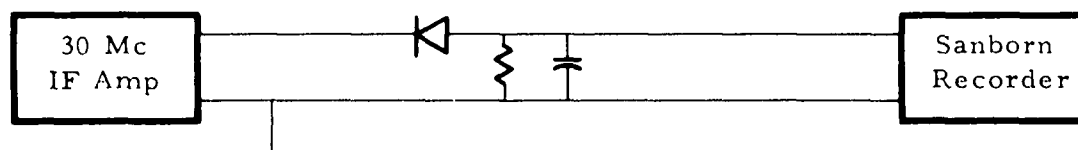


Figure 5-1 AM Envelope Detector

The 1 kw klystron transmitter was suspected of being frequency modulated at a 120 cps rate. It is well known that a klystron amplifier will be frequency modulated by the ripple voltage that is present in the power supply. The following observations support the klystron frequency modulation theory and there were no observations made that would disprove the theory. A definite conclusion could have been made if a very narrow-band spectrum analyzer had been available and a spectrum analysis had been made of the transmitter signal at the transmitter site. It was observed, after three weeks of operations, that there existed a correlation between target detections and the amount of suppression voltage required on the DC preamplifier of the Sanborn recorder. During the times when detections were made, the suppression was small; it was 5 to 6 times greater at other times. A carrier

sweeping an unbalanced discriminator will produce a DC voltage when integrated, and the DC voltage will be proportional to the frequency deviation of the carrier. Following the discovery of this correlation, the equipment was carefully observed to determine if the theory could be disproved; however, all observations supported the theory. The second observation was that the carrier signal level at the output of the notch filter, as observed on the Tektronix oscilloscope, contained a signal that was sweeping through the notch filter at a 120 cps rate. During the time when target detections were observed, the sweeping did not cause the carrier to be out of the notch filter during the majority of the time (e.g. the frequency deviation of the carrier was small although the carrier was being swept at the same 120 cps rate) as it did during times of no target detections. The discriminator was used to obtain the third observation of frequency modulation by removing the integration and observing the sweeping rate at very large amplitudes compared to the DC level. Inquiries were made into the percentage of ripple voltage on the klystron power supplies but no answers were obtained because no one at the transmitter site had ever measured it and the transmitter specifications did not list it. This was not surprising since the observed frequency deviations were of the order of 200 cps and therefore would not degrade the communications link to any appreciable extent.

During the field tests, the receiving equipment was self tested with the target simulator and always functioned properly with the exception of the discriminator offset mentioned above. The oscillator in the FRC-45 Radio Frequency Oscillator was tested before field tests and did not have frequency modulation. A tropo scatter signal contains both AM and FM but the observed frequency modulation of the carrier signal was an order of magnitude greater than that which is normally expected. Also, there were target detection periods in the early afternoon when signal fading and therefore, frequency modulation are greatest.

### 5.3 FIELD TEST RESULTS

Part of the time, targets were detected on the FM channel that were comparable to or better than, those detected on the AM channel; but during other periods of time there were only a few poor FM detections. The reason for this has been postulated above, along with supporting observations; however, final proof in the form of a spectrum analysis was not obtained because of the lack of a very narrow band spectrum analyzer.

Good detections were obtained when all equipment was operating satisfactorily. Tests of the receiving equipment by use of the Target Simulator indicated that the equipment was performing as designed with the exception of the discriminator zero offset. The discriminator offset of 29 cps caused all target crossings with doppler frequencies of less than 29 cps to have only positive voltage and therefore no negative-going-to-zero-to-positive S-curve. The target doppler frequencies that were observed for the great majority of crossings were lower than those anticipated. Very few crossings had doppler frequencies greater than 40 cps. During the daylight hours and early evening, the target crossings were very frequent, in fact, there were many times when two or three targets would be present in the beam at the same time.

A representative sampling of the many target crossings that were obtained are presented below. For the majority of the crossings presented, the two AM detections and the FM detection are shown. The AM Spectrum Analyzer displays the detections as a function of frequency and time. The low doppler frequencies of the crossings are readily apparent from this display. The AM channel of the Sanborn displays the doppler frequency implicitly as a function of time and is more representative of the power level of the target signal than the Spectrum Analyzer.

Target crossings No. 1, 2, and 3 are shown in Figure 5-2 below. The second target crossed 45 seconds after the first and the third target crossed 15 seconds after the second or 60 seconds after the first. The problem that is caused by more than one target being present in the beam is the inability to separate the effects of any one crossing. For these crossings, the integration time constant was 4 seconds and the zero doppler of the system was  $806 \text{ Mc} - 9 \text{ cps}$ . This zero doppler of  $806 \text{ Mc} - 9 \text{ cps}$  results in a first IF frequency zero doppler of  $30 \text{ Mc} + 9 \text{ cps}$  because the first local oscillator frequency is  $836 \text{ Mc}$  or  $30 \text{ Mc}$  above the carrier frequency. The zero doppler frequency in the second IF is  $5 \text{ Mc} + 9 \text{ cps}$  since the second local oscillator frequency is  $25 \text{ Mc}$ . The sign of the doppler frequency is maintained only in the case where the local oscillator is below the received frequency. Since the zero doppler frequency for these crossings was  $806 \text{ Mc} - 9 \text{ cps}$ , one would not expect to see an FM detection until the doppler frequency has reached  $+4$  to  $+10 \text{ cps}$  due to high attenuation of the target signal when it is in the notch filter. Target crossings No. 1 and No. 2 show that this is indeed what happened. Target crossing No. 3 cannot be interpreted directly because of the effect of target crossing No. 2. Target crossing No. 3 is barely visible on the AM displays.

cps

60

40

20

15

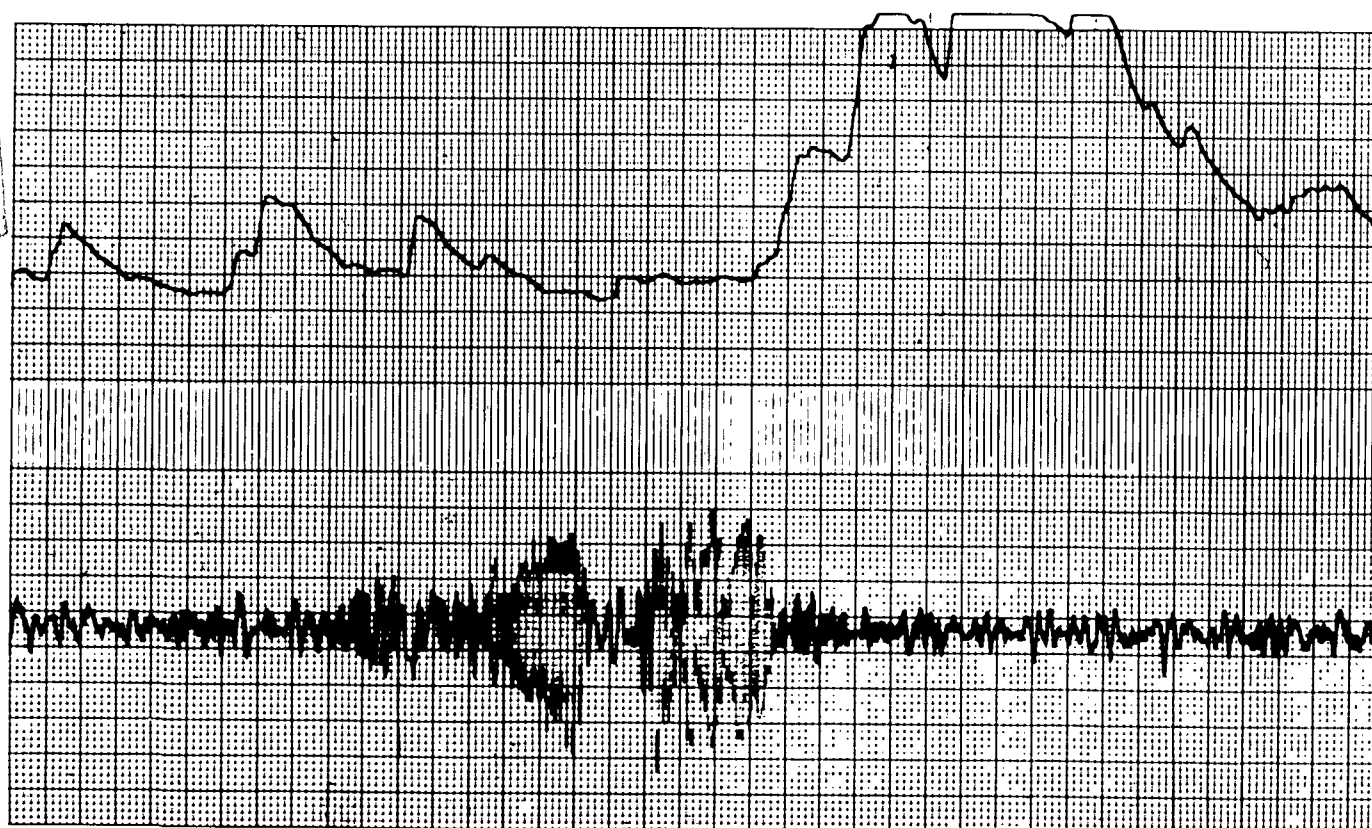
13

12

10



1



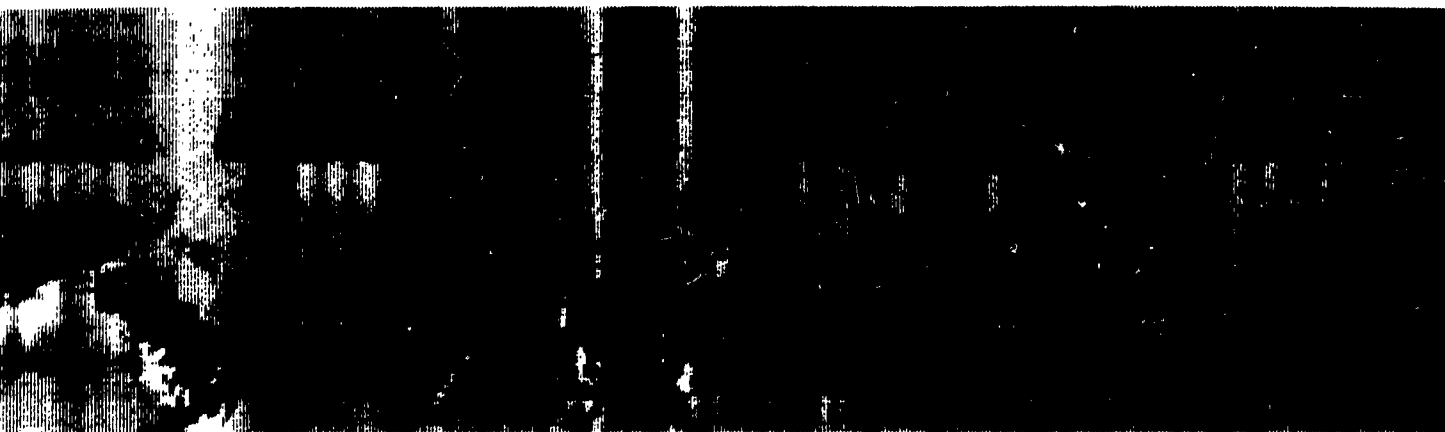
SUPPRESSION -75

ATTENUATION x 10

TC 4 sec

ZERO DOPPLER 806 Mc - 9 cps

PAPER SPEED 2.5 mm/sec



2

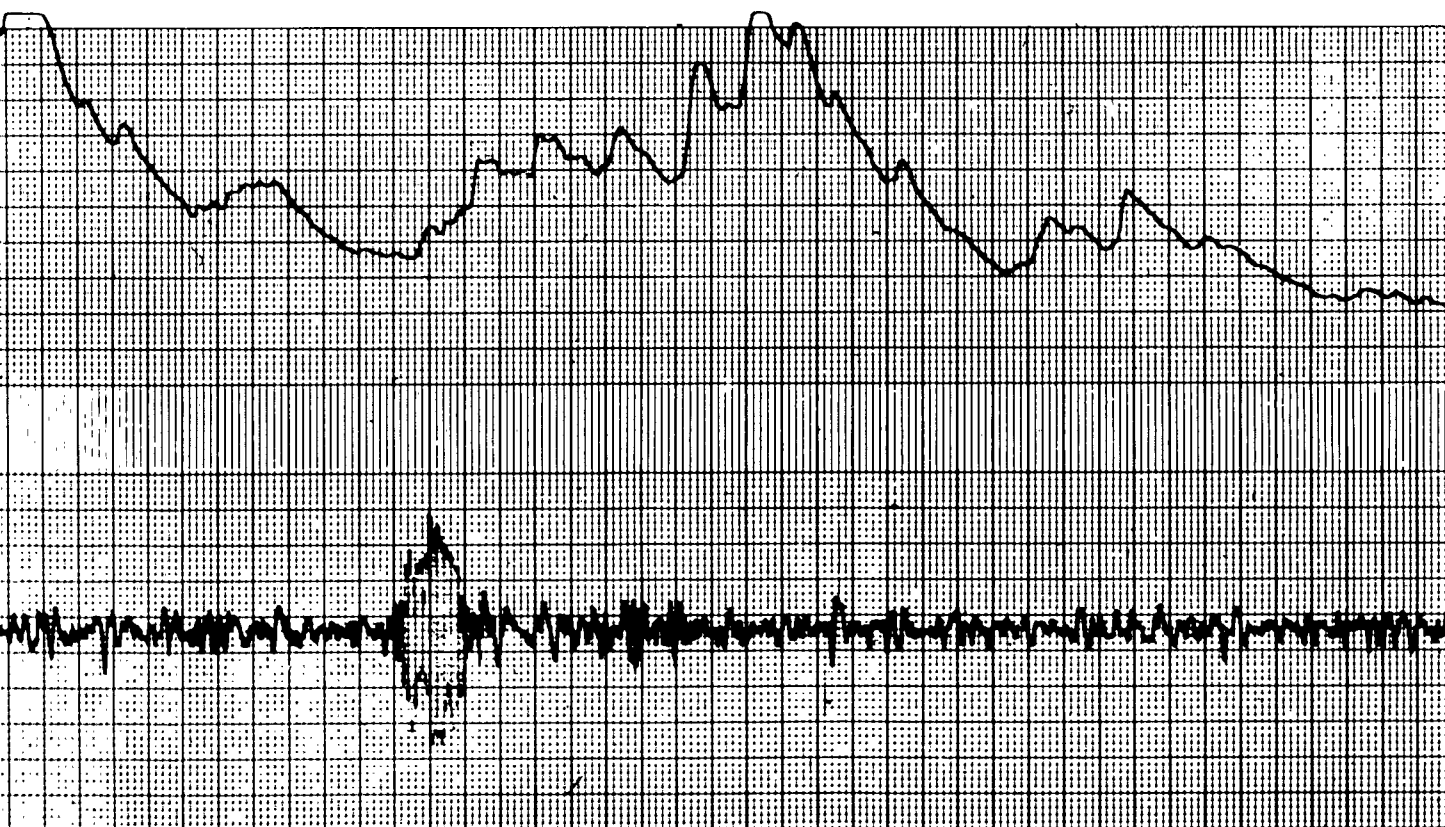


Figure 5-2 Crossings 1, 2, and 3

Target crossings No. 4 and No. 5 are shown in Figure 5-3 below. These targets were marginal detections for the AM system but are easily discerned on the FM system. All settings for target crossings No. 4 and No. 5 were the same as those for target crossings No. 1, 2, and 3.

Target crossings No. 6, No. 7, No. 8, and No. 9 as shown below in Figures 5-4, 5-5 and 5-6 were obtained during a continuous series of crossings that lasted for 6 minutes. The display appears to be fairly clean when target crossing No. 6 appears, but does not clear up again until after target crossing No. 9. This appearance of targets in the beam for long periods of time was quite common during the tests and obscured many crossings. Target crossings No. 7 and No. 8 were high-speed crossings and were observed first on the FM display and then found on the AM display by careful scrutiny. This series of four crossings was obtained with the same settings as the first five crossings.

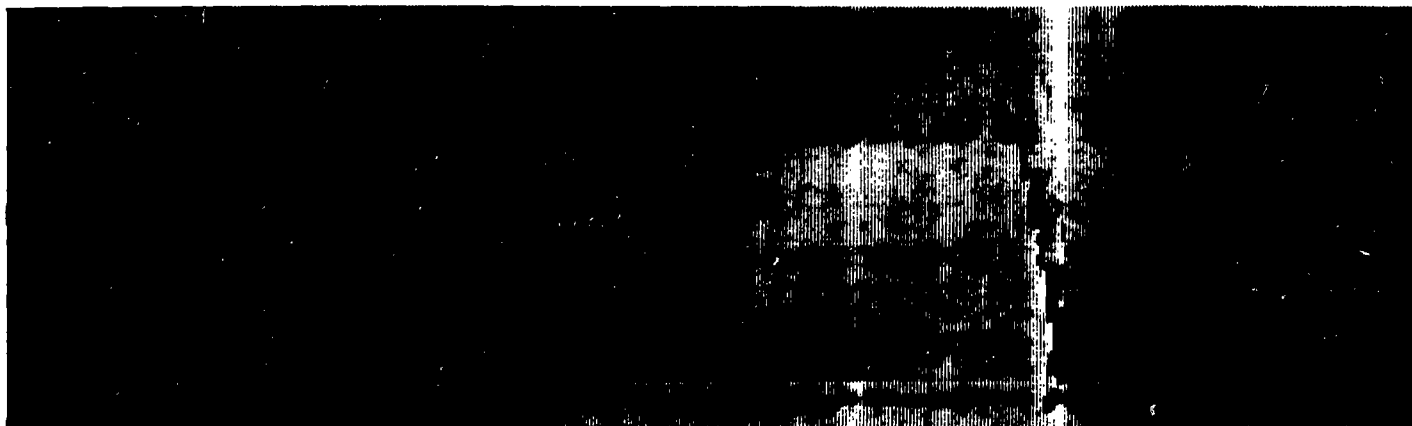
Target crossing No. 10, as shown in Figure 5-7 below, is similar to the previous crossings but has a 10 second integration time constant instead of 4 seconds.

Target crossings No. 11 and No. 12 are shown in Figure 5-8 below. The settings for these crossings are different than those used previously and the detections appear to be much clearer than those previously presented because the fluctuations about the zero frequency point of the quiescent state have been biased out by the suppression voltage of the Sanborn DC preamplifier. Both crossings are distorted and it appears that either the target changed direction in the beam or two targets were present simultaneously; the second target having a low doppler frequency. No spectrum analyzer display is shown since the Spectrum Analyzer was shut down prior to this time because it caused interference on the AM and FM displays.

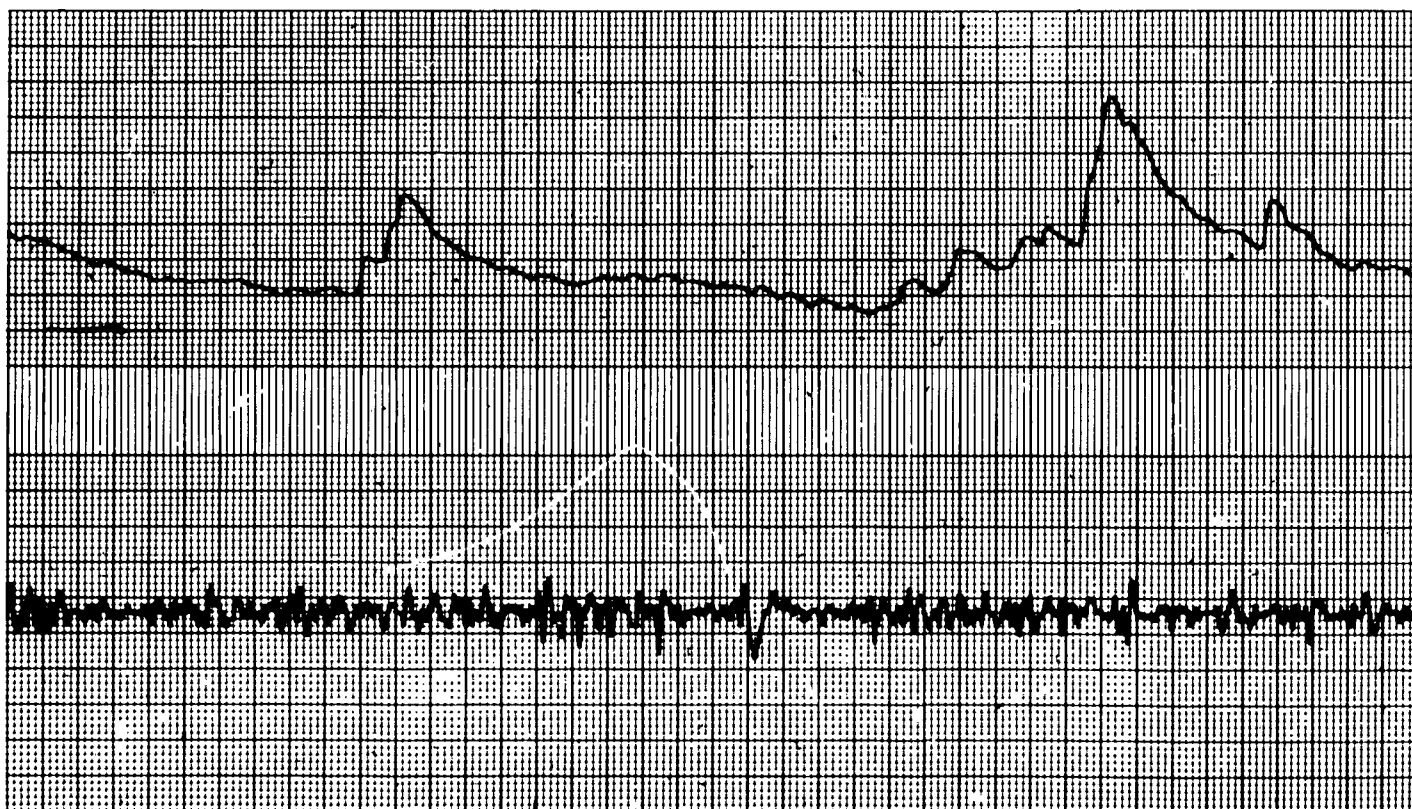
On the day before the field test was completed a series of simulated target crossings were made with the target simulator. In Figures 5-9A through 5-9F only target and carrier were present while in Figures 5-10A through 5-10F target, carrier and receiver noise were present. The transmitter was not operating during this period of time and, therefore, only atmospheric or front end noise was present. This was done to remove the unknown properties of the transmitted carrier signal and also to ensure that no real targets were present to disturb these tests.

60  
40  
20  
15  
13  
12  
10

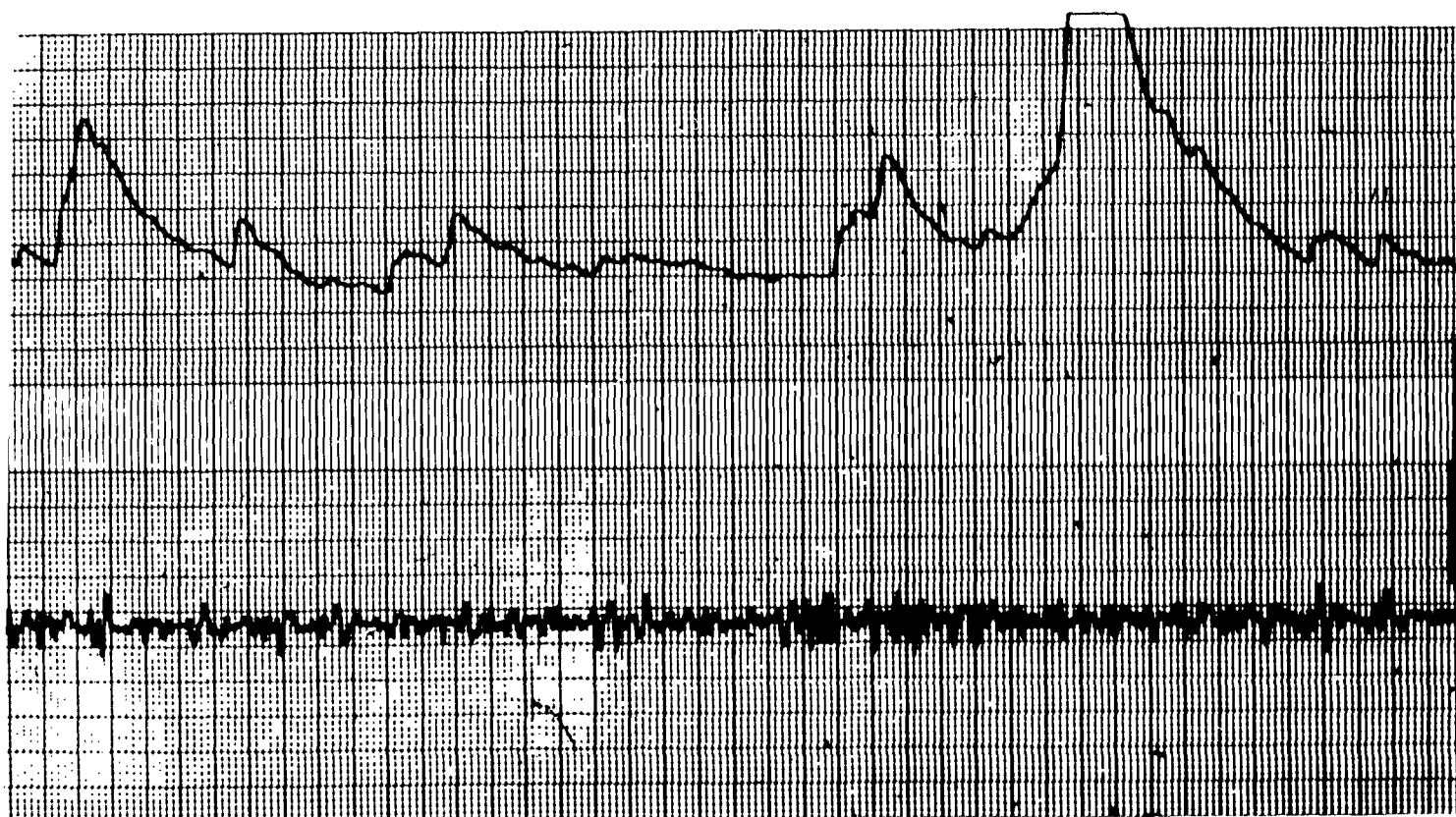
cps



1



SUPPRESSION -75  
ATTENUATION x 10  
TC 4 sec  
ZERO DOPPLER 806 Mc - 9 cps  
PAPER SPEED 2.5 mm/sec

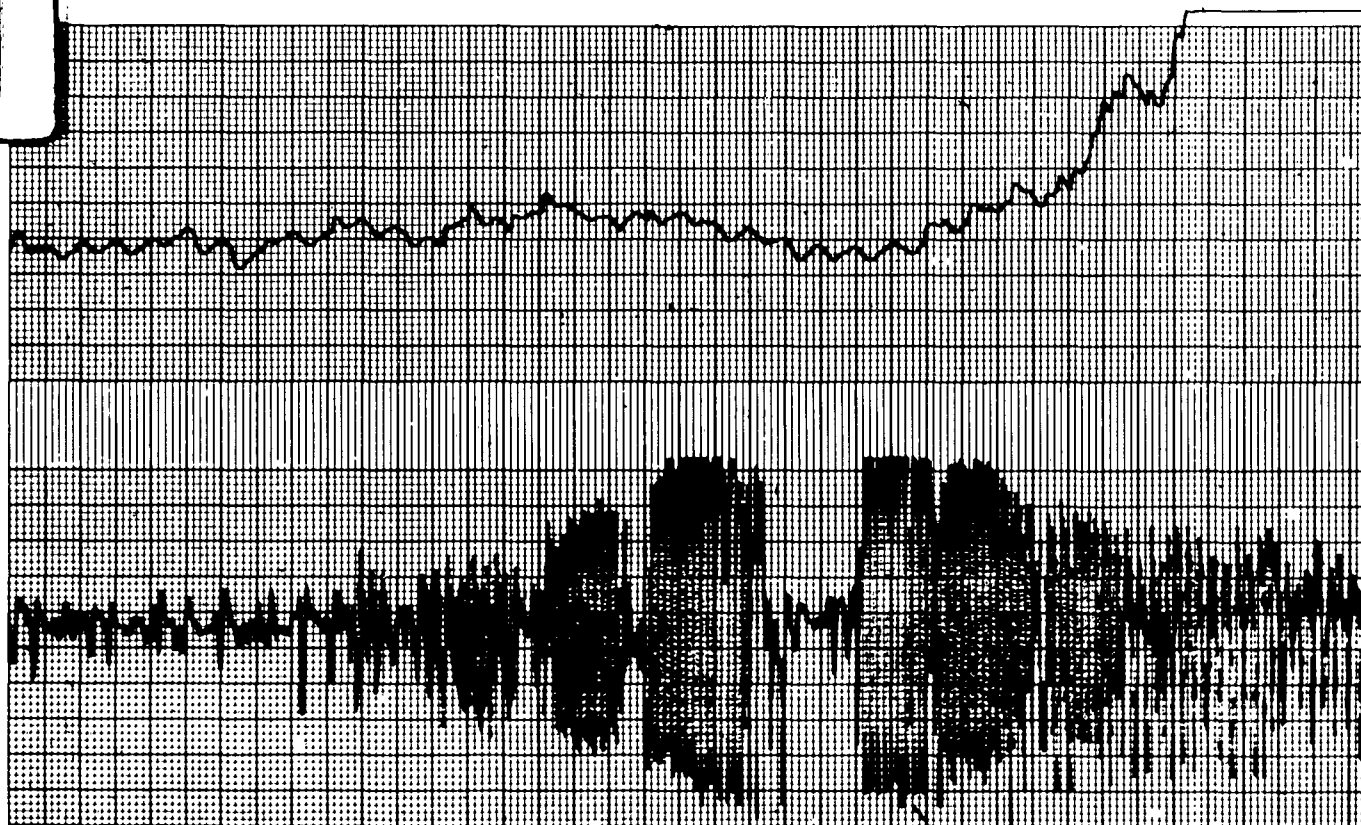


2

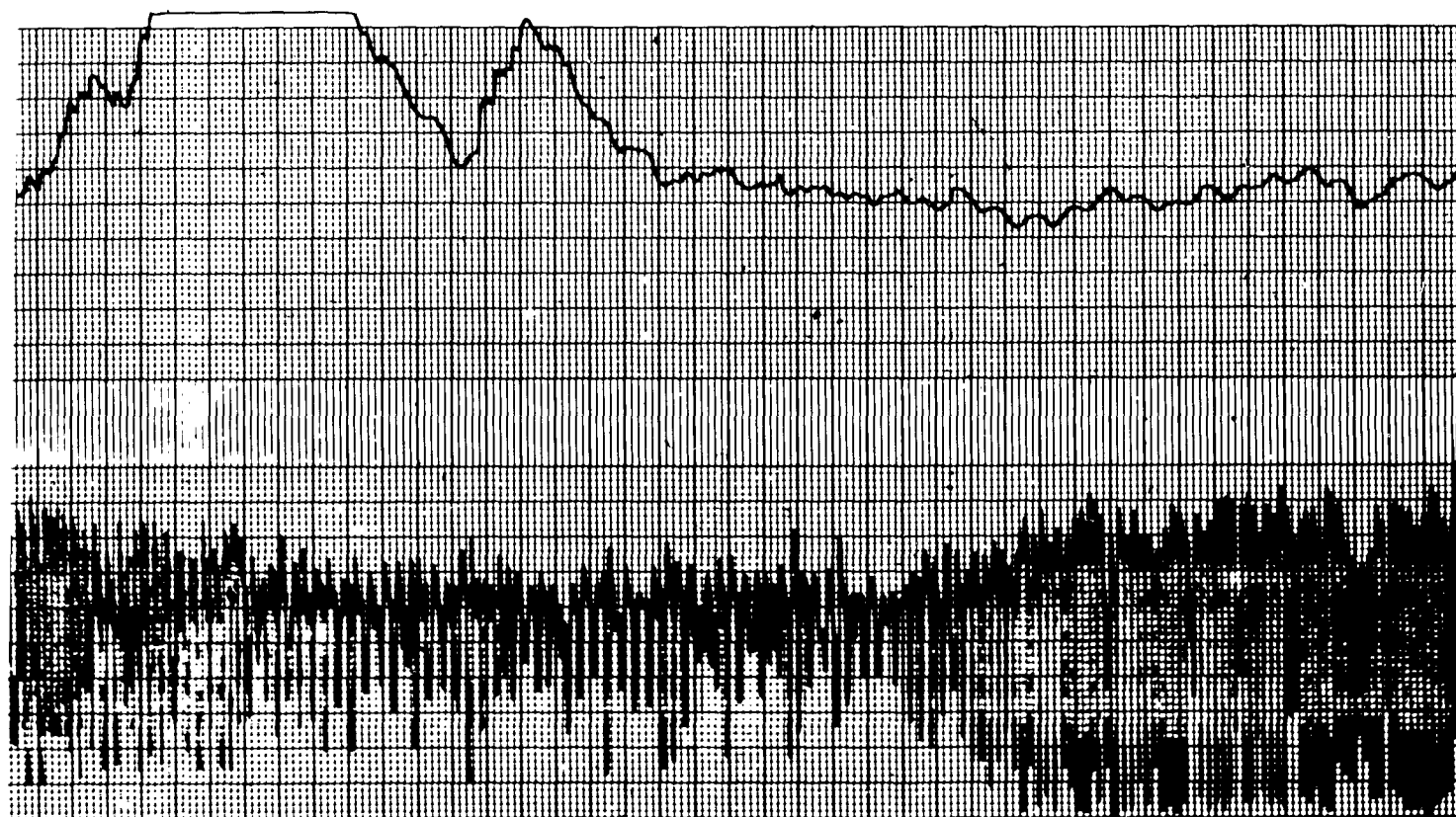
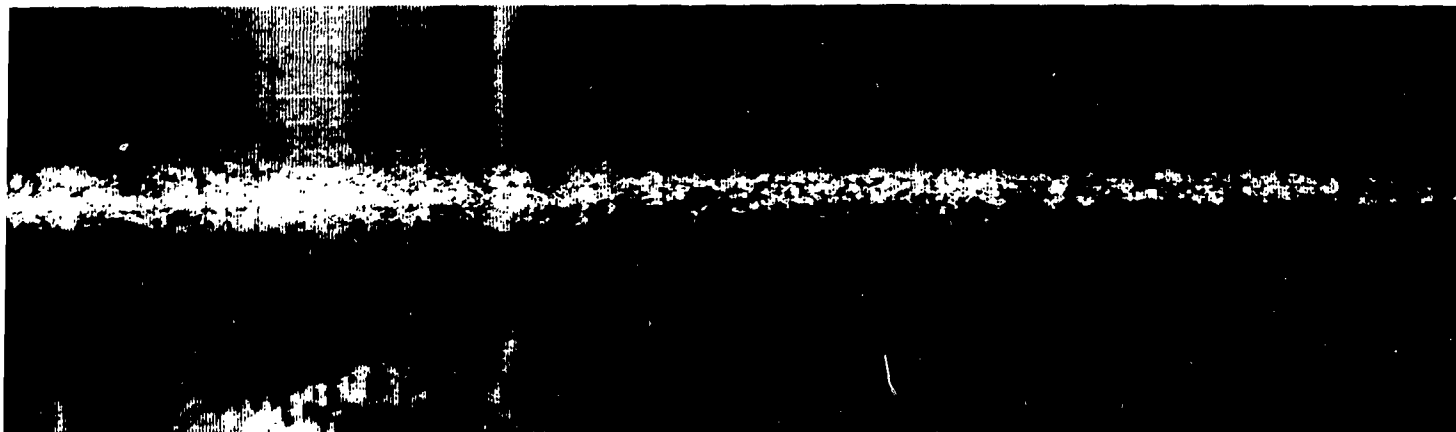
Figure 5-3 Crossings 4 and 5

60  
40  
20  
15  
13  
12  
10

1



SUPPRESSION -75  
ATTENUATION x 10  
TC 4 sec  
ZERO DOPPLER 806 Mc - 9 cps  
PAPER SPEED 2.5 mm/sec



2

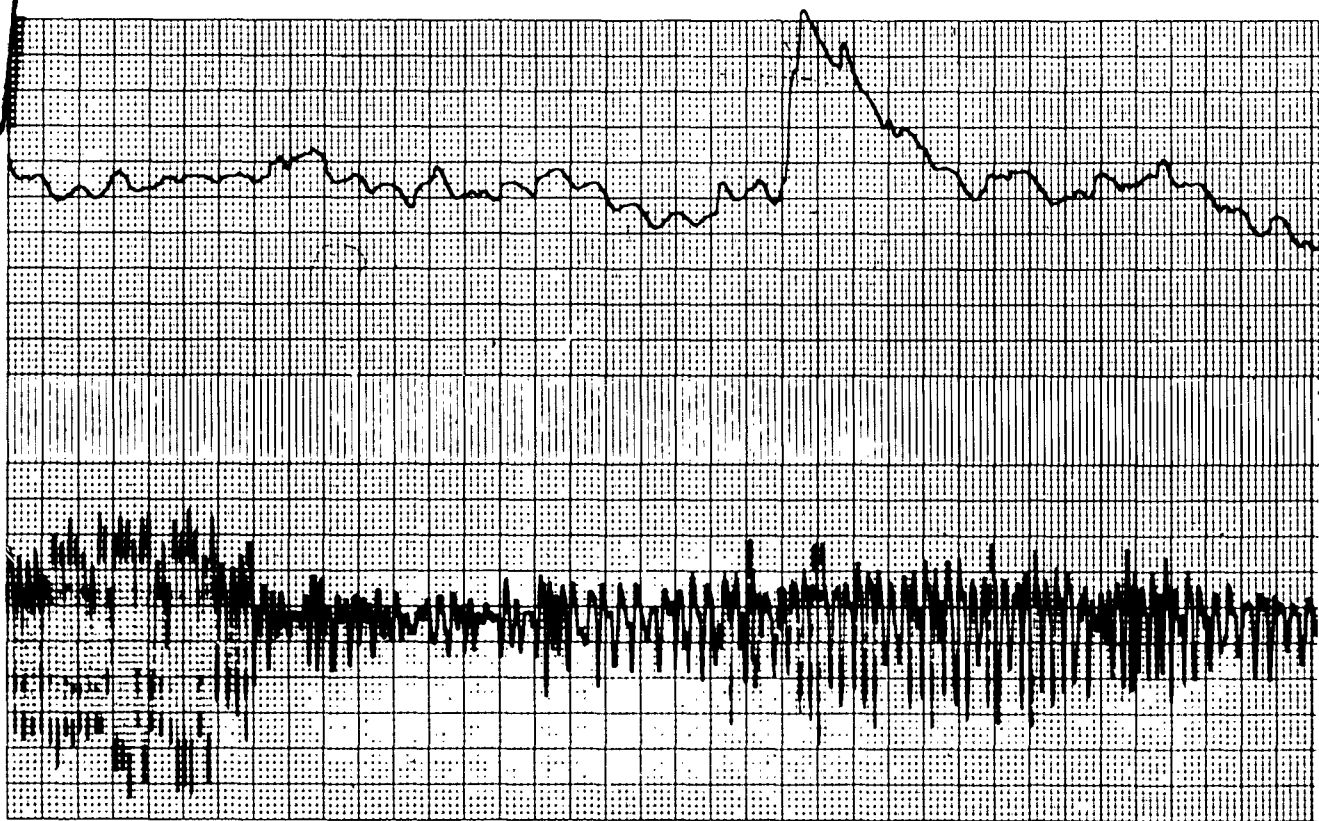
Figure 5-4 Crossings 6 and 7

60  
40  
20  
15  
13  
12  
10

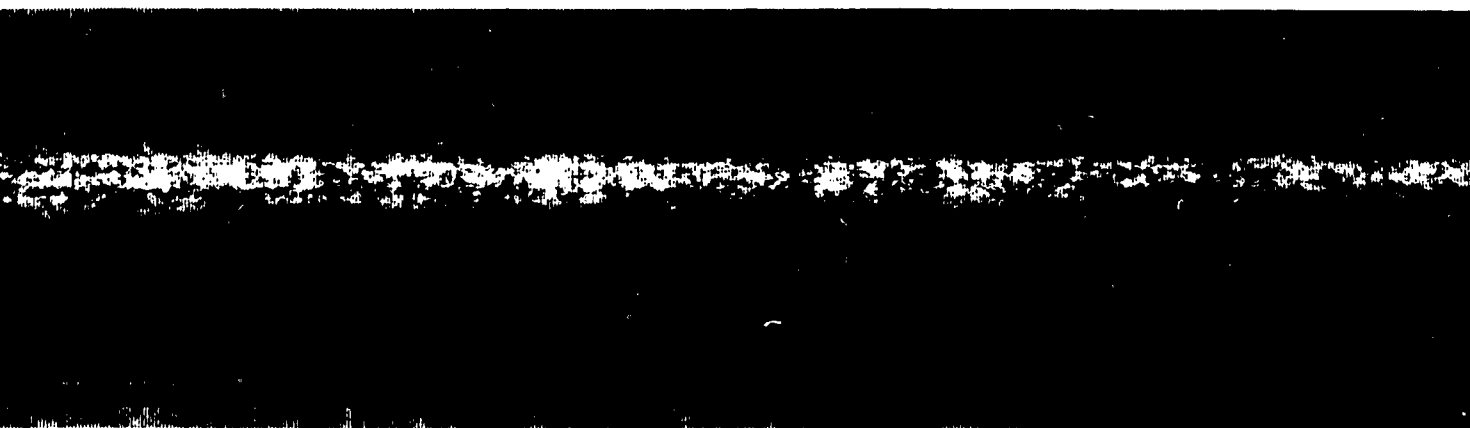
cps



1



SUPPRESSION -75  
ATTENUATION x 10  
TC 4 sec  
ZERO DOPPLER 806 Mc - 9 cps  
PAPER SPEED 2.5 mm/sec



2

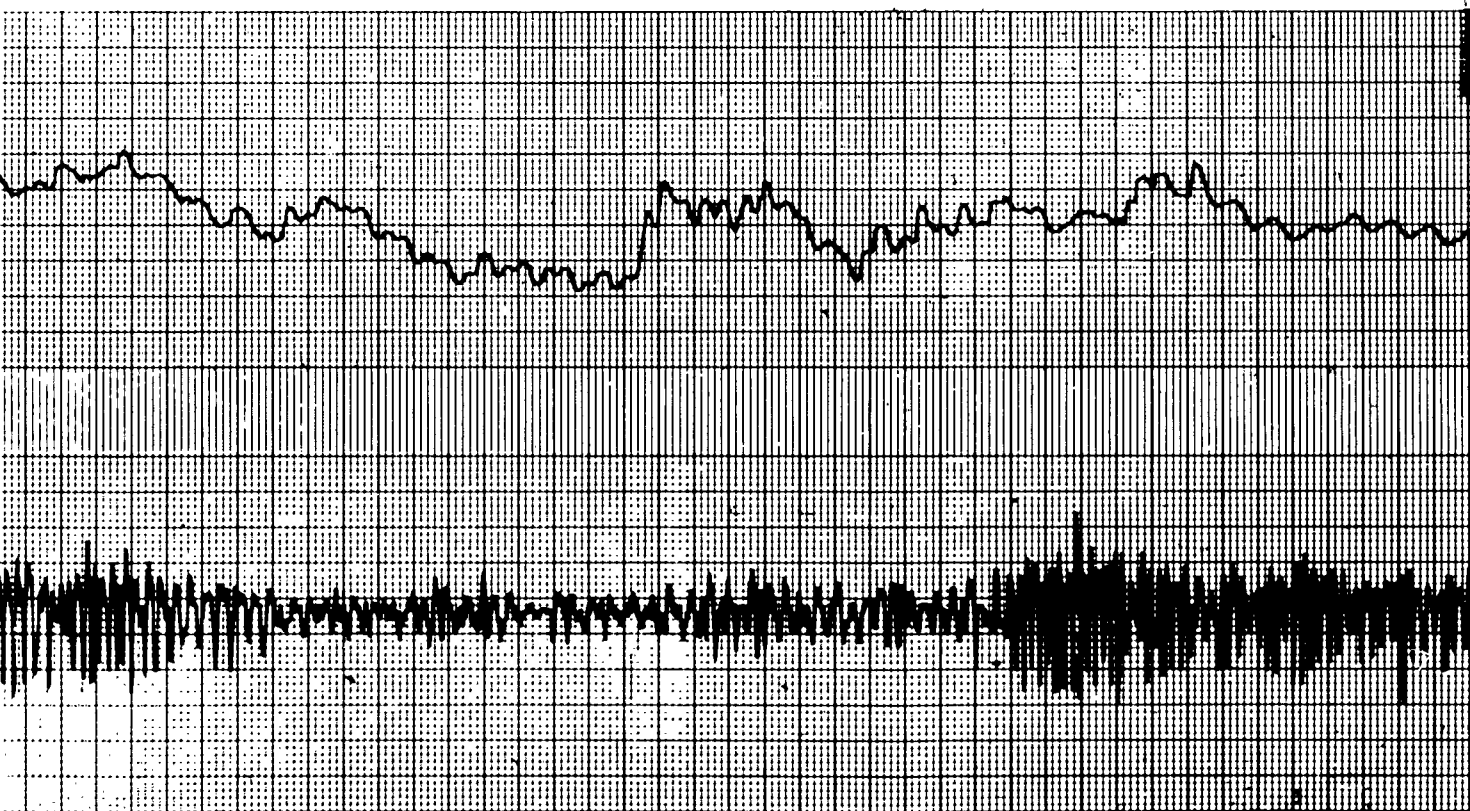
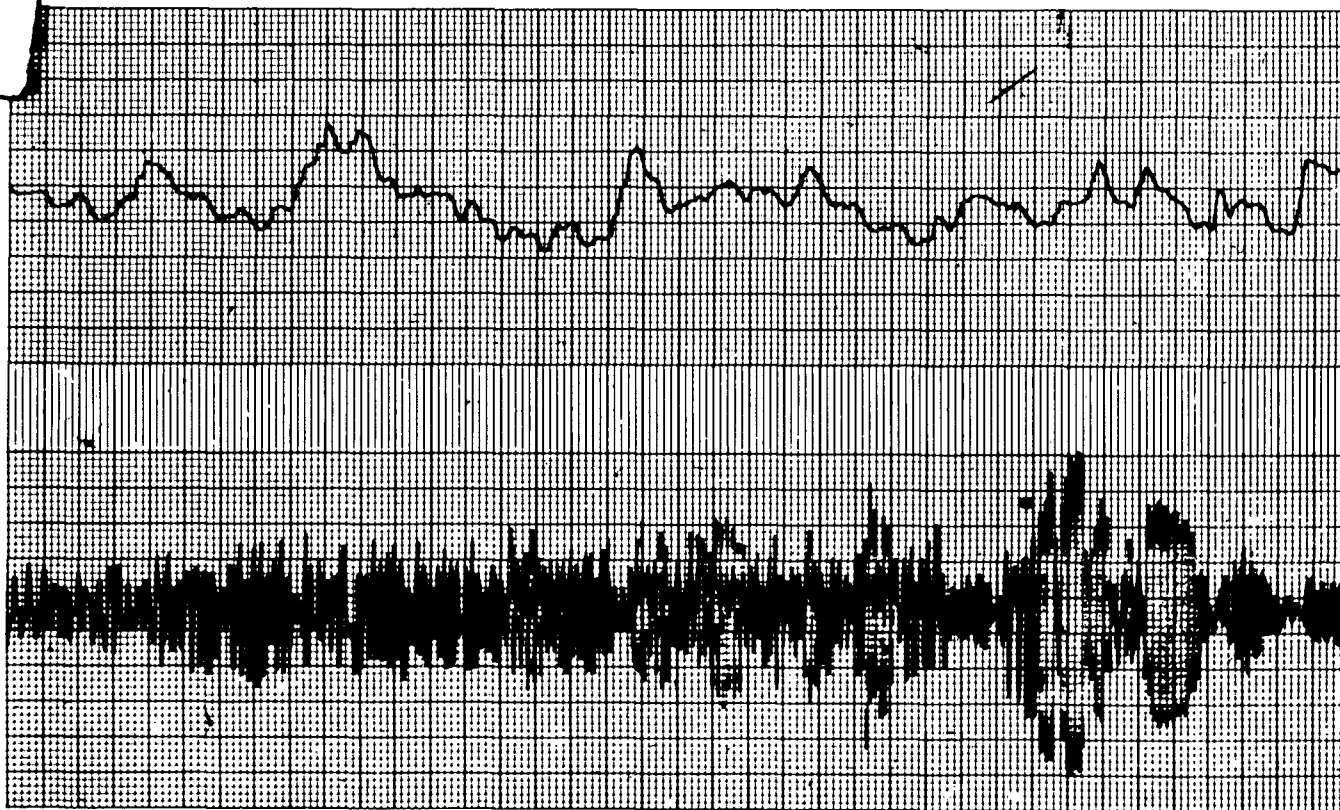


Figure 5-5 Crossing 8

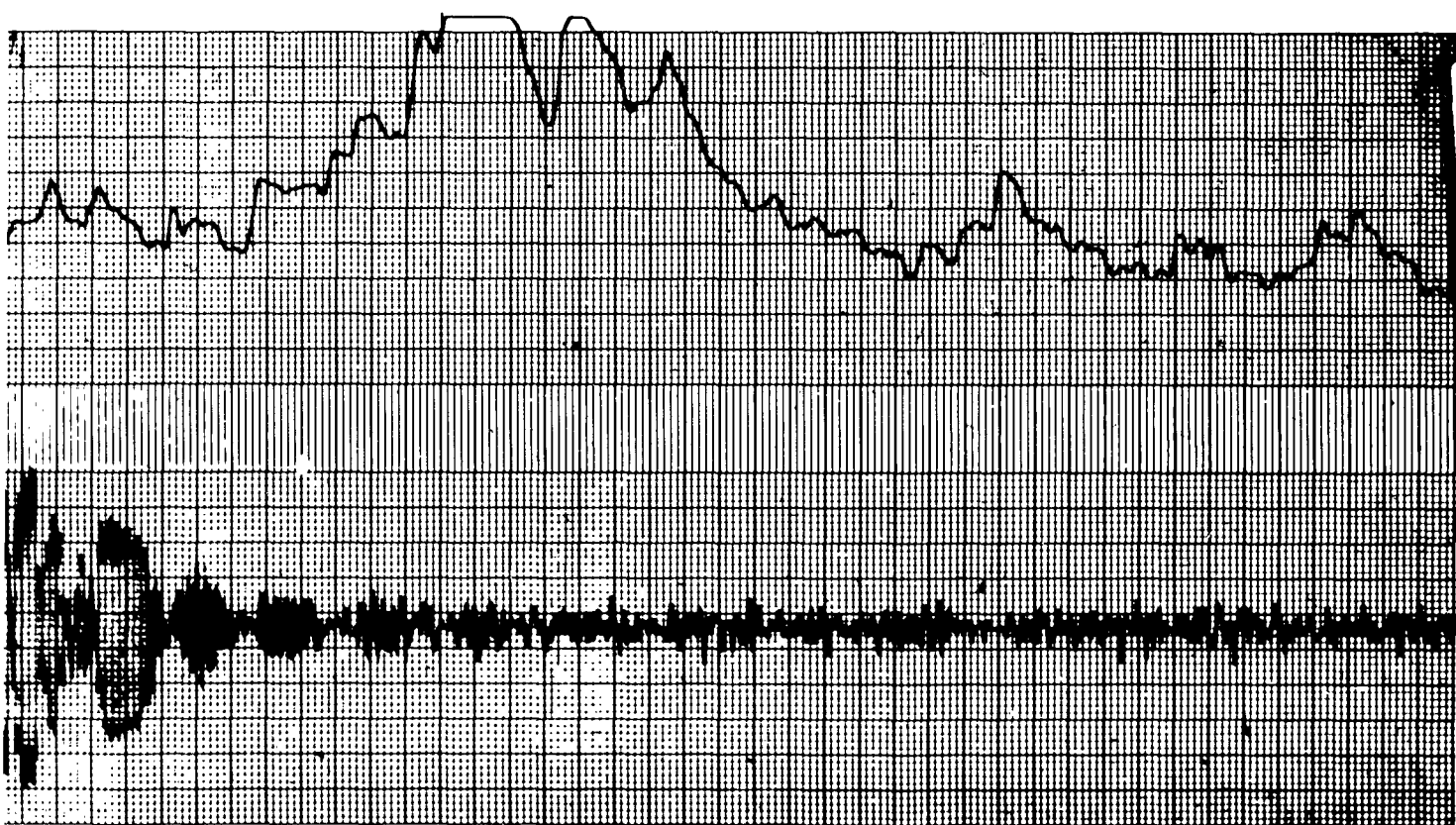
60  
40  
20  
15  
13  
12  
10

cps

1



SUPPRESSION -75  
ATTENUATION x 10  
TC 4 sec  
ZERO DOPPLER 806 Mc - 9 cps  
PAPER SPEED 2.5 mm/sec

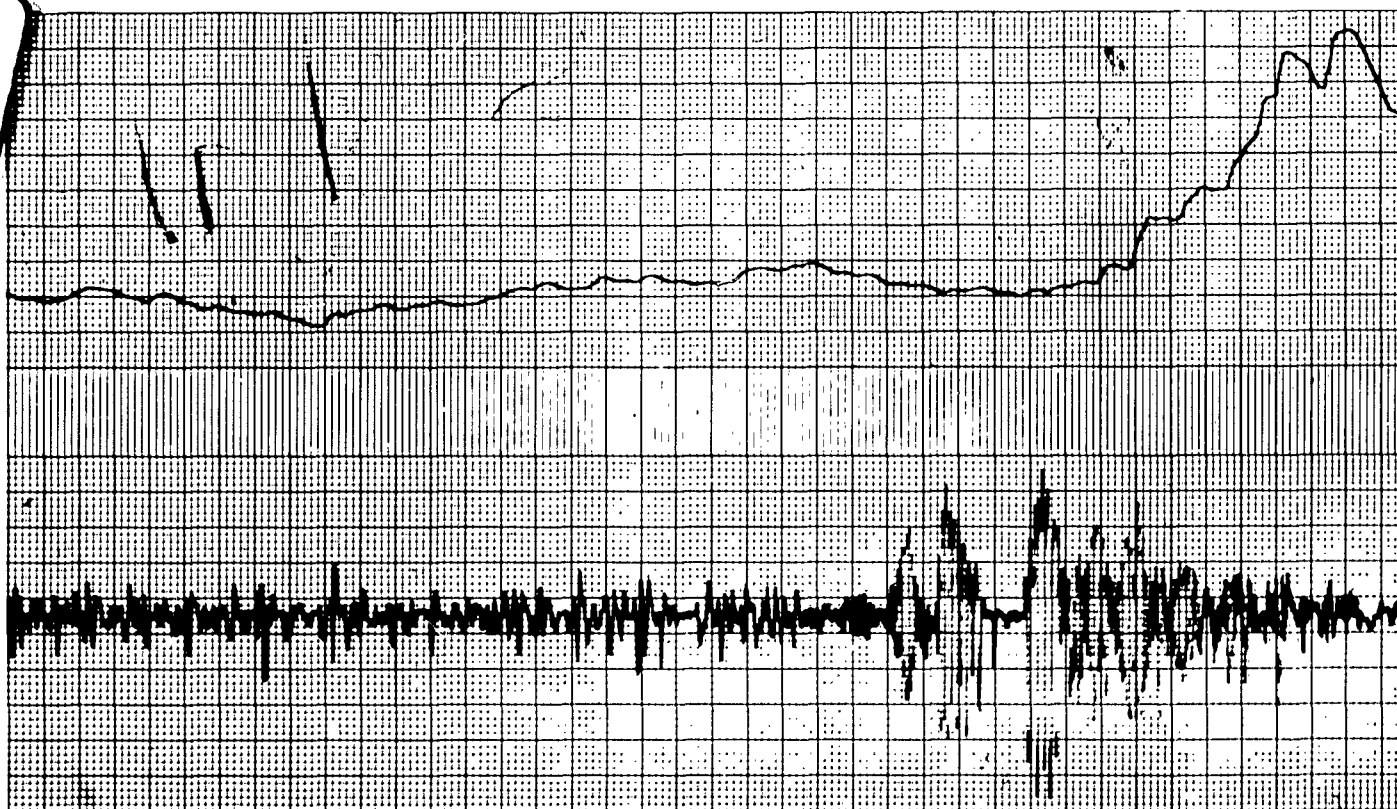


2

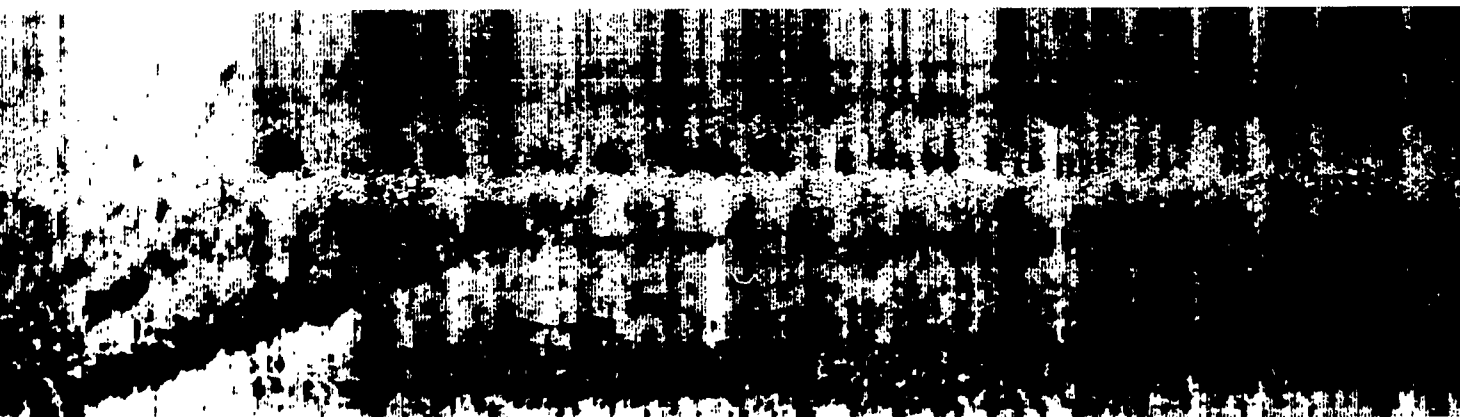
Figure 5-6 Crossing 9



1



SUPPRESSION -40  
 ATTENUATION x 10  
 TC 10 sec  
 ZERO DOPPLER 806 Mc - 9 cps  
 PAPER SPEED 2.5 mm/sec



2

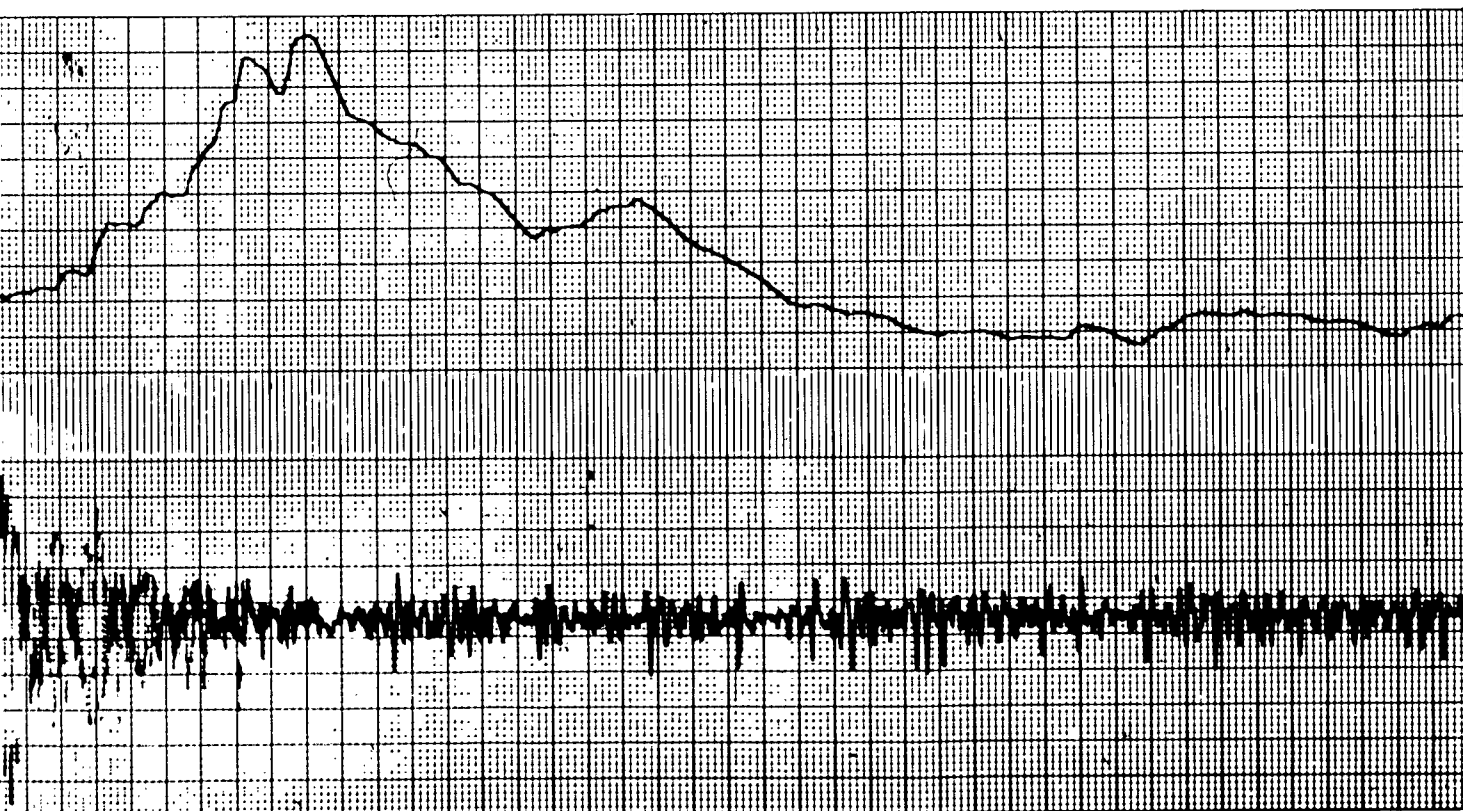
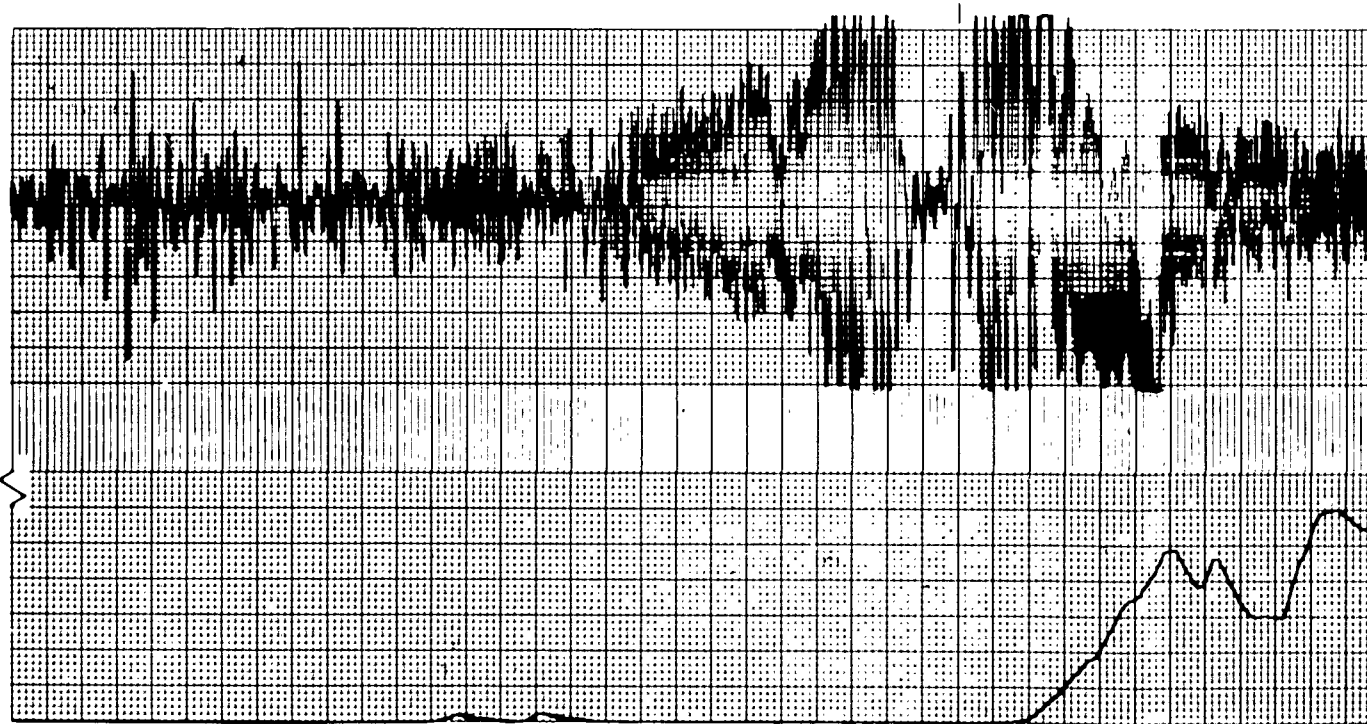
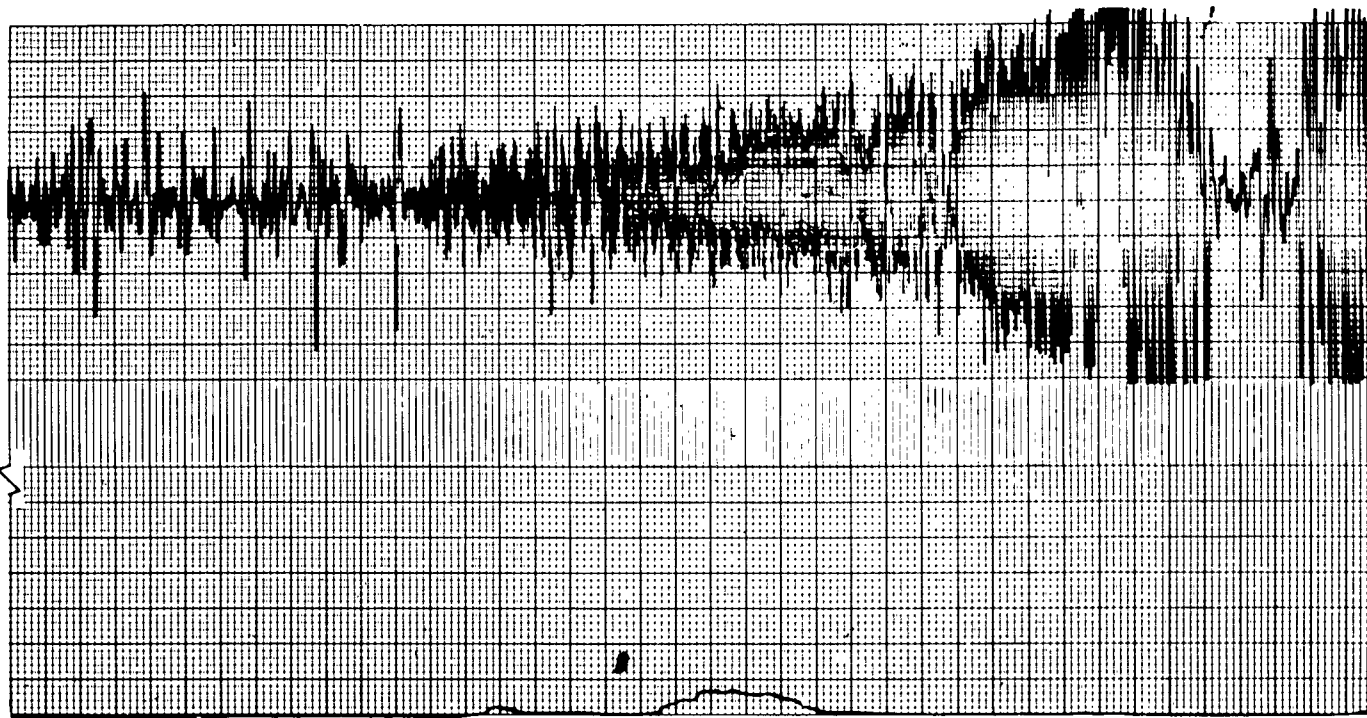


Figure 5-7 Crossing 10

1



SUPPRESSION +37  
ATTENUATION x 20  
TC 8 sec  
ZERO DOPPLER 806 Mc - 9 cps  
PAPER SPEED 2.5 mm/sec

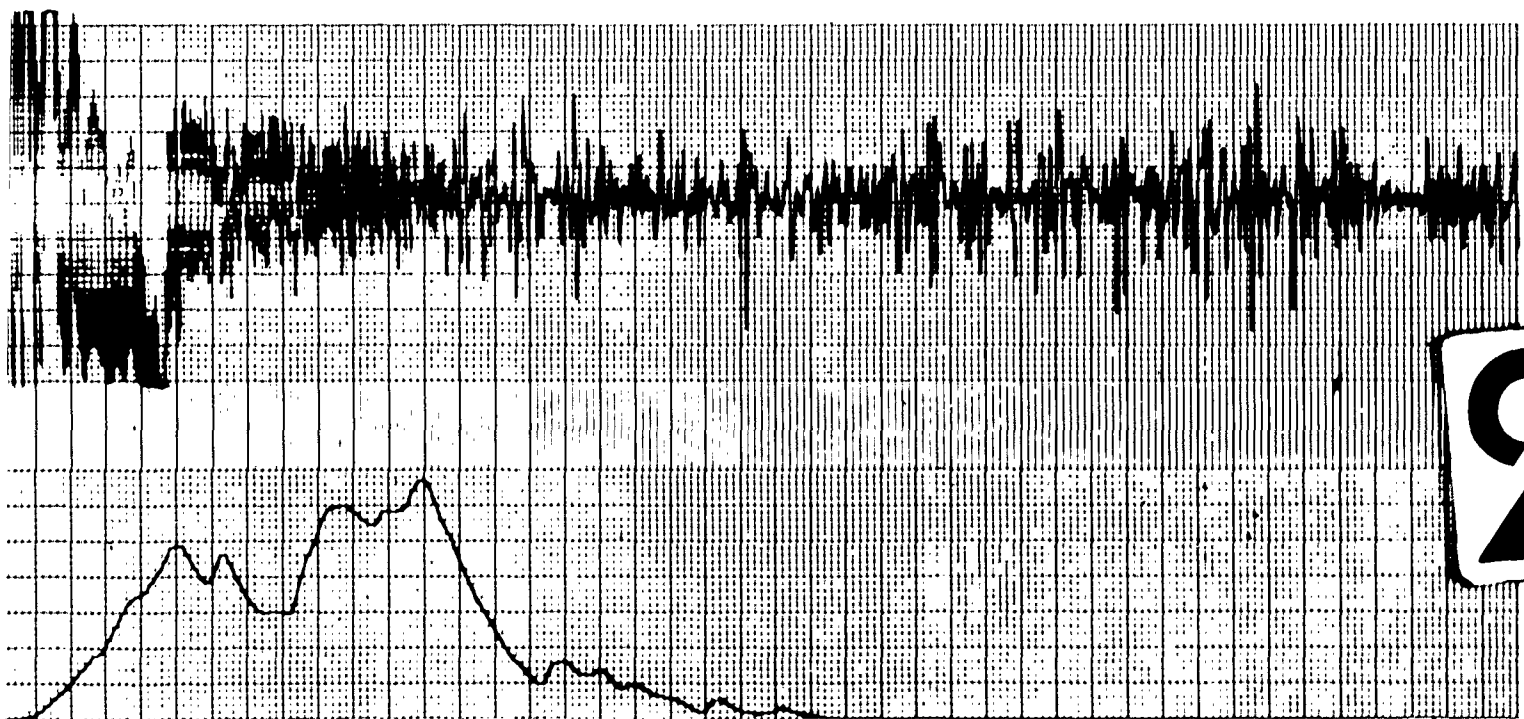
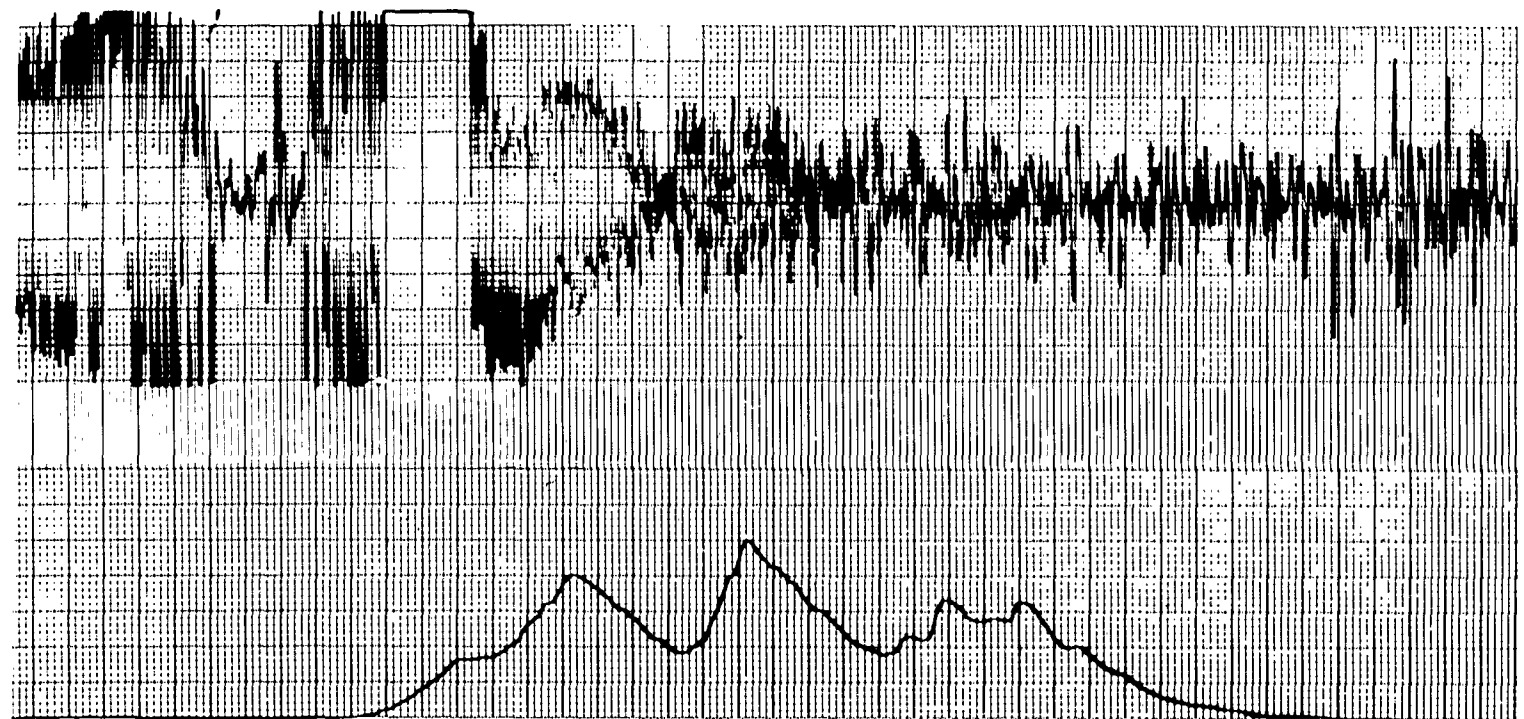
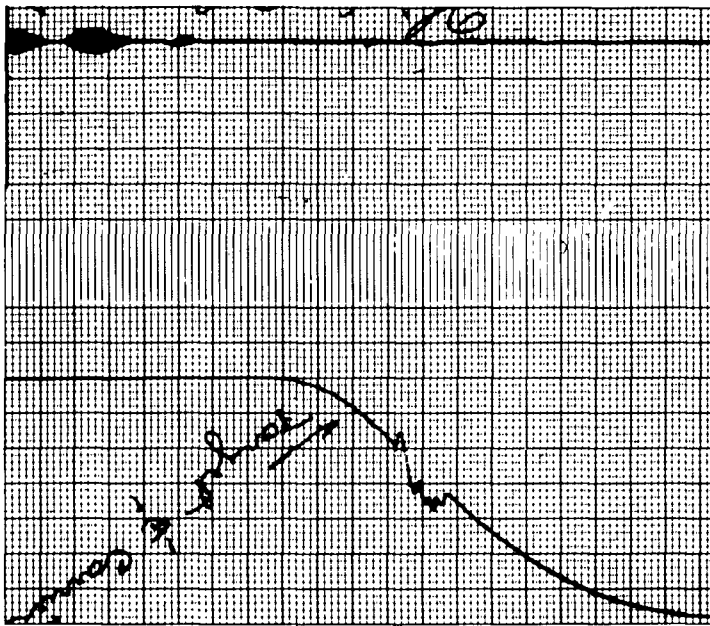
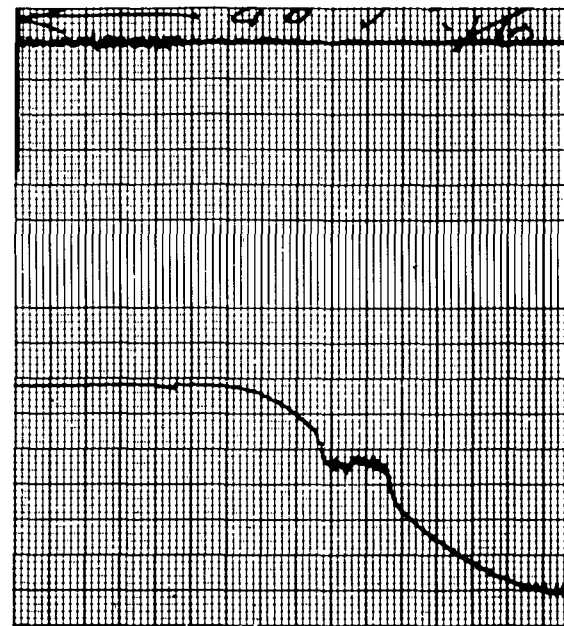


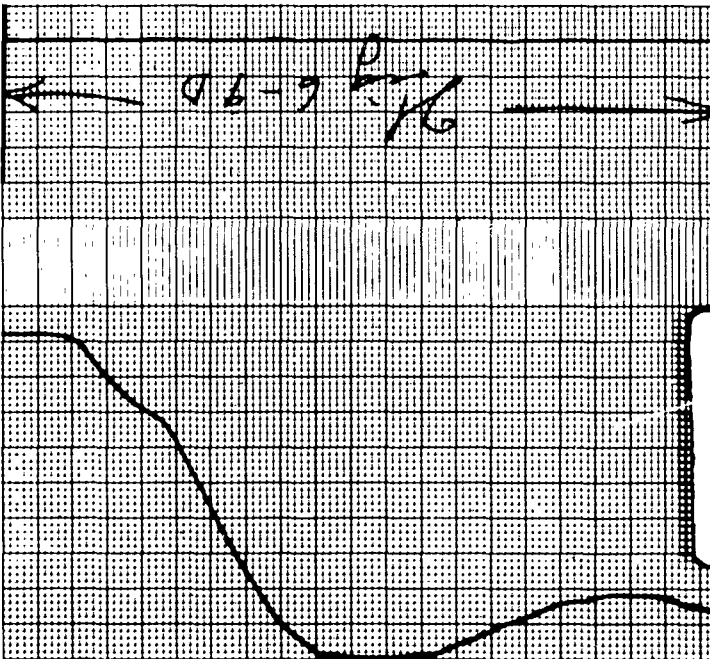
Figure 5-8 Crossings 11 and 12 (a and b)



T/C = 0 db  
 SUPPRESSION = 18  
 ATTENUATION = x 100  
 TC = 0.1 sec  
 PAPER SPEED = 2.5 mm/sec

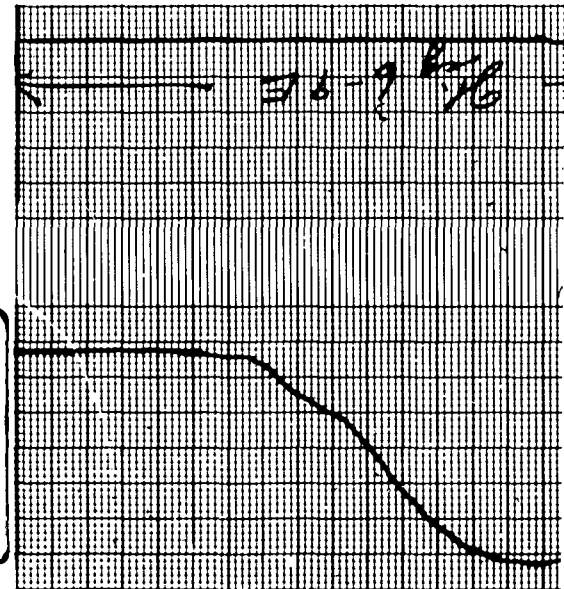


T/C = -40 db  
 SUPPRESSION = 18  
 ATTENUATION = x 100  
 TC = 0.1 sec  
 PAPER SPEED = 2.5 mm/sec

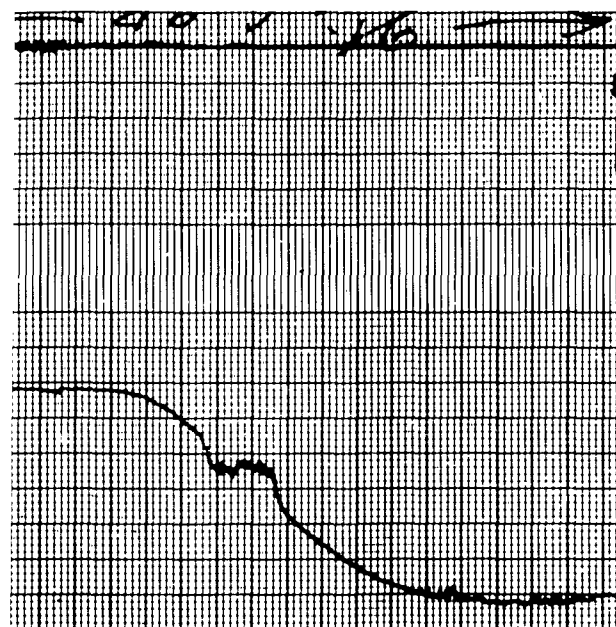


T/C = -55 db  
 SUPPRESSION = 40  
 ATTENUATION = x 20  
 TC = 8 sec  
 PAPER SPEED = 2.5 mm/sec

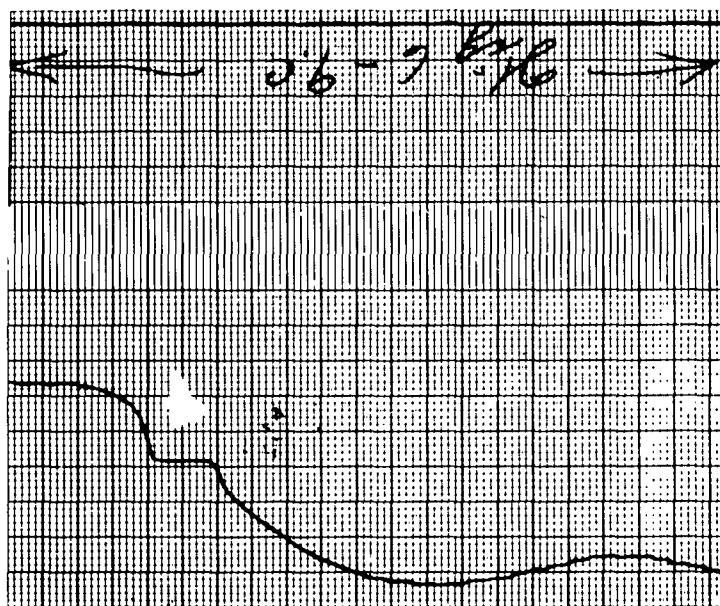
1



T/C = -60 db  
 SUPPRESSION = 75  
 ATTENUATION = x 10  
 TC = 8 sec  
 PAPER SPEED = 2.5 mm/sec



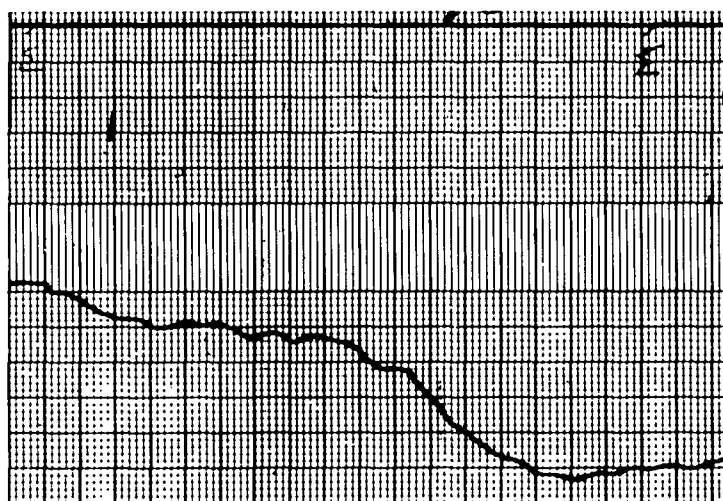
T/C = -40 db  
 SUPPRESSION = 18  
 ATTENUATION = x 100  
 TC = 0.1 sec  
 PAPER SPEED = 2.5 mm/sec



T/C = -50 db  
 SUPPRESSION = 18  
 ATTENUATION = x 100  
 TC = 0.1 sec  
 PAPER SPEED = 2.5 mm/sec



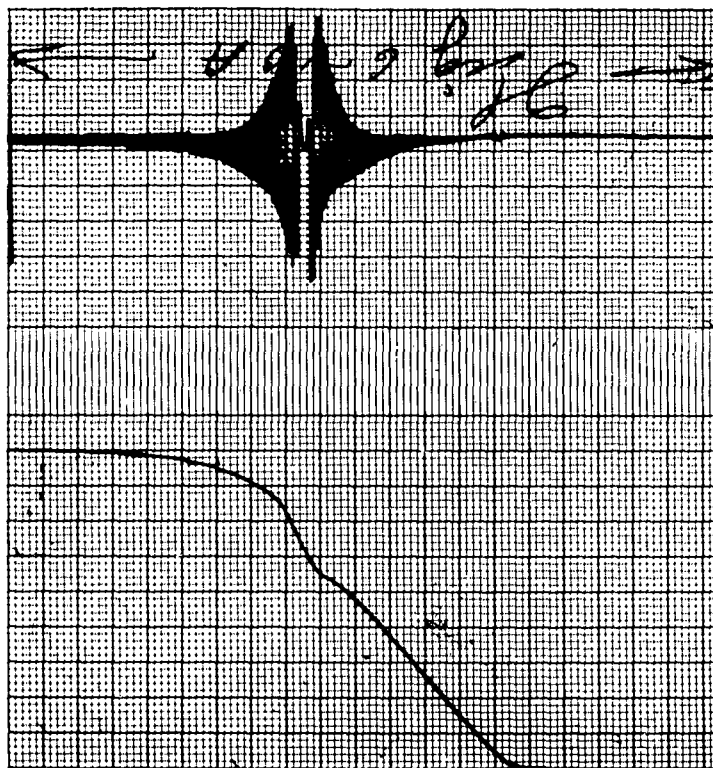
T/C = -60 db  
 SUPPRESSION = 75  
 ATTENUATION = x 10  
 TC = 8 sec  
 PAPER SPEED = 2.5 mm/sec



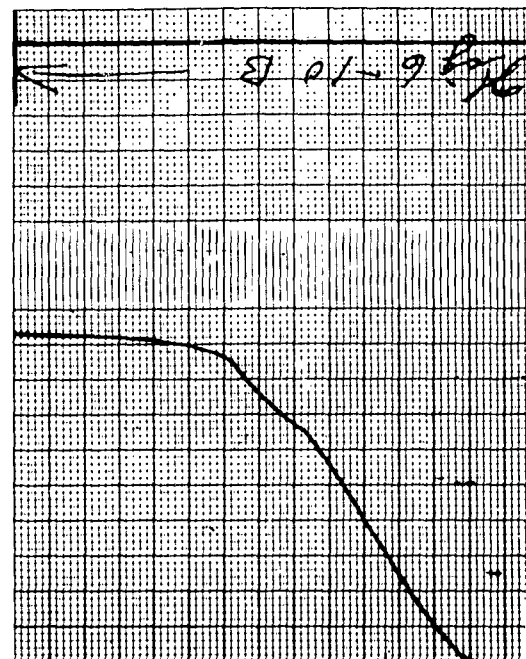
T/C = -65 db  
 SUPPRESSION = 300  
 ATTENUATION = x 5  
 TC = 8 sec  
 PAPER SPEED = 2.5 mm/sec

Figure 5-9 Simulated Target Crossings

2

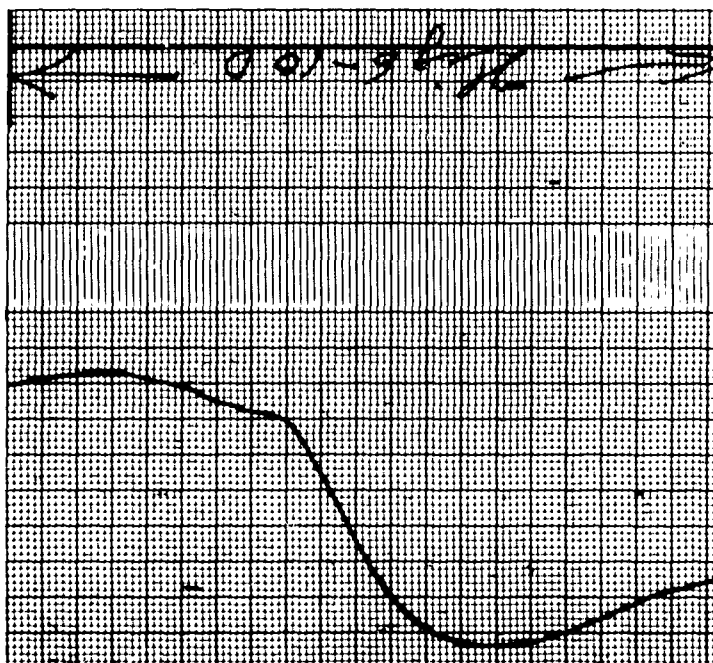


T/C = 0 db  
 SUPPRESSION = 36  
 ATTENUATION = x 50  
 TC = 8 sec  
 PAPER SPEED = 2.5 mm/sec

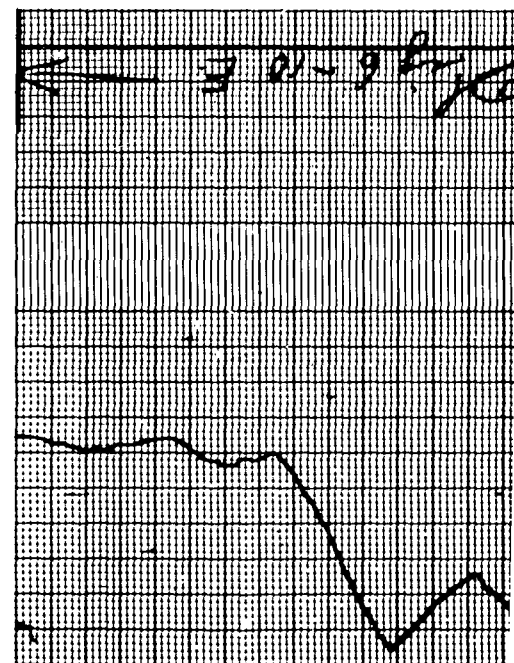


T/C = -40 db  
 SUPPRESSION = 33  
 ATTENUATION = x 50  
 TC = 8 sec  
 PAPER SPEED = 2.5 mm/sec

1



T/C = -55 db  
 SUPPRESSION = 60  
 ATTENUATION = x 20  
 TC = 8 sec  
 PAPER SPEED = 2.5 mm/sec



T/C = -58 db  
 SUPPRESSION = 46  
 ATTENUATION = x 10  
 TC = 8 sec  
 PAPER SPEED = 2.5 mm/sec

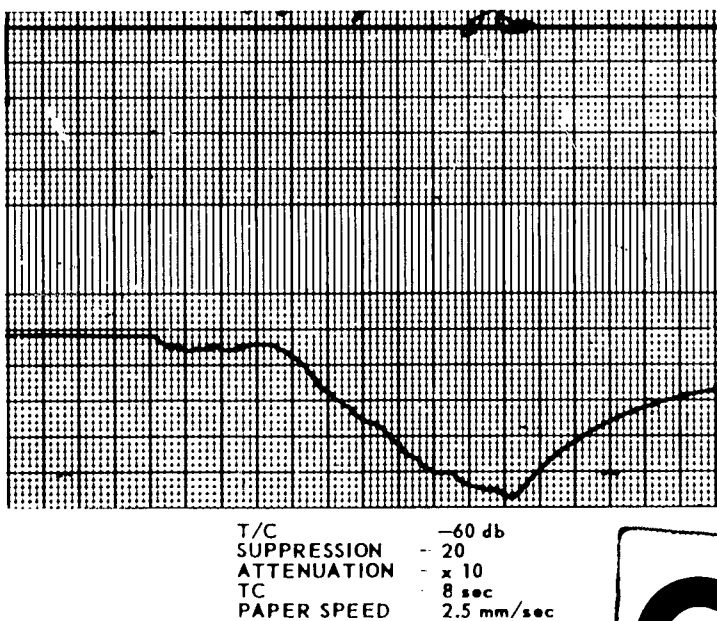
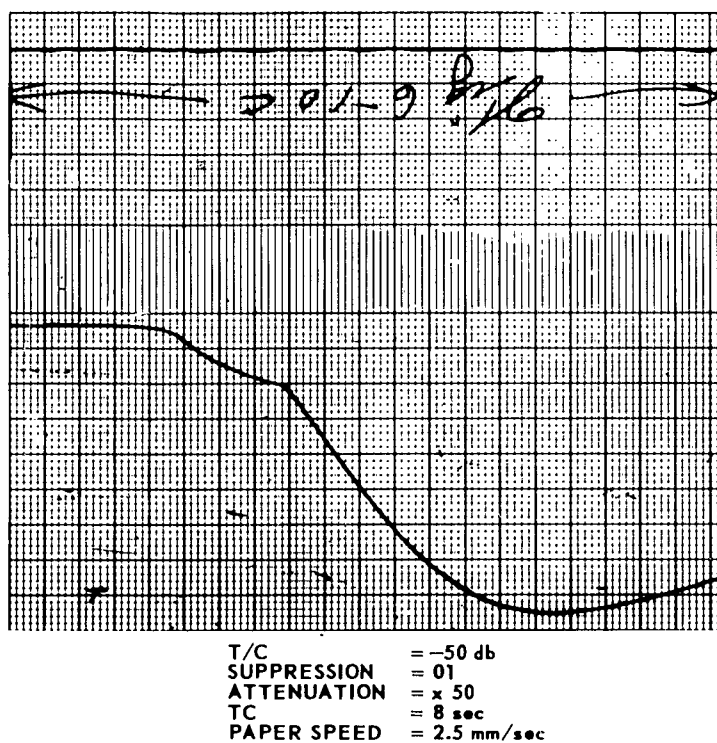
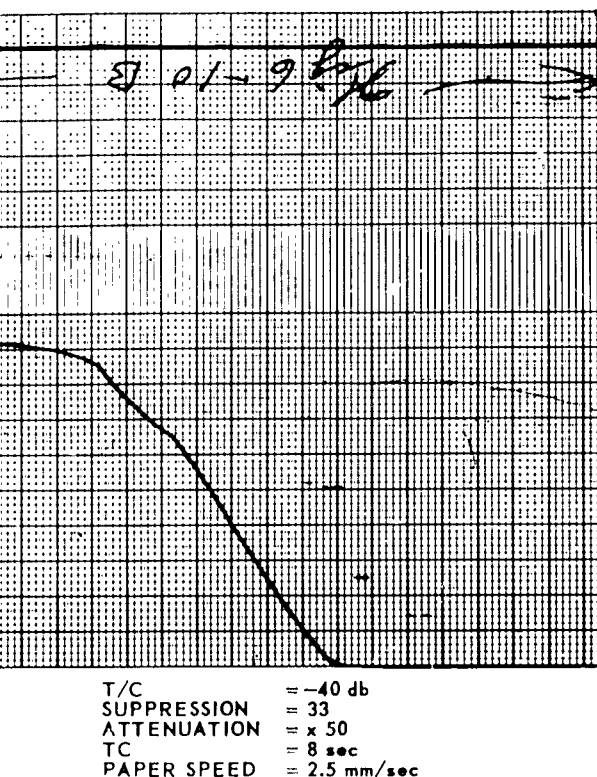


Figure 5-10 Simulated Target Crossings With Noise

The simulated target crossings in Figure 5-9 are clearly discernible without any changes in attenuation or integration time until the target to carrier (T/C) ratio is -55 db. At this point the integration time was increased from 0.1 seconds to 8 seconds and the attenuation was reduced by a factor of 20 to obtain clearly discernable target crossings until T/C = -65 db at which point target doppler frequency for these crossings was 125 cps and the low was 200 cps.

For the case presented in Figure 5-10, where noise was added to the simulated target crossings, the results are not as good. For this case, the marginal crossing occurred for T/C = -58 db and the crossings were clearly discernible up to T/C = -50 db without changes in the attenuator setting. The integration time for this series of crossings was 8 seconds and the doppler frequency was the same as above. The noise power was 5 db below the power of the target and carrier signals.

## SECTION 6

### CONCLUSIONS AND RECOMMENDATIONS FOR FUTURE STUDY

#### 6.1 CONCLUSIONS

The analysis has shown that the system is capable of detecting a very weak target signal in the presence of a very strong carrier signal and noise. Equipment tests conducted in the laboratory prior to field tests and in the field after the tests indicated that the equipment was performing correctly. However, because of the nature of the received carrier signal and the low doppler frequencies of the target aircraft, the conclusions drawn from field-tests results are subject to interpretation. Many target crossings were observed first on the FM detection system and then found on the AM display with the aid of the FM system information. In some instances when good target crossings were being obtained on both systems, FM crossings were observed but no AM detections could be found. If a controlled aircraft had been used, the time of crossing would have been known and correlated to the FM crossing.

The system has been shown to be useful for the detection of targets in noise. Unlike the AM system, it is possible to detect targets in the absence of a carrier signal; in fact, the presence of a carrier signal degrades the system to the extent that the carrier signal must be removed by filtering. Because of this, if higher transmitted frequencies are used to increase the doppler frequencies and if the antenna angles (as measured from the local tangent) are increased to reduce the tropo-scattered signal as much as possible, the resulting system will have a smaller low-altitude detection capability but a much greater detection capability against high-altitude targets such as missiles or high supersonic (Mach 3 or 4) manned vehicles.

#### 6.2 RECOMMENDATIONS FOR FUTURE STUDY

It is recommended that a spectrum analysis be made on the transmitter output to determine to what extent the carrier signal is frequency-modulated by the power supply ripple voltage. An extremely stable, narrow-band spectrum analyzer is required. It would be possible to use portions of the FM detection system as part of the spectrum analyzer.

An analysis of the application of feed-forward or feed-back around the limiters is recommended to determine if the detectability of a sub-noise-level signal could be improved by this method.

A thorough study of the discriminator should be conducted to determine if additional information can be obtained from the output before integration. Also, the discriminator should be designed for maximum noise cancellation (by including a phase shifter in each arm of the discriminator) for the external center frequency adjustment and balancing.

During the signal-to-noise analysis, it was decided that neither the wide-band nor the narrow-band FM treatment could be successfully defended. It is recommended that a more thorough analysis be pursued so that the analysis and results can be compared to one or the other standard FM analysis approach.

During the field tests many difficulties were encountered, the data-gathering efficiency was poor due to the choice of field test site. The ideal site should have had a controlled, high-speed aircraft on a tropo-scatter link that had no casual aircraft about.

## APPENDIX A

### THEORETICAL ANALYSIS

#### A.1 STATEMENT OF PROBLEM

This paper discusses the detection of a very weak target signal in the presence of a very strong carrier signal, (the target signal being less than 150 cps removed from the carrier frequency of 806 Mc). The carrier signal is considered to be stationary, since its frequency stability is  $1 \times 10^{-8}$  parts/day; the target signal is considered to be quasi-stationary, since its frequency change is linear with time and is of the order of 10 cps/sec.

A great deal of effort has been devoted to reducing the distortion of a desired signal that is caused by a slightly smaller undesired signal in the same passband of the receiver. These efforts have been directed primarily toward the enhancement of the so-called capture effect and are, therefore, not applicable to this problem.

More recently, work has been directed toward the development of methods to extract a weak signal in the presence of a stronger signal<sup>1</sup>. Some of these methods will be reviewed below. The problem of detecting the weak signal in the presence of a strong nearby signal will be analyzed and a method of detecting this signal will be presented. This method will be evaluated theoretically to determine its limits of operation as compared to the theoretical AM detection method.

#### A.2 REVIEW OF RECENTLY PROPOSED WEAK SIGNAL ENHANCEMENT SCHEMES

A comprehensive review of the schemes that have been proposed (for the enhancement of a weak signal in the presence of a stronger one) has been conducted; it was found that the only scheme that is applicable to this problem is Baghdadly's Variable-Trap Method. The methods<sup>3</sup> proposed by Wilmotte<sup>1</sup>, Baghdadly<sup>2</sup> (feed-forward method), and Farris<sup>3</sup> require two channels to process the signals before adding them together at the discriminator. In all three methods, one channel is used to derive the strong signal. The differences between the three methods are listed below.

---

<sup>1, 2, 3</sup>

References to follow on the next page.

#### A.2.1 Wilmotte's Proposal

Wilmotte uses envelope detection followed by limiting and discriminating to determine the magnitude of the difference frequency. He then adds the difference frequency signal to the strong signal after determining the sense of the difference frequency. It is not clear how Wilmotte proposes to maintain the correct sign of the difference frequency.

#### A.2.2 Baghdady's Feed-Forward Method

Baghdady proposes a "feed-forward" method in which each channel contains a different number of amplifiers, limiters and filters. In this system, Baghdady places an amplitude limiter of appropriate bandwidth before the two channels to drive the combination. If there is only one narrow band limiter in one of the channels, then the limiter that drives the combination must also be narrow-band. If, however, two or more narrow band limiters are cascaded in one of the channels, then the limiter that drives the combination need not be narrow-band. This system has been designed and tested but a report of the results could not be obtained.

- 
1. Wilmotte, R. M., "Reception of an FM Signal in the Presence of a Stronger Signal in the Same Frequency Band and Associated Results," Proc. IRE, Vol. 101, Part III No. 70, pp 69-75, March 1954
  2. Baghdady, E. J., "Frequency Modulation," Part VIII of Quarterly Progress Report, Research Laboratory of Electronics, MIT, pp 52-55, October 1957
  3. Farris, H. W., "Alternative Detection of Modulations in Co-channel FM," Technical Report No. 84, Electronic Defense Group, Dept. of EE, U of M, June 1958

#### A.2.3 H. W. Farris' Method

The method used by Farris was also a feed-forward circuit, but a linear amplifier was used in one channel. In the other channel the composite signal was hard limited to obtain the large signal by capture effect and then amplified. The two channels have the same gain but are  $180^\circ$  out of phase with respect to the large signal. The outputs of the two channels are added together to obtain the weak signal by cancellation of the strong signal before it captures the weak one. The weak signal is then amplified, limited and detected in the usual manner. The feasibility of this system has been demonstrated and evaluated. The limitations of this system are that it cannot detect a weak signal that is greater than 20 db below the strong signal and that it is sensitive to amplitude fluctuations of the strong signal.

#### A.2.4 R. E. Meek's Proposal

Meek<sup>1</sup> has proposed a method for subtraction of the strong signal by the use of a balanced modulator. This method is quite similar to that proposed by Farris but differs in the way the results are achieved. The limitations of this method are similar to those of Farris' method.

#### A.2.5 Baghdady's Variable-Trap Method<sup>2</sup>

Baghdady has proposed a variable-trap method to remove the strong signal before limiting and demodulating as shown in Figure A-1. The system, per se, could not solve the problem presented in this paper since the sharply tuned variable trap could not be tuned sharply enough to reject the strong signal without also rejecting the weak one. It will be shown below that a variation of this method can be used to solve the problem.

---

1. Meek, R. E., "Study Program for Investigation to Aid in Reduction and Prevention of UHF Interference," Progress Letter No. 38, Contract No. AF 30(602) 673, Georgia Inst. of Tech., Sept. 1956

2. Op. Cit.

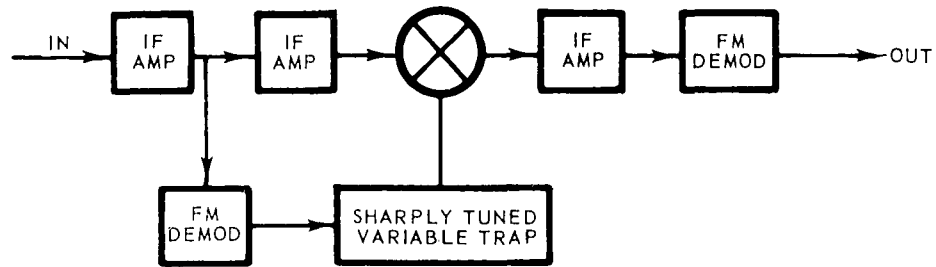


Figure A-1 Baghdady's Variable Trap Method

#### A.2.6 AM Detection

A great deal of work has been done in the area of weak target signal AM detection in the presence of a strong carrier signal and has been reported in the "SCADAR Final Report," BSR 256, June 1960.

### A.3 MATHEMATICAL ANALYSIS

#### A.3.1 Two Stationary Carriers

The system design is based on the following mathematical analysis.

Consider two unmodulated radio waves  $S_c$  and  $S_t$  arriving simultaneously at a receiver, as shown in Figure A-2.

$$S_c = E_c \cos W_c t \quad (A-1)$$

$$S_t = E_t \cos W_t t \quad (A-2)$$

$$S_s = S_c + S_t \quad (A-3)$$

$$S_s = 2E_t \left[ \cos \frac{1}{2}(W_c - W_t)t \right] \left[ \cos \frac{1}{2}(W_c + W_t)t \right] + (E_c - E_t) \cos W_c t$$

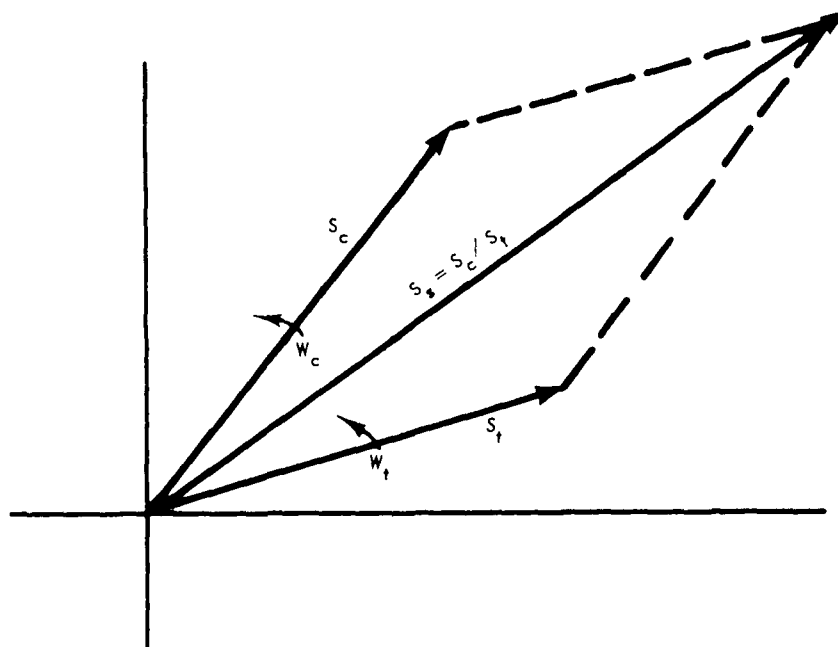


Figure A-2 Vector Diagram of Two Unmodulated Radio Waves

Therefore, the resultant voltage at the first grid of the receiver generally consists of two distinct components. One component has a mean angular frequency of  $1/2(W_c + W_t)$  and an amplitude that is fluctuating at an angular rate of  $1/2(W_c - W_t)$ . This component can be considered to be 100% amplitude modulated since the  $\cos 1/2 (W_c - W_t)t$  varies between 0 and 1. The other component is not modulated and is smaller than  $S_c$  or  $S_t$  since it has a frequency  $W_c$  and an amplitude  $E_c - E_t$ .

The resultant signal  $S_t$  can be brought into the following form by the use of the law of cosines:

$$S_s = \cos(W_c t + \theta_s) \sqrt{E_c^2 + E_t^2 + 2E_c E_t \cos(W_c - W_t)t} \quad (A-4)$$

where

$$\theta_s = \tan^{-1} \left[ \frac{E_t \sin (W_c - W_t)t}{E_c + E_t \cos (W_c - W_t)t} \right] \quad (A-5)$$

It can now be seen that in addition to AM between the limits of  $(E_c - E_t)$  and  $(E_c + E_t)$  we also have phase modulation since the equation is of the form

$$S_s = |S_s| \cos (W_c t + \theta_s) \quad (A-6)$$

Since no assumptions were made in the derivation of Equation (A-6), it will hold for all values of  $W_c$ ,  $W_t$ ,  $E_c$ , and  $E_t$ . The argument  $\alpha = W_c t + \theta_s$  can, therefore, be used to compute the equivalent FM from the relation

$$W_s = \frac{d\alpha}{dt} = W_c + \frac{d\theta_s}{dt} \quad (A-8)$$

let

$$\frac{E_t}{E_c} = A \quad (A-9)$$

$$W_c - W_t = W_d \quad (A-10)$$

then Equations (A-4) and (A-5) can be written as

$$E_s = E_c \sqrt{1 + A^2 + 2A \cos W_d t} \cos (W_c t + \theta_s) \quad (A-11)$$

and

$$\theta_s = \tan^{-1} \left[ \frac{A \sin W_d t}{1 + A \cos W_d t} \right] \quad (A-12)$$

The instantaneous frequency of the resultant wave, with  $W_d = \text{const.}$ , is

$$\begin{aligned}
 W_s &= W_c + \frac{d\theta_s}{dt} \\
 &= W_c + AW_d \left[ \frac{A + \cos W_d t}{1 + A^2 + 2A \cos W_d t} \right]
 \end{aligned}
 \tag{A-13}$$

The instantaneous frequency differs from the large signal frequency  $W_c$  by the factor

$$\frac{d\theta_s}{dt} = AW_d \left[ \frac{A + \cos W_d t}{1 + A^2 + 2A \cos W_d t} \right]
 \tag{A-14}$$

If  $W_d$  is constant in time, the instantaneous frequency as a function of time would appear as shown in Figure A-3 below if the amplitude of  $S_t$  is equal to  $A$ , where  $A > 1$  and  $E_c$  was of unit amplitude. If  $A < 1$ , the plot would be inverted with respect to  $W_c$  and the spike amplitude would be

$$\frac{AW_d}{A-1}$$

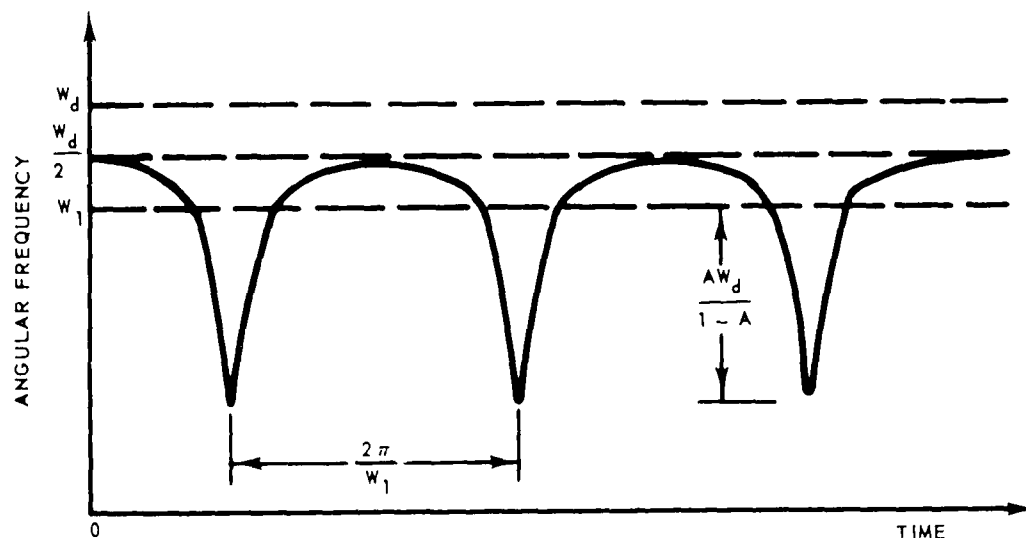


Figure A-3 Instantaneous Frequency Distribution (after Granlund<sup>1</sup>)

1. Granlund, J. "Interference in FM Reception," Technical Report No. 42, Research Laboratory of Electronics, MIT, Jan. 1949. A-7

### A.3.2 One Stationary Carrier and One Moving

The instantaneous frequency distribution for the problem considered in this report involving the two unmodulated radio waves  $S_c$  and  $S_t$  of Fig. A-2 will be more complex since the frequency difference  $[W_d = W_c - W_t]$  is linearly varying with time as will be shown in Fig. A-4.

If

$$W_d = kt \quad (A-15)$$

then (A-13) becomes

$$W_s = W_c + 2A W_d \left[ \frac{A + \cos W_d t}{1 + A^2 + 2A \cos W_d t} \right] \quad (A-16)$$

The instantaneous frequency differs from  $S_c$  by the factor

$$\frac{d\theta_s}{dt} = 2A W_d \left[ \frac{A + \cos W_d t}{1 + A^2 + 2A \cos W_d t} \right] \quad (A-17)$$

where the factor of 2 arises from the time varying property of  $W_d$ .

The instantaneous frequency distribution is shown in Figure A-4 below for a constant  $A = 1$  and a unit amplitude of  $S_c$ . If  $A = 1$  then the distribution would be inverted with respect to  $W_c$  and the spike amplitude would be

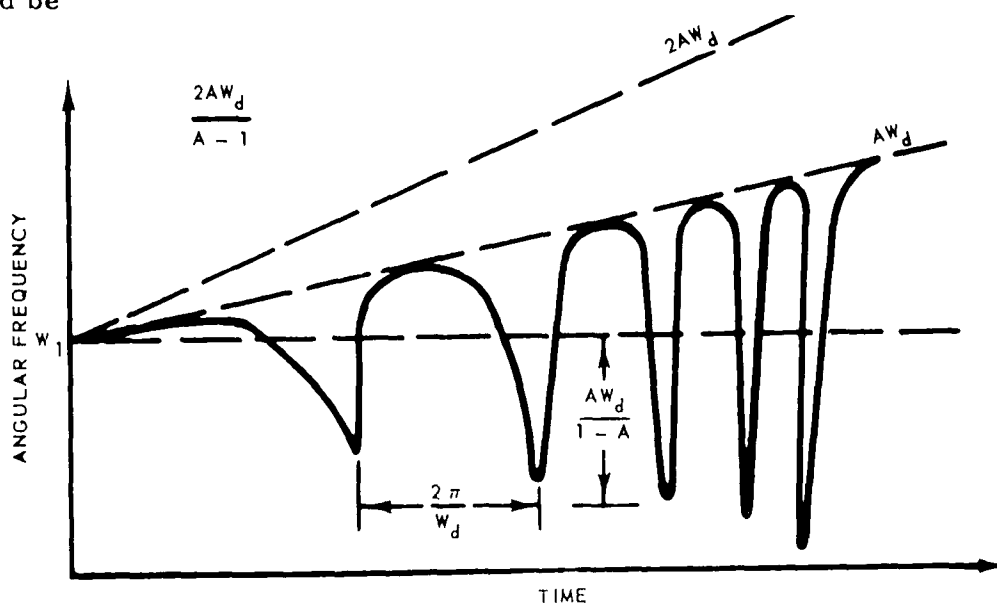


Figure A-4 Instantaneous Frequency Distribution for  $W_d = kt$  A-8

It can be seen from Figure A-3 that the average frequency is not  $W_c$  as was the case for constant  $W_d$ , but  $W_c + 2AW_d$ .

We will now return to Equation (A-11) and rewrite it in the form

$$S_s = \sqrt{E_c^2 + E_t^2 + 2E_c E_t \cos W_d t} \cos(W_c t + \theta_s) \quad (A-18)$$

Very narrow-band crystal filtering will be used to reduce  $E_c$  to a level far below that of  $E_t$  thereby making  $E_c$  negligible compared to  $E_t$ . The composite signal will then be amplified, limited, and detected in a 300 cps bandwidth discriminator. The amplification and hard limiting of the composite signal will remove the amplitude fluctuations from the composite signal so that we may now represent the composite signal by the equation

$$S_{lim} = C_1 \cos(W_c t + \theta_s) \quad (A-19)$$

where the constant  $C_1$  has been determined by the output level of the limiter. If the center frequency of the crystal discriminator is set to  $W_c$ , the output of the discriminator will be

$$S_{disc} = C_2 \frac{d\theta_s}{dt} = 2C_2 AW_d \left[ \frac{A + \cos W_d t}{1 + A^2 + 2A \cos W_d t} \right] \quad (A-20)$$

where  $C_2$  is determined by  $C_1$  and the characteristics of the discriminator.

The problem, as stated in Section A.1, is merely to detect the presence of  $S_t$ . It can be seen from Equation (A-20) that this is easily accomplished as long as  $E_t$  is able to suppress the noise of the system by the well known capture effect. Low pass filtering of the discriminator output will increase the detection capability considerably by providing long time integration. The output of the filtered discriminator will be

$$S_{out} = 2C_2 AW_d - 2C_2 A k t \quad (A-21)$$

This output can be used to drive a pen recorder to obtain a plot of discriminator output vs. time.

### A. 3.3 Signal-to-Noise Ratio

In the mathematical analysis of the signal-to-noise ratio, there arises the question of whether the incoming signal should be treated as a "narrow-band FM signal" or a "wide-band FM signal". If one chooses the quasi-stationary spectrum as the criteria and splits it into an AM portion and an FM portion, then one would conclude that it is narrow-band FM; however, if one chooses the definition of the modulation index ( $m_f$ ) as the criteria

$$m_f = \frac{\Delta f}{f_m} = \frac{\text{maximum deviation frequency}}{\text{modulating frequency}}$$

one would conclude that it is a wide-band system. The fact that the modulating frequency ( $f_m$  is caused by the target signal) is not a repetitive function and is not usually sinusoidal casts aspersions on the modulation index criteria while the quasi-stationary property causes one to doubt the validity of the spectrum criteria.

A reasonable solution to the dilemma is to treat the signals as they actually are; i. e., a carrier signal at the center of the discriminator and a target signal whose frequency differs from the carrier by the doppler. For reasons of comparison, analyses will be presented for wide-band FM signals that are greater than noise and for narrow-band signals that are greater than, equal to, or less than noise.

#### A. 3.3.1 Wide-band FM Analysis for Signals Greater than Noise

To determine the amount of frequency and amplitude modulation of the incoming signal that is caused by random noise we will use an approach that is similar to the development of the last section. In Section A. 3.1 it was shown that any arbitrary unsymmetrical sideband can be expressed as the sum of symmetrical and anti-symmetrical sideband pairs. Under the assumption that the incoming carrier is large in comparison to the noise, the symmetrical sidebands will cause amplitude modulation and the anti-symmetrical sidebands will cause frequency modulation. The degree of amplitude modulation  $M_a$  due to random noise is

$$M_a = \frac{1}{A} \sqrt{\sum_a \left[ B_{a_1}^2 + B_{a_2}^2 + 2B_{a_1} B_{a_2} \cos(\theta_{a_2} - \theta_{a_1}) \right]} \quad (\text{A-22})$$

$$M_a = \frac{1}{A} \sqrt{\sum_a \left[ B_{a_1}^2 + B_{a_2}^2 \right]} \quad (\text{A-23})$$

where:

A is the amplitude of the carrier

$B_{a_1}$  is the noise-sideband amplitude a cycles above the carrier

$B_{a_2}$  is the noise-sideband amplitude a cycles below the carrier.

The cross-product terms,

$$\sum_a 2B_{a_1} B_{a_2} \cos(\theta_{a_2} - \theta_{a_1}) = 0 \quad (A-24)$$

since the average value of  $\cos(\theta_{a_2} - \theta_{a_1})$  is a zero for any range of values

of "a" because of the random nature of the phase of noise sidebands.

Similarly, the effective degree of FM of the carrier by the random noise is

$$M_f = \frac{1}{AD} \sqrt{\sum_a a^2 \left[ B_{a_1}^2 + B_{a_2}^2 - 2B_{a_1} B_{a_2} \cos(\theta_{a_2} - \theta_{a_1}) \right]} \quad (A-25)$$

$$M_f = \frac{1}{AD} \sqrt{\sum_a a^2 \left[ B_{a_1}^2 + B_{a_2}^2 \right]} \quad (A-26)$$

where D is the maximum deviation frequency and "a" is the frequency difference between the noise and the carrier. If the carrier is at the center of a symmetrical bandpass amplifier,  $M_a$  and  $M_f$  can be integrated over the effective thermal noise voltage square vs frequency curve to obtain

$$M_a = \frac{1}{A} \sqrt{\int 2N^2 df} \quad (A-27)$$

$$M_f = \frac{1}{AD} \sqrt{\int 2a^2 N^2 df} \quad (A-28)$$

where N is the thermal noise voltage in the interval and the factor of 2 is required because N is an rms value. If we make the simplifying assumptions

that there is constant gain over the pass band B and the noise N is due to shot and thermal noise, the equations above become:

$$M_a = \frac{1}{A} \sqrt{\int_{-1/2BW_a}^{+1/2BW_a} 2N^2 da} = \frac{N}{A} \sqrt{2B_a} \quad (A-29)$$

$$M_f = \frac{1}{AD} \sqrt{\int_{-1/2BW_f}^{+1/2BW_f} 2N_a^2 da} = \frac{N}{A} \frac{B_f}{2D} \sqrt{\frac{2B_f}{3}} \quad (A-30)$$

where  $B_a$  is the bandpass of the AM system and  $BW_f$  is the bandpass of the FM system. If we now let  $F_a$  be the audio passband of the AM receiver and, as is normal,  $F_a = 1/2BW_a$ , the effective signal-to-noise ratio at the output of the receiver (referred to a 100% modulated signal) will then be

$$S/N_a = \frac{A^2}{4N^2 F_a} - 5\text{db} \quad (A-31)$$

The 5 db of degradation to the signal-to-noise ratio is the "excess noise figure"<sup>1</sup> and is due to the presence of a carrier on the noise output of a detector. If we let F be the audio passband of the FM receiver and, in this case,

$$F_f = \frac{1}{2} BW_f \quad (A-32)$$

$$S/N_f = \frac{3A^2 D^2}{4N^2 F_f^3} \quad (A-33)$$

The signal to noise improvement factor (I) will be the ratio,

- 
1. "Signal-to-Noise Ratio in AM Receivers", by E.G. Furbini and D. C. Johnson, Proc. I.R.E., Dec. 1948, pp. 1461-1466.

$$I = \frac{S/N_f}{S/N_a} = \frac{3D^2 F_a^2}{F_f^3} + 5 \text{ db} \quad (\text{A-34})$$

For the case presented in this report,

$$D \approx 100 \text{ cps}$$

$$F_a \approx 3 \text{ cps}$$

$$F_f \approx 1/8 \text{ cps}$$

$$I = \frac{3(100)^2 (3)}{(1/8)^3} + 5 \text{ db} = 83 \text{ db} \quad (\text{A-35})$$

This improvement factor  $I$  is only valid when  $S/N$  is greater than 1 at the input to the limiter and when  $\frac{\text{target signal}}{\text{carrier signal}}$  is greater than 1 after notch filtering and before limiting.

#### A. 3. 3. 2 Narrow Band FM Analysis for Signals Greater than Noise

The treatment of a narrow-band FM signal to determine the improvement ratio will proceed on the basis of the well known statement that narrow-band FM provides no  $S/N$  improvement over AM for equal bandwidths. The AM signal-to-noise ratio ( $S/N_a$ ) was determined in the previous section to be

$$S/N_a = \frac{A^2}{4 N^2 F_a} - 5 \text{ db} \quad (\text{A-31})$$

The signal-to-noise improvement factor ( $I$ ) for the narrow-band FM case will simply be

$$I = \frac{(S/N_a)_{fm}}{(S/N_a)_{am}} = \frac{(F_a)_{am}}{(F_a)_{fm}} + 5 \text{ db} \quad (\text{A-36})$$

where

$(S/N)_{a\text{ fm}}$  is the signal-to-noise ratio for the narrow-band FM system

$(S/N)_{a\text{ am}}$  is the signal-to-noise ratio for the AM system

$(F)_{a\text{ am}}$  is the audio bandwidth of the AM system

$(F)_{a\text{ fm}}$  is the audio bandwidth of the FM system

The  $(S/N)_{a\text{ fm}}$  is not degraded by the "excess noise figure" because of limiting. For the system being investigated,

$$(F)_{a\text{ am}} = 3 \text{ cps}$$

$$(F)_{a\text{ fm}} = 1/8 \text{ cps}$$

and therefore

$$I = \frac{3}{1/8} + 5 \text{ db} = 19 \text{ db} \quad (\text{A-37})$$

It can be seen, by comparing this  $I$  with that obtained for the wideband FM case in A. 3. 3. 1 that there is a tremendous improvement in the wideband case for input  $S/N$  ratios greater than one. This is exactly what one would expect for  $S/N$  greater than 1; however, the problem that is under investigation states that the  $S/N$  is less than 1 and therefore requires that we re-evaluate  $I$  for the wide-band case. This formidable task has not been attempted here since another approach will be used below for the case of signals in noise; however, it will be pointed out that the improvement threshold in a wide-band FM system occurs for  $S/N$  greater than 1 and below this threshold an equal degradation takes place.

#### A. 3. 3. 3 Analysis for Signals in Noise

The treatment that will be used in the determination of the signal-to-noise ratio for signals and noise below the limiting level is that presented by D. Slepian<sup>1</sup>. For the discriminator shown in Figure A-5 below, the input is passed through the two filters ( $F_1$  and  $F_2$ ), envelope detected, and subtracted.

---

1. Slepian, D., "Noise Output of Balanced Frequency Discriminator", Proc. I.R.E., March 1958, pp. 614.

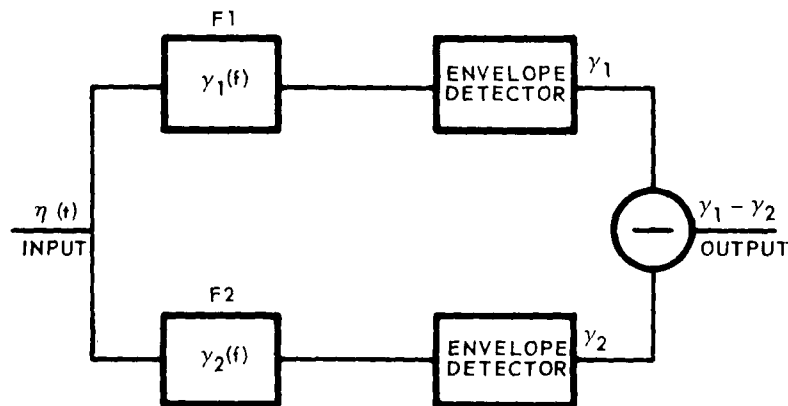


Figure A-5 Discriminator Block Diagram

Slepian has shown that the rms noise output is minimized if the phase angles of the filters are equal. That is, if filter  $F_1$  has the transfer function

$$Y_i(f) = R_i(f) + jI_i(f) = A_i(f) e^{i\phi_i(f)} \quad (i = 1, 2) \quad (\text{A-38})$$

then the rms noise is a minimum when  $\phi_1 = \phi_2$ .

The transfer functions  $Y_1$  and  $Y_2$  have conditions that are imposed by the desired discriminator shape and bandwidth. The slope of the discriminator curve should be as close to a constant as is possible in the vicinity of the center frequency  $f_o$ . That is,

$$\left. \frac{d}{df} [A_1(f) - A_2(f)] \right|_{\text{about } f_o} = -K \quad (\text{A-39})$$

The discriminator output should be zero at  $f_o$ . That is

$$\left. [Y_1(f) - Y_2(f)] \right|_{f=f_o} = 0 \quad (\text{A-40})$$

The area under the curve of  $Y_1(f)$  should be equal to the area under the curve of  $Y_2(f)$  for noise balance purposes. That is

$$\int_0^{\infty} [Y_1(f) - Y_2(f)] df = 0 \quad (A-41)$$

The above conditions are very closely realized by the transfer function (shown in Figure A-6) of the form

$$Y_1(f) = \frac{1}{1 + jQ \left[ \frac{f}{f_i} - \frac{f_i}{f} \right]} \quad (A-42)$$

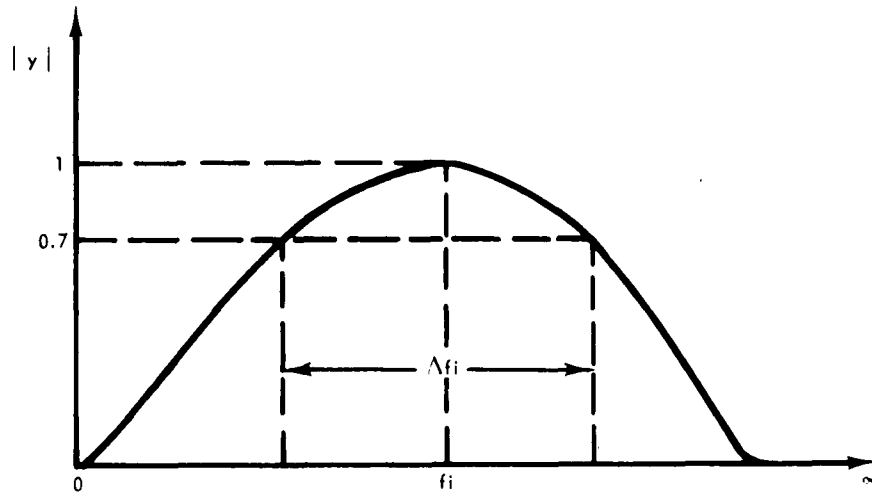


Figure A-6 Transfer Function

The rms noise output,  $\sigma^2$  is

$$\sigma^2 = (2 - \pi/2) (\alpha_1 + \alpha_2) - \pi \sqrt{\alpha_1 \alpha_2} \left[ \frac{2}{\pi} (1+h) E \left( \frac{2\sqrt{h}}{1+h} \right) - 1 \right] \quad (A-43)$$

where

$$\alpha_i = \int_0^{\infty} |Y_i(f)|^2 W(f) df \quad i = 1, 2 \quad (A-44)$$

$$h^2 = \frac{1}{\alpha_1 \alpha_2} \left| \int_0^{\infty} Y_1(f) Y_2(f) W(f) df \right|^2 \quad (A-45)$$

$$E(x) = \int_0^{\pi/2} \sqrt{1 - x^2 \sin^2 \theta} d\theta \quad (A-46)$$

The bracketed expression in (A-43),  $\left[ 2/\pi (1+h) E \left( \frac{2\sqrt{h}}{1+h} \right) - 1 \right]$ , has been evaluated in the reference above and is a monotone function of  $h$  for fixed  $Y_i$  (fixed  $Y_i$  implies fixed  $\alpha_i$ ).

The evaluation of  $\alpha_i$  will not be obtained directly due to the extreme difficulty in evaluating the integral. The integral is simplified considerably by an approximation of the transfer function as shown below.

$$\alpha_i = \int_0^{\infty} |Y_i(f)|^2 W(f) df, \quad i = 1, 2 \quad (A-44)$$

$$\alpha_i = \int_0^{\infty} Y_i(f) \bar{Y}_i(f) W(f) df, \quad i = 1, 2 \quad (A-47)$$

The term  $W(f)$  is the power spectrum of the input Gaussian noise. Since the bandwidth of the discriminator is much smaller than the bandwidth of the IF, the power spectrum is essentially flat ( $W(f) = N$  watts/cps.).

Inserting (A-42) into (A-47),

$$\alpha_i = N \int_0^{\infty} \frac{1}{1+jQ \left[ \frac{f}{f_i} - \frac{f_i}{f} \right]} \times \frac{1}{1-jQ \left[ \frac{f}{f_i} - \frac{f_i}{f} \right]} df \quad (A-48)$$

$$\alpha_i = N \int_0^{\infty} \frac{f^2 f_i^2 df}{f^2 f_i^2 + Q^2 \left[ f^2 - f_i^2 \right]^2} \quad (\text{A-48})$$

$$\alpha_i = N \int_0^{\infty} \frac{f_i^2 f^2 df}{Q^4 f^4 + f_i^2 (1-2Q^2) f^2 - Q^2 f_i^4} \quad (\text{A-49})$$

The (A-49) cannot be evaluated due to the negative value of the coefficients of the denominator polynomial. If we use the approximation

$$\frac{f}{f_i} - \frac{f_i}{f} = 2 \left[ \frac{f - f_i}{f_i} \right] \quad (\text{A-50})$$

we obtain an integral which is easily evaluated and which is a fairly close approximation to the original integral. The evaluation of both integrals at  $f = f_i$  and  $f = \infty$  yield identical values but at  $f = 0$  the values differ by a slight amount. The approximation will lead to noise output values that are slightly higher than would be obtained if the original transform function were used in the integral.

Inserting the substitutions

$$\frac{f}{f_i} - \frac{f_i}{f} = 2 \left[ \frac{f - f_i}{f_i} \right] = 2 \delta_i ; \quad (\text{A-51})$$

$$d\delta_i = \frac{df}{f_i}$$

$$\delta_i = -1 \text{ at } f = 0$$

$$\delta_i = \infty \text{ at } f = \infty$$

the equation for  $\alpha_i$  becomes

$$\alpha_i = N \int_{-1}^{\infty} \frac{f_i d\delta_i}{1 + 4Q^2 \delta_i^2} \quad (A-52)$$

$$\alpha_i = \frac{Nf_i}{4Q^2} \int_{-1}^{\infty} \frac{d\delta_i}{\delta_i^2 + \frac{1}{4Q^2}} \quad (A-53)$$

$$\alpha_i = \frac{Nf_i}{2Q} \tan^{-1} 2Q \delta_i \Big|_{-1}^{\infty} \quad (A-54)$$

If we now reinsert the original function in place of  $2\delta_i$ ,

$$\alpha_i = \frac{Nf_i}{2Q} \tan^{-1} Q \left[ \frac{f}{f_i} - \frac{f_i}{f} \right] \Big|_0^{\infty} \quad (A-55)$$

$$\alpha_i = \frac{Nf_i}{2Q} \left[ \pi/2 - (-\pi/2) \right]$$

$$\alpha_i = \frac{N\pi f_i}{2Q} = \frac{N\pi}{2} \Delta f_i \quad (A-56)$$

The evaluation of  $h^2$  is much more difficult, since it entails polynomials of a higher degree than  $\alpha_i$ , but probably can be evaluated by using the same approach.  $h^2$  will be evaluated by using an approximation method for the value of the integrals.

$$h^2 = \frac{1}{\alpha_1 \alpha_2} \left| \int_0^\infty Y_1(f) \overline{Y_2(f)} W(f) df \right|^2 \quad (\text{A-45})$$

$$h^2 = \frac{\left| \int_0^\infty Y_1(f) \overline{Y_2(f)} W(f) df \right|^2}{\left[ \int_0^\infty |Y_1(f)|^2 W(f) df \right] \left[ \int_0^\infty |Y_2(f)|^2 W(f) df \right]} \quad (\text{A-57})$$

Since  $W(f) = \text{const} = N$ , we may cancel out all the  $W(f)$ . Also, by the basic theorem for estimates of integrals,

$$\left| \int_a^b f(x) dx \right| \leq M(b-a) \leq \int_a^b |f(x)| dx \quad (\text{A-58})$$

if  $|f(x)| \leq M$  for  $a \leq x \leq b$  and  $f(x)$  is continuous for  $a \leq x \leq b$ .

$$h^2 \leq \frac{\int_0^\infty |Y_1(f) \overline{Y_2(f)}|^2 df}{\left[ \int_0^\infty |Y_1(f)|^2 df \right] \left[ \int_0^\infty |Y_2(f)|^2 df \right]} \quad (\text{A-59})$$

$$h^2 \leq \frac{M_1^2 M_2^2 (b-a)^2}{M_1^2 (b-a) M_2^2 (b-a)} \quad (\text{A-60})$$

$$h^2 \approx 1 \quad (\text{A-61})$$

The reason that one can expect  $h^2 \approx 1$  is that the transfer function  $Y_1(f)$  is very much similar to  $Y_2(f)$  for the problem under consideration.

Entering the table of Figure 2 of the reference<sup>1</sup> we find that

$$\left[ \frac{2}{\pi} (1+h) E \left( \frac{2 \sqrt{h}}{1+h} \right) - 1 \right] = T = .25$$

The rms noise output

$$\sigma^2 = (2 - \pi/2)(\alpha_1 + \alpha_2) - \pi \sqrt{\alpha_1 \alpha_2} T \quad (A-62)$$

is now evaluated by inserting  $\alpha_1$ ,  $\alpha_2$ , and T.

$$\sigma^2 = (2 - \pi/2) \frac{N\pi}{2} (\Delta f_1 + \Delta f_2) - \pi/4 \sqrt{\left( \frac{N\pi}{2} \right)^2 \Delta f_1 \Delta f_2} \quad (A-63)$$

$$\sigma^2 = (1 - \pi/4) N\pi (\Delta f_1 + \Delta f_2) - \frac{N\pi^2}{8} \sqrt{\Delta f_1 \Delta f_2} \quad (A-64)$$

Due to the discriminator symmetry,  $\Delta f_1 = \Delta f_2 = 200$  cps

$$\sigma^2 = (1 - \pi/4) N\pi (2 \Delta f_1) - \frac{N\pi^2}{8} \Delta f_1 \quad (A-65)$$

$$\sigma^2 = \left[ 2N\pi - \frac{N\pi^2}{2} - \frac{N\pi^2}{8} \right] \Delta f_1$$

$$\sigma^2 = N\pi \Delta f_1 (2 - \pi/2 - \pi/8)$$

$$\sigma^2 = N\pi \Delta f_1 (0.0345)$$

$$\sigma^2 = 0.0542 (N^2 \Delta f_1) \quad (A-66)$$

---

1. Slepian, D. op. cit.

$$^2 = 21.7N \quad (A-67)$$

That is to say, the rms noise power out of the discriminator is 21.7 times the noise per cycle at the input or, expressed in another way, the rms noise power out of the discriminator is 0.1085 times as great as the rms noise power into the discriminator. This can also be expressed as a 10 db reduction in noise power due to the discriminator.

The signal power out of the discriminator is easily obtained by the use of the slope of the discriminator curve.

$$e_{out} = e_{in} K (f_o - f) \quad (A-68)$$

where K is the slope constant,

$$e_{out} = 5/8 e_{in} \frac{f_o - f}{150} \quad (A-69)$$

$e_{out}$  is a maximum when  $e_{in}$  is at the peak frequency of the discriminator or 100 cps away from  $f_o$  for the discriminator under study, but the doppler frequencies are expected to be 100 cps or less.

$$e_{out} = 2/5 e_{in} \quad (A-70)$$

therefore

$$S_{out} = .16 S_{in} \quad (A-71)$$

To signal-to-noise ratio at the output of the discriminator is then

$$\frac{S_o}{2} = \frac{.16 S_{in}}{.054 (2 f_i N)} = 3 \frac{S_{in}}{(N 2 f_i)_{in}} \quad (A-72)$$

$$\frac{S_o}{2} = \frac{S_{in}}{(N 2 f_i)_{in}} + 5 \text{ db} \quad (A-73)$$

The improvement factor ( $I_D$ ) of the discriminator

$$I_D = 5 \text{ db} \quad (\text{A-74})$$

pertains to signals and noise that are below the threshold of limiting. If the signal is above the limiting level, the improvement factor will be greater due to the capture effect.

Post detection integration of the discriminator output will yield a further improvement factor. It was shown above that this improvement factor is a function of the bandwidth ratio

$$I_{PDI} = \frac{F_i}{F_f} \frac{200}{1/8} = 32 \text{ db} \quad (\text{A-75})$$

The improvement factor ( $I$ ) for the noise reduction due to the discriminator and filtering is

$$I = 5 + 32 = 37 \text{ db} \quad (\text{A-76})$$

The factors that must be included in the determination of the signal-to-noise improvement factor for FM over AM are the "excess noise figure" which degrades the AM system as mentioned above, and the post detection integration in the AM system.

$$I_{EN} = -5 \text{ db} \quad (\text{A-77})$$

The post detection integration for the AM case is

$$I_{PDI} = \frac{f_i}{F_a} = \frac{200}{3} = 18 \text{ db} \quad (\text{A-78})$$

The total improvement factor for FM over AM is

$$I_{TOT} = I - I_{EN} - I_{PDI} \quad (\text{A-79})$$

$$I_{TOT} = 19 \text{ db.}$$

The above improvement factor,  $I_{TOT}$ , pertains to the noise balanced discriminator with signal and noise levels below the limiter threshold.

The signal-to-noise improvement factors that have been obtained in the above analyses have shown that the FM detection system is superior to the AM detection system in all cases. The narrow-band FM analysis for signals greater than, equal to or less than noise yielded an improvement factor of 18 db while the analysis for signals in noise yielded an improvement factor of 19 db.